1995

Derivatized porphyrins and multi-porphyrin assemblies

Hongping Yuan
Iowa State University

INFORMATION TO USERS

This manuscript has been reproduced from the microfilm master. UMI films the text directly from the original or copy submitted. Thus, some thesis and dissertation copies are in typewriter face, while others may be from any type of computer printer.

The quality of this reproduction is dependent upon the quality of the copy submitted. Broken or indistinct print, colored or poor quality illustrations and photographs, print bleedthrough, substandard margins, and improper alignment can adversely affect reproduction.

In the unlikely event that the author did not send UMI a complete manuscript and there are missing pages, these will be noted. Also, if unauthorized copyright material had to be removed, a note will indicate the deletion.

Oversize materials (e.g., maps, drawings, charts) are reproduced by sectioning the original, beginning at the upper left-hand corner and continuing from left to right in equal sections with small overlaps. Each original is also photographed in one exposure and is included in reduced form at the back of the book.

Photographs included in the original manuscript have been reproduced xerographically in this copy. Higher quality 6" x 9" black and white photographic prints are available for any photographs or illustrations appearing in this copy for an additional charge. Contact UMI directly to order.

UMI

A Bell & Howell Information Company
300 North Zeeb Road, Ann Arbor, MI 48106-1346 USA
313/761-4700 800/521-0600

Derivatized porphyrins and multi-porphyrin assemblies

by

Hongping Yuan

A Dissertation Submitted to the

Graduate Faculty in Partial Fulfillment of the

Requirements for the Degree of

DOCTOR OF PHILOSOPHY

Department: Chemistry
Major: Inorganic Chemistry

Approved:

Signature was redacted for privacy.

In Charge of Major Work

Signature was redacted for privacy.

For the Major Department

Signature was redacted for privacy.

For the Graduate College

Iowa State University
Ames, Iowa

1995

1

Derivatized Porphyrins and Multiporphyrin Assemblies

Hongping Yuan

Major Professor: L. Keith Woo
Iowa State University

Porphyrin-containing multi-component systems have served a key role in the study of molecular assembly and supramolecular chemistry. These systems, however, are often very difficult to prepare and new synthetic strategies towards their preparation are of great interest.

This work describes a series of thiol-derivatized porphyrins and the corresponding Co and Zn complexes which have been synthesized from 5-(*p*-aminophenyl)-10,15,20-triphenylporphyrin, 5α,15α-bis(*o*-aminophenyl)porphyrin, and α,α,α,α-tetrakis(*o*-aminophenyl)porphyrin. These derivatized porphyrins have varying numbers of thiol appendages attached via amide linkages at different locations. Thiol-derivatized porphyrins have been demonstrated to form oriented monomolecular coatings on gold surfaces. Accordingly, gold electrodes that have been chemically modified with cobalt thiol porphyrins exhibit electrocatalytic potencies for the reduction of O_2 which vary as a function of the number and location of the thiol appendages. The monolayer formed by bis thiol-porphyrins, in which the porphyrin rings are mostly parallel to the gold surface,

has a higher electrocatalytic activity compared with that from the monolayer formed by mono thiol porphyrins where the porphyrin rings are approximately perpendicular to the gold surface. These metalloporphyrin monolayers will allow an investigation of the influence of surface architecture on chemical properties.

A series of mono-, bis- and tetra-porphyrin assemblies from monopyridylporphyrins and Pd(II) or Pt(II) ions has also been prepared. By utilizing the well defined and versatile chemistry of square planar Pt(II) and Pd(II) coordination complexes, we have been able to place porphyrin subunits at chosen positions and fixed distances around the central metal ions. The molecular structure of one bisporphyrin assembly has been determined. This straightforward synthetic strategy provides an easy method to prepare porphyrin-containing multi-component systems. This dissertation focuses on the synthesis and characterization of thiol-derivatized porphyrins and metal ion-template multi-porphyrin supramolecular assemblies.

DEDICATION

To my wife Danhong

TABLE OF CONTENTS

LIST OF ABBREVIATIONS

ACS	American Chemical Society
bipy	4,4'-bipyridyl
BTPP-Zn	2-bromo-tetraphenylporphyrinato zinc
^{t}Bu	tertiary butyl
cm	centimeter
cr	charge recombination
cs	charge separation
DBDPP-Zn	5,15-dibromo-10,20-diphenylporphyrinato zinc
DBU	1,8-diazabicyclo[5.4.0]undec-7-ene
DDQ	2,3-dichloro-5,6-dicyano-1,4-benzoquinone
DMSO	dimethyl sulfoxide
DNBCOOH	3,4-dinitrobenzoic acid
DPE	aminodiphenyletioporphyrin
dppf	1,1'-bis(diphenylphinoferrocene)
dppp	1,3-bis(diphenylphosphino)propane
eq	equation
Et	ethyl
ET	electron transfer
eV	electron volt

HOMO	highest occupied molecular orbital
IR	infrared
kcal	kilocalorie
LUMO	lowest unoccupied molecular orbital
Me	methyl
mg	milligram
MHz	megahertz
mL	milliliter
mmol	millimole
mol	mole
MQ or monoquat	4-pyridyl-4'-methylpyridinium iodide
MS{EI}	mass spectrometry by electron impact
MS{ESI}	mass spectrometry by electrospray ionization
MS{FAB}	mass spectrometry by fast atom bombardment
nm	nanometer
ns	nanosecond
NMR	nuclear magnetic resonance
OAc	acetate
OEP	octaethylporphyrinato dianion
OEt_2	diethylether
OMP	octamethylporphyrin dianion

OTf	triflate anion
PCOOH	diethyl-pentamethylporphyrin-2-acetic acid
Ph	phenyl
POR	general porphyrinato dianion
ppm	parts per million
ps	picosecond
py	pyridine
Py_4POR	*meso*-tetrapyridylporphyrin
pyPP	5-pyridyl-10,15,20-triphenylporphyrin
Py_3T	tripyridyltriazine
pyTP	5-pyridyl-10,15,20-tritolylporphyrin
solv	solvent
terpy	terpyridine
THF	tetrahydrofuran
p-TsOH	*p*-toluenesulfonic acid
TMP	*meso*-tetramesitylporphyrinato dianion
$TMP(R)_8$	β-octasubstituted-tetramesitylporphyrinato dianion
TmTP	*meso*-tetra-*m*-tolylporphyrinato dianion
TMS	trimethylsilyl
Tol	tolyl
TPP	*meso*-tetraphenylporphyrinato dianion

TPPBr	2-bromo-tetraphenylporphyrinato dianion
$TPP(Br)_4$	2,3,12,13-tetrabromo-tetraphenylporphyrinato dianion
$TPP(Br)_8$	octabromo-tetraphenylporphyrinato dianion
TTP or TpTP	*meso*-tetra-*p*-tolylporphyrinato dianion
μs	microsecond
UV-vis	ultraviolet-visible
XPS	X-ray photoelectron spectrometry

GENERAL INTRODUCTION

Dissertation organization

This dissertation contains two chapters of literature review. Chapter 1 discusses recent advances in the synthesis of porphyrins and multi-porphyrin arrays. Chapter 4 deals with the design of porphyrin-containing multi-component systems as models for the photosynthetic reaction center. Non-covalently bonded systems are discussed. The remaining chapters constitute individual papers that have been published, or are being prepared for submission. General conclusion follows the last paper.

What is a porphyrin?

Porphyrins are macrocyclic compounds which consist of four pyrrole groups bridged in the two and five (α) positions by methine units. The methine bridges are designated as the *meso* position and the two non-bridged carbon positions (C_3 and C_4) of the pyrroles are the β-pyrrole positions. A variety of functional groups can be placed at these positions without affecting the basic structural parameters of the macrocycle. The porphyrin framework has 11 conjugated double bonds and 22 π electrons. It obeys Huckel's 4n+2 rule and is aromatic. Porphyrins are semi-rigid, planar molecules with an inner hole diameter of 4 Å. The porphyrin macrocyle is thermally stable and can be sublimed at approximately 350 °C. When the two internal protons are removed from the free base porphyrin, it becomes a tetradentate chelating dianion, with the ability to coordinate a variety of different metal ions in the central cavity.

In this work, five porphyrins were used exclusively, 5,15-bis(*o*-aminophenyl)-2,8,12,18- tetraethyl-3,7,13,17-tetramethylporphyrin (DPE-$(NH_2)_2$ -- amino*di*phenyl-*e*tioporphyrin II), 5-(*p*-aminophenyl)-10,15,20-triphenylporphyrin (TPP-NH_2), 5,10,15,20-tetrakis(*o*-aminophenyl)porphyrin (TPP-$(NH_2)_4$), 5-(4-pyridyl)-10,15,20-triphenylporphyrin (pyPP) and 5-(4-pyridyl)-10,15,20-tritolylporphyrin (pyTP). In pyPP or pyTP (Figure 1), the pyridyl group and the three aryl groups (phenyl for MpyPP, *p*-tolyl for pyTP) are located in the *meso* positions and hydrogens are at the β-pyrrole positions. Figure 2a shows the bis(aminophenyl)porphyrin, DPE-$(NH_2)_2$. This molecule has two aminophenyl groups situated at opposing *meso* positions, and hydrogens at the other two *meso* positions. Ethyl and methyl groups occupy the β-pyrrole positions such that the porphyrin has C_{2v} symmetry. TPP-NH_2 (Figure 2b) has hydrogens at the β-pyrrole positions and phenyl groups at each of the *meso* positions, one of which bears an amino group in the *para* position. The amino groups in these porphyrins can be employed to make porphyrin derivatives or porphyrin containing multi-component systems.

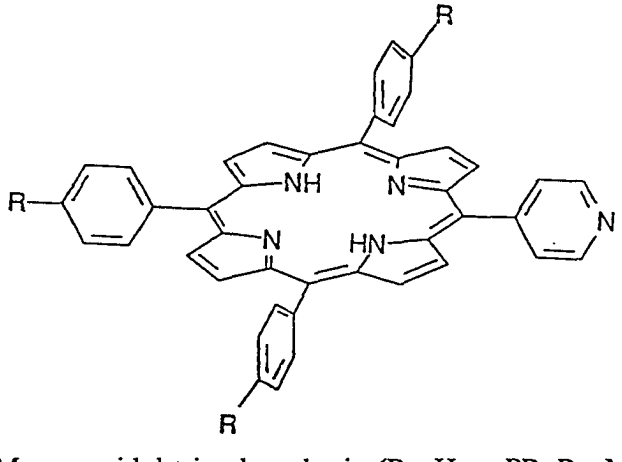

Figure 1: Mono-pyridyl triarylporphyrin (R= H, pyPP; R= Me, pyTP)

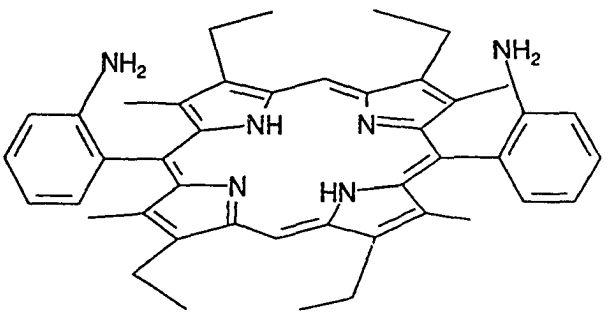

a

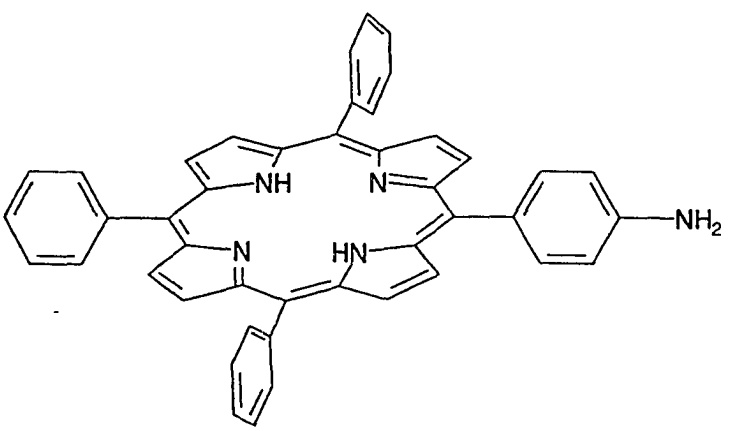

b

Figure 2: a) Aminodiphenyl etioporphyrin (DPE-$(NH_2)_2$)
b) Aminophenyl triphenylporphyrin (TPP-NH_2)

Porphyrins are excellent spectroscopic tags in both UV-vis and ^1H NMR spectroscopies. Because of the aromaticity of the porphyrin core, strong absorptions are observed in the near UV and visible regions of the electromagnetic spectrum. A typical UV-vis spectrum exhibits an intense absorption band between 350 and 500 nm known as the Soret band, with a molar absorptivity on the order of 10^5 $M^{-1}cm^{-1}$. Several less intense peaks called Q-bands can be observed from 450 nm to 700 nm with molar absorptivities of 10^3-10^4 $M^{-1}cm^{-1}$. Proton NMR spectroscopy can reveal much about the molecular symmetry of the porphyrin complexes. When the 2-fold symmetry of the bis(*o*-aminophenyl)porphyrin (DPE-$(NH_2)_2$) is maintained on the NMR timescale, the ^1H NMR spectrum exhibits a single resonance for the meso protons. However, in the lower symmetry compounds TPP-NH_2, pyPP and pyTP, the β-pyrrole protons split into multiplets.

Why study porphyrins?

Porphyrin chemistry encompasses a rich and diverse research field. It spans the areas of organic, inorganic, physical, biochemistry and materials science. All transition metals and many metalloid elements in a wide range of oxidation states can form metalloporphyrin complexes. The organometallic chemistry of metalloporphyrins and catalytic systems using metalloporphyrins have been studied extensively. Also, metalloporphyrins provide a good system for the study of group transfer reactions.

Porphyrin and porphyrin related structures play a very important role in biological

systems. The most predominant are iron hemes. The heme group is iron protoporphyrin IX. It is found in the hemoglobin-myoglobin and cytochrome families. In many organisms, O_2 transport, storage, and activated are frequently mediated by heme proteins. In mammals, oxygen is transported by the hemoglobin and stored by myoglobin. In the terminal step of respiration involving reduction of oxygen to water, electrons are transported via a series of cytochrome to cytochrome oxidase transfer steps. Cytochrome oxidase contains two iron porphyrins and two copper ions. The heme group is also found in peroxidases and catalases, which are involved in the oxidation of organic compounds with H_2O_2. The active site of vitamin B_{12} utilizes a corrin, a related structure to porphyrin, which plays an important role in biological systems. Chlorophyll consists of a chlorin, a reduced porphyrin, which captures sunlight for photosynthesis. This process is the important light-harvesting phenomenon that converts solar energy to support the whole ecosystem in the planet. Extensive work has been done to mimic the above systems using synthetic porphyrins.

The research presented here focuses on the preparation of thiol-derivatized porphyrins and the applications of these porphyrins to construct monolayers on gold surfaces with special chemical properties. Also, studies on assembling pyridyl porphyrin subunits around metal ions to build multi-porphyrin assemblies is presented.

CHAPTER 1: PORPHYRIN SYNTHESES AND MODIFICATIONS: A LITERATURE REVIEW

Synthesis of *meso*-tetra-substituted porphyrins

Synthesis of *meso*-substituted porphyrins was reported by Rothemund[1] in 1936. Early procedures involved treating benzaldehyde with pyrrole in pyridine in a sealed bomb at 140 to 220 °C over a period of 24 to 48 hours. This method yielded 4 to 5% of H_2TPP, *meso*-tetraphenylporphyrin, with variable amounts of tetraphenylchlorin. However, the reactions conditions were so severe that few only a substituted benzaldehydes could be converted to the corresponding porphyrins. Improved synthetic procedures have been developed over the years, and are reviewed in *The Porphyrins*.[2]

One of the most important modifications of the Rothemund reaction was reported by Adler and Longo.[3] This modification involved the aerobic condensation of benzaldehyde and pyrrole in refluxing propionic acid (141 °C). Under these relatively mild conditions, a wider selection of substituted benzaldehydes have been converted to the corresponding porphyrins in multigram quantities with yields of up to 20%. Some disadvantages are still inherent in this method. For example, attempts at making porphyrins from benzaldehydes bearing sensitive functional groups such as hydroxyl, thiol, and amino groups failed under these reaction conditions. Moreover, tar-like side products cause purification problems especially with porphyrins that do not readily crystallize or precipitate at the end of the reaction.

Recently, Lindsey and co-workers developed a more general procedure for the synthesis of *meso*-substituted porphyrins.[4] In this method, pyrrole and aldehyde undergo acid-catalyzed condensation to form a porphyrinogen under equilibrium conditions. Porphyrin is produced upon addition of 2,3-dichloro-5,6-dicyano-1,4-benzoquinone (DDQ) or 2,3,5,6-tetrachloro-1,4-benzoquinone (*p*-Chloranil, TCQ) as an oxidant. This strategy, based on the examination of equilibrium cyclization and biomimetic studies of porphyrin biosynthesis, is centered around three hypotheses: 1) Tetraphenylporphyrinogen should be the thermodynamically favored product when benzaldehyde and pyrrole are condensed under appropriate conditions. Thus, reaction conditions which reach equilibrium prior to oxidation should favor high yields of the porphyrin. 2) High temperature is not necessary since benzaldehyde and pyrrole are reactive molecules. 3) Synthetic conditions sufficiently mild for equilibrium to be achieved should also be compatible with an unprecedented variety of substituted benzaldehydes, thereby allowing new functionalized porphyrins to be obtained in good yield. In general, Lindsey's procedure is compatible with a wide variety of substituted benzaldehydes and porphyrin yields are around 30-40%. When this procedure is applied to synthesize porphyrins with 2,6-disubstituted benzaldehydes, a co-catalyst, $BF_3 \cdot OEt_2$-ethanol, is needed to overcome steric barriers. However, this method can not be used for in the synthesis of porphyrins with aldehydes bearing large ortho substitutents such as 9-anthraldehyde, 2,4,6-triphenyl benzaldehyde. Also, very electron poor groups such as 2,6-dinitrobenzaldehyde and 2,6-bis(trifluoromethyl)benzaldehyde fail to undergo condensation under these conditions.

Moreover, the optimal yields are obtained with low concentrations (0.01 M pyrrole and aldehyde), requiring large volumes of solvent for gram-scale preparations. Lindsey *et al.*[5] subsequently found that by increasing the concentration of the acid catalyst, porphyrins could be synthesized in yields of 20-30% by condensation of pyrrole and benzaldehyde at 0.1 M concentrations. For example, reaction mixtures with 0.1 M mesitaldehyde and pyrrole with BF_3-ethanol as a cocatalyst afforded H_2TMP in yields up to 15%. Lindsey's method is complementary in nature to the Adler-Longo procedure.

Therien *et al.*[6] have found a method for the synthesis of *meso*-substituted porphyrins which bear strong electron withdrawing groups such as perfluoroalkyl for which conventional methods failed. The mechanism of porphyrin formation is shown in Figure 1, where R_f represents the perfluoroalkyl groups. The intermediate 2,2,3,3,4,4,4-heptafluoro-1-(2-pyrrolyl)-1-butanol was condensed in benzene using *p*-TsOH as catalyst. During the reaction, water was removed by azeotropic distillation with a Dean-Stark trap to shift the equilibrium towards porphyrinogen formation. DDQ was added to oxidize the porphyrinogen to the final porphyrin product in an overall yield of 37%.

Synthesis of porphyrin precursor dipyrromethanes

5,15-Substituted porphyrins have important applications in building multi-porphyrin arrays.[7] Mixed aldehyde condensations can be used as a synthetic process for 5,15-substituted porphyrins, but isolating the desired product from other isomers and other side products is usually difficult and sometimes impossible. Direct approaches to

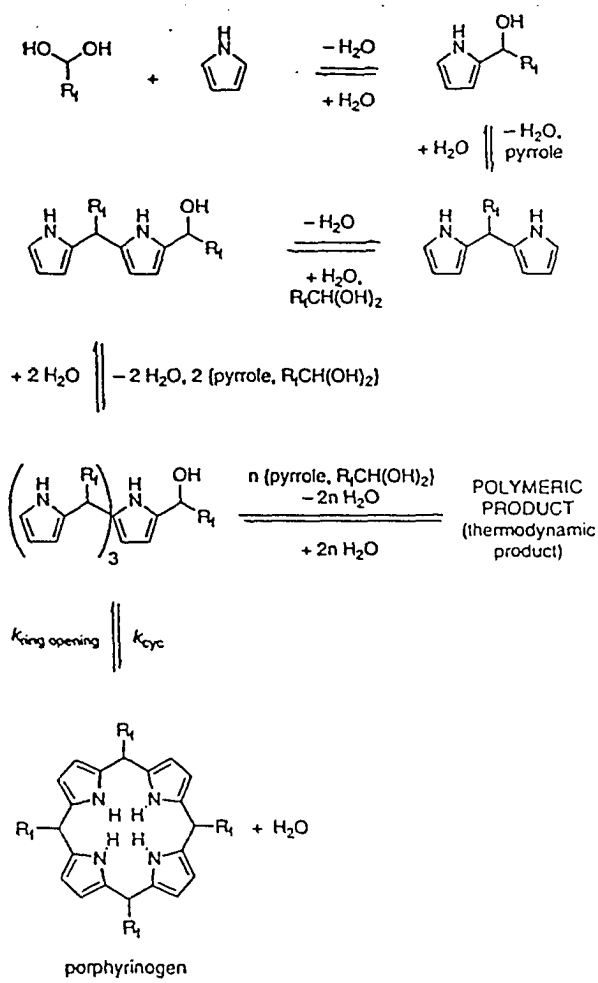

Figure 1. Mechanism of porphyrin formation (reprinted with permission from *J. Org. Chem.* **1994**, *59*, 6943. Copyright © 1993 ACS)

5,15-disubstituted porphyrins are provided by condensation of dipyrromethanes with aldehydes. There are four different methods currently available for the synthesis of dipyrromethanes, each distinguished by the position of substituents on dipyrromethane.

The synthesis of 2,2'-dipyrromethane involves a two-step procedure starting from pyrrole and thiophosgene.[8] Treatment of pyrrole with thiophosgene produces 2,2'-dipyrrothione. Subsequent reduction of 2,2'-dipyrrothione with sodium borohydride provides 2,2'-dipyrromethane.

Preparation of dipyrromethanes with substitutents on the β-pyrrole positions (β-substituted dipyrromethanes) have often required laborious syntheses.[9] Verkade and Tang have developed a relatively simple route for synthesizing β-substituted dipyrromethanes in high yield.[10] In the presence of the strong, nonionic super-base $P(MeNCH_2CH_2)_3N$, 3,4-disubstituted pyrrole-2-esters can be made from β-acetoxy-α-nitroalkanes (or α-nitroalkenes) and isocyanoacetates at low temperatures and in quantitative yield. Since superbase salts are virtually insoluble in nonpolar and weakly polar solvents, the pyrrole product can be easily isolated by filtration. The 3,4-disubstituted pyrrole-2-esters are coupled with paraformaldehyde to form dipyrromethane di-esters. Subsequent decarboxylation of the esters produced β-substituted dipyrromethanes. This procedure provides easy access to β-substituted dipyrromethanes.

Lindsey and Lee reported that the reaction of an aldehyde with a large excess of pyrrole (1: 30-70) at room temperature produces a *meso*-substituted, β-unsubstituted dipyrromethanes.[11] The reaction is catalyzed with trifluoroacetic acid or $BF_3 \cdot OEt_2$. The

dipyrromethane is purified by crystallization or by flash chromatography and isolated in 47-86% yield. The reaction is compatible with aliphatic or aromatic aldehydes, including 2,6-disubstituted benzaldehyde.

Rose *et al.* found that condensation of 2,6-dinitrobenzaldehyde with substituted pyrroles in a 2:1 ratio does not produce the *meso*-aryl dipyrromethane. Instead, the reaction afforded the one-to-one condensation product.[12] However, they have used a similar strategy in condensing 2,6-diacetamidobenzaldehyde with a β-substituted pyrrole to form the *meso*-aryl dipyrromethane. Condensation of this *meso*-substituted dipyrromethane in CH_2Cl_2 with $HC(OMe)_3$ in the presence of a catalytic amount of CCl_3COOH affords 5,15-bis(2,6-diacetamidophenyl)octaalkylporphyrin. The 5,15-bis(2,6-diaminophenyl)porphyrin can be made by hydrolysis of this acetamidophenylporphyrin.[13]

Synthesis of β-octa-substituted porphyrins

Octamethylporphyrin (H_2OMP) was first prepared by Fischer and Walach in 1926 by heating 3,4-dimethylpyrrole in formic acid.[14] Treibs and Haberele[15] reported a 77% yield of H_2OMP from the reaction of 3,4-dimethylpyrrole with formaldehyde in acetic acid and pyridine.

Octaethylporphyrin (H_2OEP) is one of the most important and widely used synthetic porphyrins because of its high symmetry and good solubility. It has been prepared by self-condensation of 2-N,N'-diethylaminomethyl-3,4-diethylpyrrole,[16] ethyl 5-N,N'-diethylaminomethyl-3,4-diethylpyrrole-2-carboxylate,[17] or 3,4-diethyl-5-

hydroxymethylpyrrole-2-carboxylic acid under oxidative conditions.[18] It has also been prepared by direct condensation of 3,4-diethylpyrrole with aqueous formaldehyde on a small scale.[19] All of these syntheses derive from the same ethyl 3,4-diethyl-5-methylpyrrole-2-carboxylate. This precursor is prepared from a "reverse Knorr" reaction of ethyl propionylacetate with 2,4-pentanedione, and requires several steps.

Recently, several groups[20] have developed a new method for the synthesis of ethyl 3,4-diethyl-5-methylpyrrole-2-carboxylate. Starting from β-acetoxy-α-nitroalkanes (or α-nitroalkenes) and isocyanoacetates in the presence of a nonionic base such as DBU or guanidine, the pyrrole ester could be synthesized in high yield (80-90%). Verkade and Tang[10] improved this procedure further by using the superbase $P(MeNCH_2CH_3)_3N$ in place of DBU or guanidine. The product forms in quantitative yield and is easy purified. Verkade and Tang have also found that the reaction of 5,5'-bis(methoxycarbonyl)-3,3',4,4'-tetraethyldipyrromethane with LiCl, $(CH_2O)_n$, H_2O in DMSO at 200-210°C for 2 hours produced H_2OEP in 67% yield. This one-pot procedure greatly simplifies the synthesis of H_2OEP.

Porphyrin modification

Kruper and coworkers developed alternative synthetic routes to unsymmetrically functionalized porphyrins. They synthesized mono(*p*-nitrophenyl)triphenylporphyrin through regiospecific aryl nitration of readily available tetraphenylporphyrin.[21] The mono(*p*-nitrophenyl)triphenylporphyrin can be easily reduced to mono(*p*-aminophenyl)-

triphenyl porphyrin. This aminoporphyrin can be employed as the starting material to make different derivatized porphyrins such as thiol-derivatized porphyrins[22] and halogenated porphyrins.[23]

Tetraarylporphyrins have been used to make novel structures such as the "picket fence", "pocket", and "picnic-basket" porphyrins,[24] the "capped" porphyrins,[25] the "bridged" porphyrins,[26] the "baskethandle" porphyrins,[27] and the "gyroscope" porphyrin.[13] These derivatives have been studied as models of natural hemoproteins. Our group has developed a series difunctionalized porphyrin ligands based on 5,15-bis(*o*-aminophenyl)porphyrin, which were used to prepare multinuclear transition-metal complexes.[28]

Synthesis of porphyrins via metal-mediated cross-coupling

The attachment of unusual organic moieties to the porphyrin periphery often involves elaborate synthetic strategies and tedious separation procedures.[29] Typical routes to porphyrins bearing one or more different *meso*- or β-substitutents involve condensation of appropriate aldehydes with various monopyrroles,[30] substituted dipyrromethanes,[31] or prefabricated 1,19-dideoxybiladienes.[32] In addition to purification and separation problems, other limitations include: 1) the sensitivity of the cyclization step in a porphyrin synthesis to the steric and electronic features of substitutents at the *meso* and the β-pyrrole positions and 2) the potential incompatibility of the reactants with the condensation condition (i.e. protic or Lewis acid catalysts[4] or

high temperature[33]).

Some researchers have utilized metal-mediated cross-coupling methodologies to put special appendages on readily available porphyrins. This strategy has provided an alternative method for the synthesis of substituted porphyrins. Therien *et al.*[34] reported the synthesis of new substituted porphyrins based on Pd-catalyzed coupling of halogenated porphyrins and organometallic reagents. For example, $Pd(PPh_3)_4$ can catalyze the coupling of (5,15-dibromo-10,20-diphenylporphyinato)zinc (DBDPP-Zn) or (2-bromo-tetraphenylporphinato)zinc (BTPP-Zn) with organozinc chloride or organotributyltin. $Pd(dppf)Cl_2$ (dppf = 1,1'-bis(diphenylphinoferrocene)) was also used as a catalyst. Figure 2 outlines the proposed reaction sequence and lists the variety of alkyl, vinyl, and aryl moieties coupled to BTPP-Zn. The authors found that: 1) the complete conversion of reactants to products took place for each organometallic reagent; 2) the reaction time depended only on the catalyst used; and 3) the reaction is not sensitive to such factors as steric constraints, the basicity of the organometallic reagent, or electronic properties of substituted groups on the organometallic reagent. Catalytic conversion of DBDPP-Zn to 5,15-disubstituted-10,20-diphenylporphinato zinc complexes provides a facile route to a wide range of mixed *meso*-substituted porphyrins.

Dolphin *et al.* have synthesized mixed *meso*-substituted porphyrins.[35] They found that the treatment of 5,15-diphenylporphyrin with 1.5 equivalents of bis(trifluoroacetoxy)-iodobenzene-iodine (1.2:1) gave 10-iodo-5,15-diphenylporphyrin in yields greater than 70%. These conditions are designed to avoid multiple iodination since

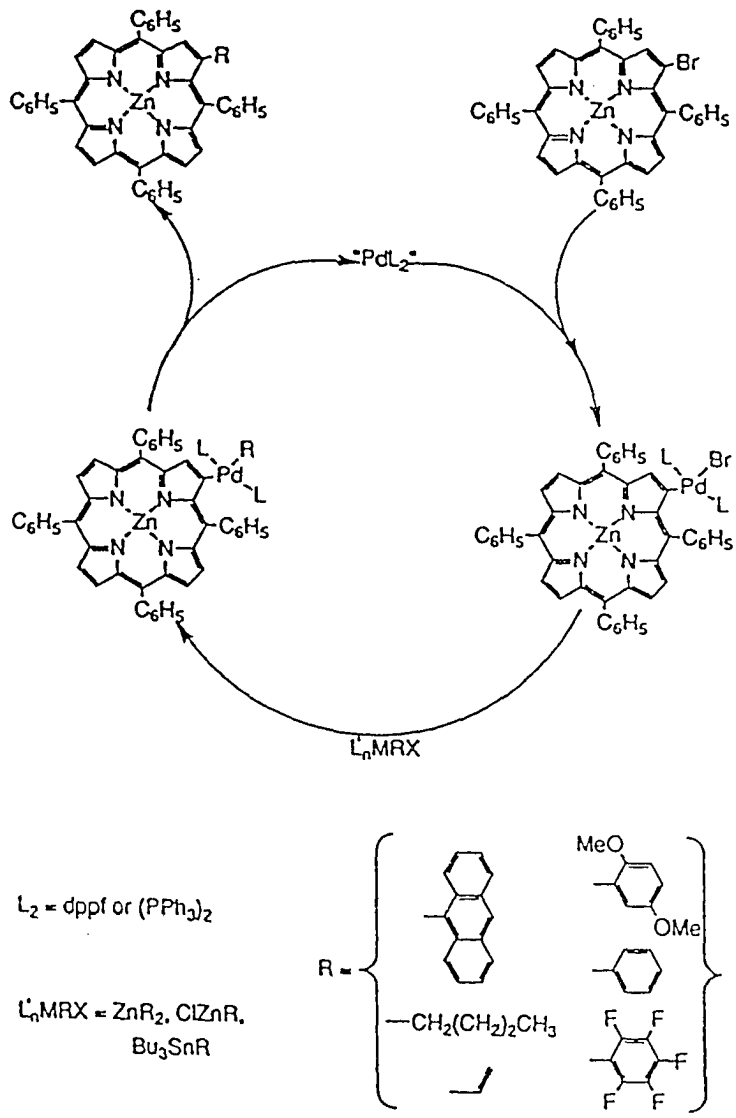

Figure 2. Metal-mediated porphyrin synthesis (reprinted with permission from *J. Org. Chem.* **1993**, *58*, 5983. Copyright © 1993 ACS).

subsequent addition occurs at a β-pyrrole position and leads to a mixture of regioisomers. The 10-iodo-5,15-diphenyl-porphyrinato zinc complex was treated with a range of monosubstituted alkynes in the presence of a catalytic amount of $Pd(PPh_3)_2Cl_2$ and copper(I) iodide to produce the corresponding 10-alkynyl-5,15-diphenylporphyrinato zinc(II) complexes in 50-90% yield. This coupling reaction was carried out under ambient temperature and pressure, making it a practical method for tethering biologically active moieties to porphyrins. For example, 17α-ethynyltestosterone and 17α-ethynylestradiol have been linked to 5,15-diphenylporphyrin in this manner. This method offers a powerful tool for attaching substitutents to a porphyrin through a common acetylenic linkage to give isomerically pure products.

Lier and Ali[36] reported that a variety of Ni, Cu, and Zn complexes of β-monohalosubstituted porphyrins, such as 2-bromo-tetraphenylporphyrin, 2-bromo-3,7,8,12,13,17,18-heptaethyl-porphyrin, and 3-iodo-deuteroporphyrin IX dimethylester, undergo palladium(II)-catalyzed carbon-carbon coupling reactions with a series of terminally substituted acetylenic derivatives to form the corresponding mono acetylenic porphyrins. They have also synthesized a few disubstituted porphyrins by using the corresponding dihalogentated porphyrin precursors. These reactions are usually heated to 80-85 °C for 10 to 48 hours and the yields are around 60-90%. The reaction between 5-(*p*-iodophenyl)-10,15,20-triphenylporphyrinato zinc(II) and terminally alkynes was fast and quantitative at room temperature, yielding the corresponding 5-[(*p*-acetylenic)phenyl]-10,15,20-triphenylporphyrinato zinc(II).

Chan *et al.*[37] reported the synthesis of β-aryl substituted porphyrins by employing the Suzuki cross coupling reaction[38] with β-bromoporphyrins. 2-Bromo-5,10,15,20-tetraphenylporphyrin (H_2TPPBr), 2,3,12,13-tetrabromo-5,10,15,20-tetraphenylporphyrin [$H_2TPP(Br)_4$] and 2,3,7,8,12,13,17,18-octabromo-5,10,15,20-tetraphenylporphyrin [$H_2TPP(Br)_8$] all underwent smooth cross-coupling reactions with aryl boronic acids to give β-aryl tetraphenylporphyrins in moderate to high yields (50-88%) in the presence of a catalytic amount of $Pd(PPh_3)_4$. This method can also be employed to prepare sterically hindered β-octasubstituted tetramesitylporphyrins $H_2TMP(R)_8$ (R= Me, Ar) from $H_2TMP(Br)_8$. One advantage of this method is that it can be directly applied to free-base porphyrins.

The above examples show that the metal-mediated, cross-coupling method provides several important advantages to the fabrication of elaborate porphyrins: 1) catalytic, quantitative conversion of reactants to products allows efficient derivatization of the porphyrin periphery, 2) mild reaction conditions permit the incorporation of organic groups that are sensitive to heat and acid, 3) purification and isolation of products is fast, and, 4) the procedure is generally suitable for the construction of a wide range of porphyrin compounds.

Synthesis of porphyrin dimers and oligomers via metal-mediated cross-coupling

Lindsey *et al.*[39] have synthesized pentameric porphyrins arrays. Tetra(4-iodo-2,6-dimethylphenyl)porphyrin was employed as the core unit and was coupled to 5-(4-

ethynylphenyl)-10,15,20-tris(mesityl)porphyrinato zinc with a catalytic amount of $Pd(PPh_3)_4$ to afford the pentamer as the major product (Figure 3). In the pentamer, fluorescence excitation and emission studies on Zn4Fb1 and Zn4Cu1 indicate that the energy is funneled from the peripheral zinc porphyrins to the central porphyrin such that the fluorescence quantum yield of the zinc porphyrins are reduced 12- to 14-fold. The energy transfer from zinc porphyrin to free base porphyrins was shown to have greater than 90% efficiency.

Sanders and coworkers have synthesized cyclic porphyrin oligomers using the Glaser coupling (eq. 1).[40] This coupling reaction oxidatively combines two terminal

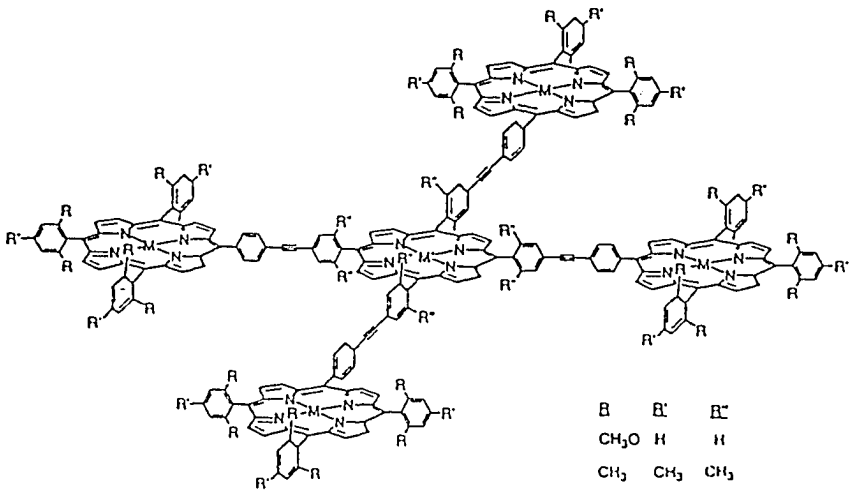

M = Zn, M' = 2H, Zn4Fb1; M = Zn, M' = Cu, Zn4Cu1

Figure 3. Porphyrin pentamer (adopted from *J. Am. Chem. Soc.* **1993**, *115*, 7519).

acetylenes to give a butadiyne linkage in essentially a quantitative yield. Under Glaser

$$Ar\text{-}C{\equiv}C\text{-}H + H\text{-}C{\equiv}C\text{-}Ar + [O] \rightarrow Ar\text{-}C{\equiv}C\text{-}C{\equiv}C\text{-}Ar + H_2O \quad (1)$$

coupling conditions, 5,15-bis(*m*-ethynylphenyl)porphyrin or its Zn complex produced a complex mixture of porphyrin oligomers. Using templates to organize the reactants allows preparation of cyclic dimers, trimers and tetramers (Figure 4).[41, 42] When 4,4'-bipyridine (bipy) was used as the template, the yield of the cyclic dimer was tripled. The first step in this template reaction is the combination of two porphyrin units to yield a linear dimer. Then either intramolecular cyclization occurs to provide cyclic dimer or reaction with a further monomer porphyrin yields a linear porphyrin trimer.[33] The bipy template aligns the reactive ends of the intermediate to increase the rate of intramolecular cyclization.

Similarly, *meso*-tetra-(4-pyridyl)porphyrin, Py_4POR, was found to enhance the cyclization of linear porphyrin dimers to form a cyclic tetramer in yields greater than 70%. Conversion of a linear porphyrin tetramer to the cyclic tetramer by Py_4POR occurs in yields greater than 90%.

Tripyridyltriazine, Py_3T, was used as a template for the cyclic trimer. Under Glaser coupling conditions, 5,15-bis(*m*-ethynylphenyl)porphyrin could be converted to cyclic trimer in yields of 50% in the presence of Py_3T. An analogous trimer which incorporated a platinum spacer between the alkynes, was synthesized by condensation of an acetylenic porphyrin with trans-$Pt(PR_3)_2Cl_2$.[43] This cyclic porphyrin trimer with platinum spacers has a larger cavity than the butadiyne-linked cyclic porphyrin trimer.

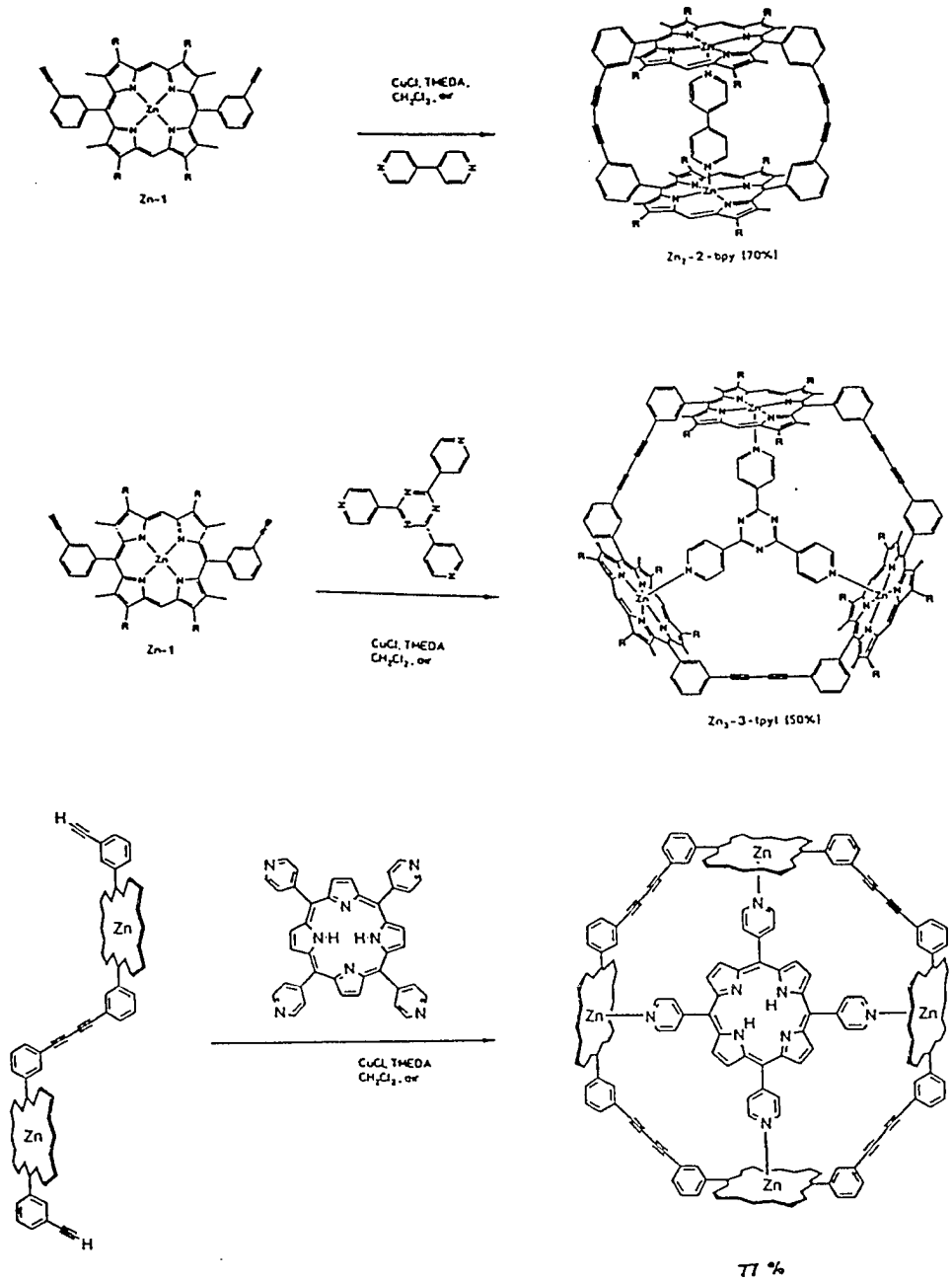

Figure 4. The formation of cyclic porphyrin oligomers by template. (adopted from *Angew. Chem. Int. Ed. Engl.* **1990**, *29*, 1400 and *Acc. Chem. Res.* **1993**, *26*, 469).

The cyclic porphyrin trimer has been shown to accelerate an intermolecular Diels-Alder reaction *exo*-selectively, making the *exo*-isomer the only detectable product (Figure 5).[44] In addition, it has the ability to catalyze acyl transfer reactions.[45] This chemistry represents an important step in the development of enzyme mimics, because its major role is in recognition and orientation events that are decoupled from the reaction itself.[46] Accordingly, it should be possible to bring together a wide range of different reactive pairs by changing the substituents on the amine ligand; or by changing the geometry of the host and the nature of the recognition event. Rational changes in synthetic design could allow a systematic study of the importance of such factors as host flexibility and quality of fit in supramolecular catalysis.

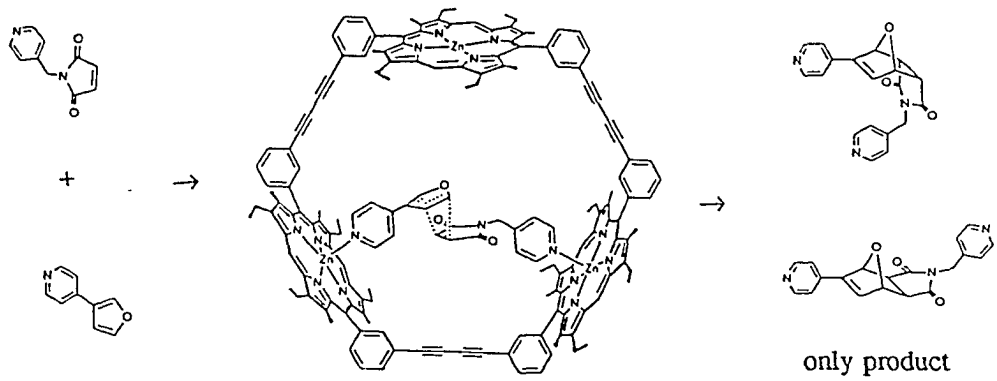

Figure 5. *exo*-Selective Diels-Alder reaction catalyzing by porphyrin terimer (adopted from *J. Chem. Soc., Chem. Commun.* **1993**, 458).

The following two chapters discuss our work on the synthesis of thiol-derivatized porphyrins and the study of thiol-derivatized porphyrin monolayers on gold.

References

1. (a) P. Rothemund, *J. Am. Chem. Soc.* **1936**, *58*, 625. (b) P. Rothemund, *J. Am. Chem. Soc.* **1939**, *61*, 2912.
2. *The Porphyrins*, Dolphin, D., Eds.; Academic Press: New York, NY, 1978, V.2, Chap. 3-6, pp. 85-288.
3. (a) Adler, A. D.; Longo, F. R.; Shergalis, W. *J. Am. Chem. Soc.* **1964**, *86*, 3145-3149. (b) Adler, A. D.; Longo, F. R.; Finarelli, J. D.; Goldmacher, J.; Assour, J.; Korsakoff, L. *J. Org. Chem.* **1967**, *32*, 476.
4. (a) Lindsey, J. S.; Hsu, H. C.; Schreiman, I. C. *Tetrahedron Lett.* **1986**, *27*, 4969-4970. (b) Lindsey, J. S; Schreiman, I. C.; Hsu, H. C.; Kearney, P. C.; Marguerettaz, A. M. *J. Org. Chem.* **1987**, *52*, 827-836. (c) Wagner, R. W.; Lawrence, D. S.; Lindsey, J. S. *Tetrahedron Lett.* **1987**, *28*, 3069-3070. (d) Lindsey, J. S.; Wagner, R. W. *J. Org. Chem.* **1989**, *54*, 828-836.
5. (a) Corken, L. A.; Plouvier, J. C.; Lindsey, J. S. *Chemom. Intell. Lab. Syst.* **1992**, *17*, 95-105. (b) Lindsey, J. S.; MacCrum, K. A.; Tyhonas, J. S.; Chuang, Y.-Y. *J. Org. Chem.* **1994**, *59*, 579-587.

6. DiMagno, S. G.; Williams, R. A.; Therien, M. J; *J. Org. Chem.* **1994**, *59*, 6943-6948.

7. (a) Prathapan, S.; Johnson, T. E.; Lindsey, J. S. *J. Am. Chem. Soc.* **1993**, *115*, 7519-7520. (b) Wagner, R. W.; Lindsey, J. S. *J. Am. Chem. Soc.* **1994**, *116*, 9759-9760. (c) Lindsey, J. S.; Prathapan, S.; Johnson, T. E.; Wagner, R. W. *Tetrahedron* **1994**, 50, 8941-8968. (d) Wagner, R. W.; Lindsey, J. S.; Turowska-Tyrk, I.; Scheidt, W.R. *Tetrahedron* **1994**, 50, 11097-11112.

8. (a) Chong, R.; Clezy, P. S.; Liepa, A. J.; Nichol, A. W.; *Aust. J. Chem.* **1969**, *22*, 229. (b) Clezy, P. S.; Smythe, G. A. *Aust. J. Chem.* **1969**, *22*, 239.

9. (a) Clesy, P. S.; Liepa, A. J. *Aust. J. Chem.* **1970**, *23*, 2443. (b) Young, R.; Chang, C. K. *J. Am. Chem. Soc.* **1985**, *107*, 898-909.

10. Tang, J. S.; Verkade, J. G.; *J. Org. Chem.* **1994**, *59*, 7793-7802.

11. Lee, C.-H.; Lindsey, J. S. *Tetrahedron*, **1994**, *50*, 11427-11440.

12. Lecas-Nawrocka, A.; Levisallles, J.; Mariacher, C.; Rose, E. *Can. J. Chem.*, **1984**, *62*, 2059-2062.

13. (a) Lecas-Nawrocka, A.; Levisalles, J.; Mariacher, C.; Renko, Z.; Rose, E. *Can. J. Chem.*, **1984**, *62*, 2054-2058. (b) Lecas, A.; Levisalles, J.; Renko, Z.; Rose, E. *Tetrahedron Lett.*, **1984**, *25*, 1563-1566. (c) Lecas-Nawrocka, A.; Renko, Z.; Rose, E. *Tetrahedron Lett.* **1985**, *26*, 1019-1022. (d) Boitrel, B; Lecas, A.; Renko, Z.; Rose, E. *New J. Chem.*, **1989**, *13*, 73-99.

14. Fischer, H.; Walach, B. *Justus Liebigs Ann. Chem.* **1926**, *450*, 164.

15. Treibs, A. Haberle, N. *Justus Liebigs Ann. Chem.* **1968**, *718*, 183.

16. (a) Eisner, U.; Lichtarowicz, A.; Linstead, R. P. *J. Chem. Soc.* **1957**, 733. (b) Eisner, U.; Linstead, R. P.; Parkes, E. A.; Stephen, E. *J. Chem. Soc.* **1956**, 733. (c) Whitlock, H. W.; Hanauer, R. *J. Org. Chem.* **1968**, *33*, 2169.

17. (a) Paine, J. B.,III; Kirshner, W. B.; Moskowitz, D. W.; Dolphin, D. *J. Org. Chem.*, **1976**, *41*, 3857. (b) Wang, C.-B.; Chang, C. K. *Synthesis*, **1979**, 548.

18. Inhoffen, H. H.; Fuhrhop, J. H.; Voight, H.; Brockmann, H., Jr. *Ann. Chem*, **1966**, *695*, 133.

19. (a) Cheng, D. O.; LeGoff, E. *Tetrahedron Lett.* **1977**, *34*, 1469. (b) LeGoff, E.; Cheng, D. O., In *Porphyrin Chemistry Advances*; Longo, F. R. Ed.; Ann Arber Science Publishers, **1979**; pp. 153-156

20. Barrton, D. H. R.; Kervagore, J.; Zard, S. *Tetrahedron* **1990**, *46*, 7587. (b) Ono, N.; Kawamura, H.; Bougauchi, M. *Tetrahedron* **1990**, *46*, 7483. (c) Ono, N.; Kawamura, H.; *Bull. Chem. Soc. Jpn.* **1988**, *61*, 4470. (d) Sessler, J. L.; Mozattari, A.; Johnson, M. *Org Synth.* **1992**, *70*, 68.

21. (a) Kruper, W. J.; Chamberlin, T. A. *U.S. Patent* 4,746,735, **1987**. (b) Kruper, W. J.; Chamberlin, T. A.; Kochanny, M. *J. Org. Chem.* **1989**, *54*, 2753-2756.

22. (a) Zak, J.; Yuan, H.; Ho, M.; Woo, L. K.; Porter, M. D. *Langmuir*, **1993**, *9*, 2772-2774. (b) Yuan, H.; Woo, L. K., manuscript in preparation.

23. Kufrevich, S. V.; Ali, H.; van Lier, J. E. *J. Chem. Soc., Perkin Trans. 1*, **1994**, 2767-2774.

24. (a) Collman, J. P.; Gagne, R. R.; Halbert, T. R.; Marchon, J. C.; Reed, C. A. *J. Am. Chem. Soc.* **1973**, *95*, 7878. (b) Collman, J. P.; Brauman, J. I; Collins, T. J.; Iverson, B. L.; Land, G.; Pettman, R. B.; Sessler, J. L.; Waters, M. A. *J. Am. Chem. Soc.* **1983**, *105*, 3083. (c) Collman, J. P.; Brauman, J. I; Fitzgerald, J. P.; Hampton, P. D.; Naruta, Y.; Sparapany, J. W.; Ibers, J. A. *J. Am. Chem. Soc.* **1988**, *110*, 3477.

25. Baldwin, J. E.; Cameron, J. H.; Crossley, M. J.; Dagley, I. J.; Hall, S. R.; Klose, T. J. *J. Chem. Soc., Dalton Trans.* **1984**, 1739.

26. Battersby, A. R.; Hartley, S. G.; Turnbull, M. D. *Tetrahedron Lett.* **1978**, *32*, 3169.

27. (a) Gerothanassis, I. P.; Loock, B.; Momenteau, M. *J. Chem. Soc., Chem. Commun.*, **1992**, 598. (b) Momenteau, M.; Loock, B.; Tetreau, C.; Lavalette, D.; Croisy, A.; Schaeffer, C.; Huel, C.; Lhoste, J. M. *J. Chem. Soc., perkin Trans. 2*, **1987**, 598.

28. (a) Woo, L. K.; Maurya, M. R.; Tolppi, C. J.; Jacobson, R. A.; Yang, S.; Rose, E. *Inorg. Chim. Acta* **1991**, *182*, 41. (b) Woo, L. K.; Maurya, M. R. *Inorg. Chem.* **1991**, *30*, 4671. (c) Woo, L. K.; Maurya, M. R.; Jacobson, R. A.; Yang, S.; Ringrose, S. L. *Inorg. Chem.* **1992**, *31*, 913. (d) Woo, L. K.; Maurya, M. R. *Inorg. Chim. Acta* **1993**, *212*, 337-340.

29. *Porphyrins and metalloporphyrins*; Smith, K. D., ed,; Elsevier: New York, 1975.

30. Kim, J. B.; Adler, A. D.; Longo, F. R. In *The Porphyrins*; Dolphin, D., Ed.; Academic Press: London, **1978**, Vol. I.

31. Paine, J. B. In *The Porphyrins*; Dolphin, D., Ed.; Academic Press: London, **1978**, Vol. I.

32. Johnson, A. W. In *The Porphyrins*; Dolphin, D., Ed.; Academic Press: London, **1978**, Vol. I.

33. Adler, A. D.; Sklar, L.; Longo, F. R.; Finarelli, J. D.; Finarelli, M. G. *J. Heterocyclic Chem.* **1968**, *5*, 669-678.

34. (a) Dimago, S. G.; Lin, V. S.-Y.; Therien, M. J. *J. Am. Chem. Soc.* **1993**, *115*, 2513-2515. (b) Dimago, S. G.; Lin, V. S.-Y.; Therien, M. J. *J. Org. Chem.* **1993**, *58*, 5983-5993. (c) Lin, V.S.-Y.; Dimago, S. G.; Therien, M. J. *Science (Washington, D.C.)* **1994**, *264*, 1105-1111.

35. Boyle, R. W.; Johnson, C. K.; Dolphin, D. *J. Chem. Soc., Chem. Commun.*, **1995**, 527-528.

36. Ali, H.; Van Lier, J. E. *Tetrahedron*, **1994**, *50*, 11933-11944.

37. (a) Chan, K. S.; Zhou, X.; Lou, B.-S.; Mak, T. C. W. *J. Chem. Soc., Chem. Commun.*, **1994**, 271-272. (b) Zhou, X.; Zhou, Z.-Y.; Mak, T. C. W.; Chan, K. S. *J. Chem. Soc., Perkin Trans. 1*, **1994**, 2519-20.

38. (a) Oh-e, T.; Miyaura, N.; Suzuki, A. *J. Org. Chem.*, **1993**, *58*, 2201. (b) Suzuki, A. *Pure Appl. Chem.*, **1994**, *68*, 213.

39. Prathapa, S.; Johnson, T.; Lindsey, J. S. *J. Am. Chem. Soc.* **1993**, *115*, 7519-7520.

40. Anderson, H. L.; Sanders, J. K. M. *J. Chem. Soc., Chem. Commun.* **1989**, 1714-15.

41. Anderson, H. L.; Sanders, J. K. M. *Angew. Chem. Int. Ed. Engl.* **1990**, *29*, 1400-1404.

42. Anderson, S.; Anderson, H. L.; Sanders, J. K. M. *Acc. Chem. Res.* **1993**, *26*, 469-475.

43. Mackay, L. G.; Anderson, H. L.; Sanders, J. K. M. *J. Chem. Soc., Chem. Commun.*, **1992**, 43-44.

44. (a) Walter, C. J.; Sanders, J.K. M. *Angew. Chem. Int. Ed. Engl.* **1995**, *34*, 217-219. (b) Walter, C. J.; Anderson, H. L.; Sanders, J.K. M. J. Chem. Soc., Chem. Commun. **1993**, 458-460.

45. Mackay, L. G.; Wylie, R. S.; Sanders, J. K. M. *J. Am. Chem. Soc.* **1994**, *116*, 3141-3142.

46. (a) Avis, J. M.; Fersht, A. R. *Biochemistry* **1993**, *32*, 5321; Johnson, K.; Allemann, R. K.; Widmer, H.; Benner, S. A. *Nature (London)* **1993**, *365*, 530.

CHAPTER 2: SYNTHESIS AND CHARACTERIZATION OF THIOL-DERIVATIZED PORPHYRIN AND METALLOPORPHYRIN COMPLEXES

A paper to be submitted to *Tetrahedron*

Hongping Yuan and L. Keith Woo*[1]

Abstract

A series thiol-derivatized porphyrins and the corresponding Co and Zn complexes were synthesized from 5-(*p*-aminophenyl)-10,15,20-triphenylporphyrin (H_2TPP-NH_2), and 5α,15α-bis(*o*-aminophenyl)porphyrin (H_2DPE-$(NH_2)_2$). These derivatized porphyrins have a different number of thiol appendages attached via amide linkages at different locations. The thiol-derivatized porphyrins made from H_2TPP-NH_2, H_2TPP-NHC(O)$(CH_2)_n$SH (n = 2, 4, 5, 10), have one alkyl-thiol appendage attached to the porphyrin through an amide linkage on the *p*-aminophenyl position. The derivatives made from H_2DPE-$(NH_2)_2$ have two alkyl-thiol appendages attached to the porphyrin through amide linkages on the *o*-aminophenyl positions on the same face of the porphyrin ring. These thiol-derivatized porphyrins are important adsorbates for the preparation of thiol-porphyrin monolayers on gold.

Introduction

Thiol-derivatized porphyrins have been studied as model systems for cytochrome P-450.[2] Recently, thiol-derivatized porphyrins have captured attention in the application of porphyrin monomolecular layers on gold surfaces and the study of the electrocatalytic properties of the these monolayers.[3,4] A key feature in these studies was the design of derivatized porphyrins in which the numbers and locations of alkyl thiol appendages on the porphyrin ring could be manipulated readily.

The aldehyde-pyrrole condensation reaction can not be used to directly prepare these compounds since the thiol group is incompatible with the normal procedures for porphyrin synthesis.[5] Thiol-derivatized porphyrins must be synthesized indirectly by attaching a functional group to the porphyrin and subsequently converting it into a thiol.

We report here the full details for the preparation of thiol-derivatized porphyrins and metalloporphyrins in which only one specific isomer is present. The pure atropisomer, 5α,15α-bis(*o*-aminophenyl)porphyrin (H_2DPE-$(NH_2)_2$), was used as a starting material. Also mono thiol-derivatized porphyrins with two, four, five and ten methylene units in the thiol appendage were synthesized and characterized.

Experimental

General All reagents were analytical grade. CH_2Cl_2 and $CHCl_3$ were distilled from CaH_2. All the NMR solvents were dried with molecular sieves. Literature procedures were used to prepare 6-(tritylthio)hexanoic acid, 6-(tritylthio)hexanoyl

chloride,[2] 5-(*o*-aminophenyl)-10,15,20-triphenylporphyrin (H_2TPP-NH_2) (**1**),[6] and 5α,15α-bis(*o*-aminophenyl)-2,8,12,18-tetraethyl-3,7,13,17-tetramethylporphyrin, or aminodiphenyletioporphyrin H_2DPE-$(NH_2)_2$ (**2**).[7] The acylating reagents 3-(tritylthio)-propionyl chloride and 11-(trirylthio)undecanoyl chloride were prepared from the corresponding acid by standard methods[8] and used *in situ*.

UV-visible data were obtained using a Hewlett-Packard HP 8452A diode-array spectrophotometer. ^{1}H NMR spectra were recorded on a Nicolet NT300 spectrometer or on a Varian VXR 300-MHz spectrometer. IR spectra were recorded from KBR pellets on a BIO-RAD Digilab FTS-7 spectrometer. Elemental analyses were performed by Atlantic Microlabs, Norcross, Georgia.

Preparations

3-(tritylthio)propionic acid ($Ph_3CSCH_2CH_2COOH$). 3-Mercaptopropionic acid (0.53 g, 5.0 mmol) and triphenyl methanol (1.30 g, 5.00 mmol) were dissolved by gentle shaking in trifluoroacetic acid (9.0 mL). The clear solution was set aside for 15 minutes at ambient temperature and the trifluoroacetic acid was removed under reduced pressure. The residue was washed with water and dried in vacuo to produce 1.65 g of white solid (mp 150-151 °C, 90%). ^{1}H NMR ($CDCl_3$, ppm): 10.15 (bs, 1H, COO*H*), 7.42-7.14 (m, 15H, C_6H_5), 2.44 (t, 2H, J = 7.2 Hz, -CH_2-), 2.22 (t, 2H, J = 7.2 Hz, -CH_2-).

11-(tritylthio)undecanoic acid. Trityl mercaptan (5.4 g, 20 mmol) was dissolved in 100 mL of H_2O and EtOH (1:1, v/v) in a 250-mL, three-necked flask fitted with a gas

inlet. After the system had been flushed with N_2, K_2CO_3 (2.76 g, 20.0 mmol) was added, and the mixture was stirred until gas evolution had ceased (about 2 hours). A solution of 11-bromoundecanoic acid (3.96 g, 15.0 mol) and K_2CO_3 (2.07 g, 15.0 mol) in 50 mL of H_2O and EtOH (1:1, v/v) was added, and the resulting mixture was heated at reflux for 12 hours. The solution was cooled to ambient temperature and the pH of the solution was adjusted to 6 by adding concentrated hydrochloric acid, resulting in the precipitation of a small amount of a yellow solid. The slurry was transferred to a separatory funnel and extracted with CH_2Cl_2 (3 x 50 mL). The organic fractions were combined and washed with H_2O (2 x 100 mL) and brine (2 x 100 mL). After drying the solution over $MgSO_4$ and filtering, solvent was removed under reduced pressure to produce a yellow oil. Recrystallization of the product from CH_2Cl_2/hexane gave a yellow crystalline material: mp 68-69 °C, yield 5.90 g (86%). ^{1}H NMR ($CDCl_3$, ppm): 10.1 (bs, 1H, COO*H*), 7.41-7.16 (m, 15H, C_6H_5), 2.33 (t, 2H, J = 7.5 Hz, -CH_2-), 2.11 (t, 2H, J = 7.2 Hz, -CH_2-), 1.61 (m, 2H, -CH_2-), 1.40-1.1 (m, 14H, -CH_2-).

***meso*-{*p*-[3-(Tritylthio)propionamido]phenyl}triphenylporphyrin, H_2TPP-NHC(O)$(CH_2)_2$SCPh$_3$ (3).** The aminophenylporphyrin H_2TPP-NH_2, **1**, (315 mg, 0.500 mmol) was dissolved in 50 mL of CH_2Cl_2 containing 0.5 mL of pyridine. To this mixture was added a solution of 3-(tritylthio)propionyl chloride (385 mg, 1.05 mmol) in CH_2Cl_2 (50 mL). The mixture was stirred at ambient temperature for 12 h and quenched with 10% NH_4OH (100 mL). The organic layer was removed and the aqueous phase was extracted with CH_2Cl_2 (3 x 20 mL). The combined organic fractions were washed with

1M NaOH solution (1 x 100 mL), saturated NaCl solution (2 x 100 mL), and water (2 x 100 mL), dried over $MgSO_4$, filtered, and evaporated to dryness. The residue was eluted from a silica gel flash column (25 x 2.5 cm) with CH_2Cl_2. The first band was collected. Solvent was removed under reduced pressure to yield 400 mg of purple powder (87%). A slight amount of contamination with $Ph_3CSCH_2CH_2CO_2H$ often occurs but does not interfere with subsequent reactions. Silica TLC analysis shows one spot in: CH_2Cl_2, CH_2Cl_2/hexane (1:1) and $CHCl_3$. ^1H NMR (CD_2Cl_2, ppm): 8.86 (m, 8H, β-pyrrole H), 8.22 (d, 6H, J = 6.0 Hz, phenyl-H_o), 8.16 (d, 2H, J = 7.8 Hz, aminophenyl-H_o), 7.87 (d, 2H, J = 7.8 Hz, aminophenyl-H_m), 7.79 (m, 9H, phenyl-$H_{m,p}$), 7.55-7.20 (m, 16H, trityl, N*H*CO), 2.70 (t, 2H, J = 6.9 Hz, -CH_2-), 2.34 (t, 2H, J = 6.9 Hz, -CH_2-), -2.77 (s, 2H, internal pyrrole H). IR (KBr): ν_{CO} = 1695 cm^{-1} (broad). UV-vis (CH_2Cl_2, nm): 420 (Soret), 516, 552, 592, 648.

***meso*-[*p*-(5-Bromopentanamido)phenyl]triphenylporphyrin, H_2TPP-NHC(O)$(CH_2)_4$Br (4).** Aminophenylporphyrin **1** (250 mg, 0.400 mmol) was dissolved in 100 mL of CH_2Cl_2. A solution of 5-bromovaleryl chloride (200 mg, 1.00 mmol) and pyridine (0.5 mL) in 50 mL CH_2Cl_2 was added and the resulting mixture was stirred at ambient temperature for 8 h. After quenching the reaction with 10% NH_4OH (80 mL), the organic phase was separated, washed with saturated NaCl solution, dried by $MgSO_4$, and filtered. Solvent was removed under reduced pressure and the residue was recrystallized from CH_2Cl_2/ether/hexane to give 275 mg of **4** (87%). Silica TLC analysis shows one spot in: CH_2Cl_2, CH_2Cl_2/hexane (1:1) and $CHCl_3$. ^1H NMR ($CDCl_3$, ppm):

8.82 (m, 8H, β-H), 8.18 (m, 8H, phenyl-H_o, aminophenyl-H_o), 7.89 (d, 2H, J = 8.1 Hz, aminophenyl-H_m), 7.75 (m, 9H, phenyl-$H_{m,p}$), 7.45 (s, 1H, N*H*CO), 3.53 (t, 2H, J = 6.0 Hz, -CH_2-), 2.56 (t, 2H, J = 6.8 Hz, -CH_2-), 2.04 (m, 4H, -CH_2-), -2.79 (s, 2H, internal N*H*). UV-vis (CH_2Cl_2, nm): 420 (Soret), 516, 552, 592, 648. MS{EI} Calcd. (found) m/e: 792.78 (793.6) $[MH]^+$.

***meso*-[*p*-[(5-tritylthio)pentanamido]phenyl]triphenylporphyrin, H_2TPP-NHC(O)$(CH_2)_4$SCPh$_3$ (5).** Trityl mercaptan (550 mg, 2.00 mmol), H_2TPP-NHC(O)$(CH_2)_4$Br, **4**, (160 mg, 0.200 mmol), and K_2CO_3 (300 mg, 2.20 mmol) were mixed in 100 mL acetonitrile and the mixture was stirred at ambient temperature for 12 h under N_2. To this solution, water (100 mL) and CH_2Cl_2 (100 mL) were added. The organic phase was separated, washed with water (3 x 100 mL), and dried over $MgSO_4$. The solvent was removed under reduced pressure and the residue was eluted down a silica flask column (25 cm x 2.5 cm) with CH_2Cl_2. The first band was collected and taken to dryness under reduced pressure to yield 130 mg (66%) of **5**. Silica TLC analysis shows one spot in: CH_2Cl_2, CH_2Cl_2/hexane (1:1) and $CHCl_3$. ^{1}H NMR (CD_2Cl_2, ppm): 8.88 (m, 8H, β-H), 8.22 (d, 6H, J = 4.5 Hz, phenyl-H_o), 8.15 (d, 2H, J = 8.0 Hz, aminophenyl-H_o), 7.89 (d, 2H, J = 8.0 Hz, aminophenyl-H_m), 7.78 (m, 9H, phenyl-$H_{m,p}$), 7.56 (s, 1H, N*H*CO), 7.50-7.15 (m, 15H, trityl), 3.54 (t, 2H, J = 6.2 Hz, -CH_2-), 2.50 (t, 2H, J = 6.8 Hz, -CH_2-), 2.05 (m, 4H, -CH_2-), -2.79 (s, 2H, internal N*H*). IR (KBr): ν_{CO} = 1668 and 1695 cm^{-1}. UV-vis (CH_2Cl_2, nm): 420 (Soret), 516, 552, 592, 648.

***meso*-{*p*-[(Tritylthio)hexanamido]phenyl}triphenylporphyrin, H_2TPP-NHC(O)$(CH_2)_5SCPh_3$ (6).** This compound was prepared from aminophenylporphyrin **1** (220 mg, 0.350 mmol) and 6-(tritylthio)hexanoyl chloride (385 mg, 1.05 mmol) according to the same procedure for the preparation of H_2TPP-NHC(O)$(CH_2)_2SCPh_3$, **3**. Silica TLC analysis shows one spot in: CH_2Cl_2 (R_f = 0.65), CH_2Cl_2/hexane (1:1) and $CHCl_3$. Yield: 300 mg (85%). ^{1}H NMR (CD_2Cl_2, ppm): 8.87 (m, 8H, β-H), 8.22 (m, 6H, phenyl-H_o), 8.15 (d, 2H, J = 8.4 Hz, aminophenyl-H_o), 7.86 (d, 2H, J = 8.4 Hz, aminophenyl-H_m), 7.77 (m, 9H, phenyl-$H_{m,p}$), 7.46 (d, 6H, J = 7.2 Hz, trityl-H_o), 7.35-7.21 (m, 10H, trityl-$H_{m,p}$, N*H*CO), 2.40 (t, 2H, J = 7.4 Hz, -CH_2-), 2.23 (t, 2H, J = 7.1 Hz, -CH_2-), 1.70 (m, 2H, -CH_2-), 1.48 (m, 4H, -CH_2-), -2.82 (s, 2H, internal N*H*). IR (KBr): ν_{CO} = 1695 cm^{-1} (broad). UV-vis (CH_2Cl_2, nm): 420 (Soret), 516, 552, 592, 648.

***meso*-{*p*-[(Tritylthio)undecanamido]phenyl}triphenylporphyrin, H_2TPP-NHC(O)$(CH_2)_{10}SCPh_3$ (7).** This compound was prepared from aminophenylporphyrin **1** (250 mg, 0.400 mmol) and $Ph_3CS(CH_2)_{10}C(O)Cl$ (410 mg, 0.800 mmol) by the method used for the preparation H_2TPP-NHC(O)$(CH_2)_2SCPh_3$, **3**. Yield: 350 mg (82%). Silica TLC analysis shows one spot in: CH_2Cl_2, CH_2Cl_2/hexane (1:1) and $CHCl_3$. ^{1}H NMR (CD_2Cl_2, ppm): 8.87 (m, 8H, β-H), 8.22 (d, 6H, J = 6.3 Hz, phenyl-H_o), 8.17 (d, 2H, J = 8.1 Hz, aminophenyl-H_o), 7.92 (d, 2H, J = 8.1 Hz, aminophenyl-H_m), 7.79 (m, 9H, phenyl-$H_{m,p}$), 7.55 (s, 1H, N*H*CO), 7.43-7.19 (m, 15H, trityl), 2.49 (t, 2H, J = 7.5 Hz, -CH_2-), 2.16 (t, 2H, J = 7.2 Hz, -CH_2-), 1.80 (m, 2H, -CH_2-), 1.40-1.15 (m, 14H, -CH_2-), -2.83 (s, 2H, internal N*H*). UV-vis (CH_2Cl_2, nm): 418 (Soret), 514, 550, 590, 646.

***meso*-[*p*-(3-Mercaptopropionamido)phenyl]triphenylporphyrin, H_2TPP-NHC(O)$(CH_2)_2$SH (8).** H_2TPP-NHC(O)$(CH_2)_2SCPh_3$, **3**, (96 mg, 0.10 mmol) and mercuric acetate (105 mg, 0.330 mmol) were placed in a 250-mL side-arm, round-bottomed flask. Under a stream of argon, CH_2Cl_2 (50 mL) and absolute EtOH (50 mL) were added and the mixture was stirred at ambient temperature for 4 h. Over this time, the solution turned dark green in color. Hydrogen sulfide was then bubbled through the mixture at a moderate rate for 0.5 hour and the mixture was stirred for another hour under a H_2S atmosphere. The murky brown suspension was filtered through a Celite pad and rinsed with CH_2Cl_2 to remove precipitated HgS. The solution was washed with saturated NaCl solution (2 x 200 mL), dried over $MgSO_4$, filtered, and evaporated to dryness under reduced pressure to produce a purple oil. The residue was eluted down a silica gel column (25 x 2.5 cm) by CH_2Cl_2. The first band was collected and dried under reduced pressure. The product was isolated as a black-purple powder (40 mg, yield = 56%). Silica TLC analysis shows one spot in: CH_2Cl_2, CH_2Cl_2/hexane (1:1) and $CHCl_3$. ^{1}H NMR ($CDCl_3$, ppm): 8.83 (s, 8H, β-H), 8.18 (m, 8H, phenyl-H_o, aminophenyl-H_o), 7.89 (d, 2H, J = 8.1 Hz, aminophenyl-H_m), 7.75 (m, 9H, phenyl-$H_{m,p}$), 7.57 (s, 1H, N*H*CO), 3.03 (dt, 2H, J = 8.4, J = 6.2 Hz, -C*H*$_2$-SH), 2.84 (t, 2H, J = 6.2 Hz, -C*H*$_2$-), 1.84 (t, 1H, J = 8.4 Hz, S*H*), -2.80 (s, 2H, internal N*H*). UV-vis (CH_2Cl_2, nm): 418 (Soret), 514, 550, 588, 644.

***meso*-[*p*-(5-Mercaptopentamido)phenyl]triphenylporphyrin, H_2TPP-NHC(O)$(CH_2)_4$SH (9).** This compound was synthesized according to the procedure for

H_2TPP-NHC(O)$(CH_2)_2$SH, **8** except that H_2TPP-NHC(O)$(CH_2)_4SCPh_3$, **5**, (98 mg, 0.10 mmol) was used in the place of H_2TPP-NHC(O)$(CH_2)_2SCPh_3$, **3**. Yield: 49 mg (65%). Silica TLC analysis shows one spot in: CH_2Cl_2, CH_2Cl_2/hexane (1:1) and $CHCl_3$. ^{1}H NMR ($CDCl_3$, ppm): 8.87 (m, 8H, β-H), 8.22 (m, 6H, phenyl-H_o), 8.16 (d, 2H, J = 8.2 Hz, aminophenyl-H_o), 7.90 (d, 2H, J = 8.2 Hz, aminophenyl-H_m), 7.79 (m, 9H, phenyl-$H_{m,p}$), 7.57 (s, 1H, N*H*CO), 3.55 (t, 2H, J = 6.2 Hz, -CH_2-), 2.52 (t, 2H, J = 6.0 Hz, -CH_2-), 2.02 (m, 4H, -CH_2-), -2.81 (s, 2H, internal N*H*). The SH resonance was not observed. IR (KBr): ν_{CO} = 1660 cm^{-1} (broad). UV-vis (CH_2Cl_2, nm): 420 (Soret), 516, 552, 588, 646. MS{EI} Calcd. (found) m/e: 745.94 (745.9) $[M]^+$.

***meso*-[*p*-(6-Mercaptohexanamido)phenyl]triphenylporphyrin, H_2TPP-NHC(O)$(CH_2)_5$SH (10).** The same procedure for synthesizing H_2TPP-NHC(O)$(CH_2)_2$SH, **8** was adopted, using H_2TPP-NHC(O)$(CH_2)_5SCPh_3$, **6**, (150 mg, 0.150 mmol) in place of H_2TPP-NHC(O)$(CH_2)_2SCPh_3$, **3**. Yield: 96 mg (84%). Silica TLC analysis shows one spot in: CH_2Cl_2 (R_f = 0.55), CH_2Cl_2/hexane (1:1) and $CHCl_3$. ^{1}H NMR ($CDCl_3$, ppm): 8.83 (m, 8H, β-H), 8.20 (d, 6H, J = 6.4 Hz, phenyl-H_o), 8.15 (d, 2H, J = 8.2 Hz, aminophenyl-H_o), 7.89 (d, 2H, J = 8.2 Hz, aminophenyl-H_m), 7.74 (m, 9H, phenyl-$H_{m,p}$), 7.43 (s, 1H, N*H*CO), 2.61 (dt, J = 7.8 Hz, J = 7.0 Hz, 2H, -CH_2-SH), 2.53 (t, 2H, J = 7.2 Hz, -CH_2-), 1.88 (m, 2H, -CH_2-), 1.73 (m, 2H, -CH_2-), 1.61 (m, 2H, -CH_2-), 1.40 (t, 1H, J = 7.8 Hz, S*H*), -2.80 (s, 2H, internal N*H*). IR (KBr): ν_{CO} = 1695 cm^{-1} (broad). UV-vis (CH_2Cl_2, nm): 420 (Soret), 516, 552, 588, 646. MS{EI} Calcd. (found) m/e: 759.97 (760.1) $[M]^+$.

***meso*-[*p*-(11-Mercaptoundecanamido)phenyl]triphenylporphyrin, H_2TPP-NHC(O)$(CH_2)_{10}$SH (11).** H_2TPP-NHC(O)$(CH_2)_{10}$SH, **11** was prepared in an analogous manner as H_2TPP-NHC(O)$(CH_2)_2$SH, **8** using H_2TPP-NHC(O)$(CH_2)_{10}SCPh_3$, **7** (107 mg, 0.100 mmol) instead of H_2TPP-NHC(O)$(CH_2)_2SCPh_3$, **3**. Yield: 47 mg (57%). Silica TLC analysis shows one spot in: CH_2Cl_2, CH_2Cl_2/hexane (1:1) and $CHCl_3$. ^{1}H NMR ($CDCl_3$, ppm): 8.82 (br, 8H, β-H), 8.18 (m, 8H, phenyl-H_o, aminophenyl-H_o), 7.90 (d, 2H, J = 7.8 Hz, aminophenyl-H_m), 7.75 (m, 9H, phenyl-$H_{m,p}$), 7.43 (s, 1H, N*H*CO), 2.52 (t, 2H, J = 7.2 Hz, -C*H*$_2$-), 1.86 (m, 2H, -C*H*$_2$-), 1.62-1.20 (m, 16H, -C*H*$_2$-), -2.81 (s, 2H, internal NH). The SH resonance was not observed. UV-vis (CH_2Cl_2, nm): 418 (Soret), 514, 550, 590, 646. MS{EI} Calcd. (found) m/e: 829.38 (829.3) $[M]^+$.

[*meso*-{*p*-[(6-Tritylthio)propionamido]phenyl}triphenylporphyrinato]cobalt(II), Co[TPP-NHC(O)$(CH_2)_2SCPh_3$] (12). H_2TPP-NHC(O)$(CH_2)_2SCPh_3$, **3**, (195 mg, 0.200 mmol) was dissolved in $CHCl_3$ (20 mL) and MeOH (2 mL). A solution of $Co(OAc)_2 \cdot 4H_2O$ (100 mg, 0.400 mmol) and NaOAc (33 mg, 0.40 mmol) dissolved in 5 mL MeOH was added and the reaction was stirred at ambient temperature. After four hours, the mixture was washed with water (3 x 100 mL), dried over $MgSO_4$, and concentrated to 2 mL under reduced pressure. Hexane was added to precipitate red crystals which were filtered, washed with ether, hexane and dried in vacuo (190 mg, yield = 93%). Silica TLC analysis shows one spot in: CH_2Cl_2, $CHCl_3$ and $CHCl_3$/ethyl acetate (5:1). UV-vis (CH_2Cl_2, nm): 412 (Soret), 528.

[*meso*-{*p*-[(6-Tritylthio)hexanamido]phenyl}triphenylporphyrinato]cobalt(II), Co[TPP-NHC(O)(CH_2)$_5$SCPh$_3$] (13). Compound **13** was prepared from H_2TPP-NHC(O)(CH_2)$_5$SCPh$_3$, **6**, (200 mg, 0.200 mmol) and Co(OAc)$_2$·4H_2O (250 mg, 0.400 mmol) by the same method used for the preparation of Co[TPP-NHC(O)(CH_2)$_2$SCPh$_3$], **12**. Yield: 185 mg (87%). Silica TLC analysis shows one spot in: CH_2Cl_2, $CHCl_3$ and $CHCl_3$/ethyl acetate (5:1). IR (KBr): ν_{CO} = 1695 cm^{-1} (broad). UV-vis (CH_2Cl_2, nm): 410 (Soret), 528.

[*meso*-{*p*-[(11-Tritylthio)undecanamido]phenyl}triphenylporphyrinato] cobalt(II), Co[TPP-NHC(O)(CH_2)$_{10}$SCPh$_3$] (14). This complex was prepared from H_2TPP-NHC(O)(CH_2)$_{10}$SCPh$_3$, **7** (220 mg, 0.200 mmol) and Co(OAc)$_2$·4H_2O (250 mg, 0.400 mmol) by the same method used for the preparation of Co[TPP-NHC(O)(CH2)$_2$SCPh$_3$], **12**. Silica TLC analysis shows one spot in: CH_2Cl_2, $CHCl_3$ and $CHCl_3$/ethyl acetate (5:1). Yield: 205 mg (91%). UV-vis (CH_2Cl_2, nm): 412 (Soret), 528, 580.

[*meso*-{*p*-[(6-Tritylthio)hexanamido]phenyl}triphenylporphyrinato]zinc(II), Zn[TPP-NHC(O)(CH_2)$_5$SCPh$_3$] (15). The synthesis of this compound was similar to the procedure used for Co[TPP-NHC(O)(CH_2)$_5$SCPh$_3$], **13**. Zn(OAc)$_2$·2H_2O (220 mg, 1.00 mmol) was used in place of Co(OAc)$_2$·4H_2O. Red crystals were isolated (180 mg, 85%). Silica TLC analysis shows one spot in: CH_2Cl_2 (R_f = 0.60), $CHCl_3$ and CH_2Cl_2/hexane (1:1). ^{1}H NMR (CD_2Cl_2, ppm): 8.93 (m, 4H, β-H), 8.91 (d, 2H, J = 4.6 Hz, β-H), 8.84 (d, 2H, J = 4.6 Hz, β-H), 8.22 (d, 6H, J = 8.0 Hz, phenyl-H_o), 7.95 (d, 2H, J = 8.4 Hz,

aminophenyl-H_o), 7.76 (m, 9H, phenyl-$H_{m,p}$), 7.41 (m, 6H, trityl-H_o), 7.31-7.20 (m, 9H, trityl-$H_{m,p}$), 6.95 (s, 1H, N*H*CO), 6.92 (d, 2H, J = 8.4 Hz, aminophenyl-H_m), 2.11 (t, 2H, J = 7.2 -CH_2-), 1.51 (s, 4H, H_2O), 1.25 (m, 4H, -CH_2-), 1.01 (m, 2H, -CH_2-), 0.86 (m, 2H, -CH_2-). IR (KBr): ν_{CO} = 1655 and 1695 cm^{-1}. UV-vis (CH_2Cl_2 nm): 420 (Soret), 548, 592. Anal. Calcd. (found) for $C_{69}H_{45}N_5OSZn{\cdot}2H_2O$: C, 75.23 (75.44), H, 5.21 (4.78), N, 6.36 (6.62).

{*meso*-[*p*-(3-Mercaptopropionamido)phenyl]triphenylporphyrinato}cobalt(II), Co[TPP-NHC(O)(CH_2)$_2$SH] (16). Compound Co[TPP-NHC(O)(CH_2)$_2$SCPh$_3$], **12** (100 mg, 0.100 mmol) and mercuric acetate (100 mg, 0.320 mmol) were placed in a 250-mL side-arm, round-bottomed flask. Under a stream of argon, CH_2Cl_2 (50 mL) and absolute EtOH (50 mL) were added, and the mixture was stirred at ambient temperature for 4 h. Hydrogen sulfide was then bubbled through the mixture at a moderate rate for 0.5 hour. After stirring for another hour under a H_2S atmosphere, the brown suspension was filtered through a Celite pad, and rinsed with CH_2Cl_2 to remove precipitated HgS. The CH_2Cl_2 solution was washed several times with saturated NaCl solution (2 x 200 mL), dried over $MgSO_4$, and filtered. Solvent was removed under reduced pressure and the residue was recrystallized from CH_2Cl_2/Hexane to produce a brown powder. Yield: 55 mg (71%). Silica TLC analysis shows one spot in: CH_2Cl_2, $CHCl_3$ and $CHCl_3$/ethyl acetate (5:1). UV-vis (CH_2Cl_2, nm): 412 (Soret), 528. MS{EI} Calcd. (found) m/e: 774.22 (774.2) $[M]^+$.

{[*meso*-[*p*-(6-Mercaptohexanamido)phenyl]triphenylporphyrinato}cobalt(II), Co[TPP-NHC(O)(CH_2)$_5$SH] (17). This compound was synthesized by a route analogous to the method used for the preparation of Co[TPP-NHC(O)(CH_2)$_2$SH], **16**. Co[TPP-NHC(O)(CH_2)$_5$SCPh$_3$], **13**, (80 mg, 0.076 mmol) and $Hg(OAc)_2$ (80 mg, 0.25 mmol) were used. Yield: 45 mg (73%). Silica TLC analysis shows one spot in: CH_2Cl_2, $CHCl_3$ and $CHCl_3$/ethyl acetate (5:1). IR (KBr): ν_{CO} = 1694 cm^{-1} (broad). UV-vis (CH_2Cl_2, nm): 412 (Soret), 526, 580. MS{EI} Calcd. (found) m/e: 816.22 (816.2) $[M]^+$.

{*meso*-[*p*-(11-Mercaptoundecanamido)phenyl]triphenylporphyrinato}cobalt(II), Co[TPP-NHC(O)(CH_2)$_{10}$SH] (18). The compound was prepared from Co[TPP-NHC(O)(CH_2)$_{10}$SCPh$_3$], **14** (170 mg, 0.150 mmol) and $Hg(OAc)_2$ (150 mg, 0.480 mmol) by an analogous method used for the preparation of Co[TPP-NHC(O)(CH_2)$_2$SH], **16**. Yield: 87 mg (66%). Silica TLC analysis shows one spot in: CH_2Cl_2, $CHCl_3$ and $CHCl_3$/ethyl acetate (5:1). UV-vis (CH_2Cl_2, nm): 412 (Soret), 528, 580. MS{EI} Calc. (found) m/e: 886.30 (886.3) $[M]^+$.

[*meso*-[*p*-(6-Mercaptohexanamido)phenyl]triphenylporphyrinato]zinc(II), Zn[TPP-NHC(O)(CH_2)$_5$SH] (19). This complex was prepared from Zn[TPP-NHC(O)(CH_2)$_5$SCPh$_3$], **15** (105 mg, 0.100 mmol) by the same route used for the preparation of Co[TPP-NHC(O)(CH_2)$_2$SH], **16**. Yield: 62 mg (75%). Silica TLC analysis shows one spot in: CH_2Cl_2 (R_f = 0.40), $CHCl_3$ and $CHCl_3$/ethyl acetate (5:1). ^1H NMR ($CDCl_3$, ppm): 8.92 (m, 8H, β-H), 8.19 (d, 6H, J = 6.8 Hz, phenyl-H_o), 8.11 (d, 2H, J = 8.0 Hz, aminophenyl-H_o), 7.75 (m, 11H, phenyl-$H_{m,p}$, aminophenyl-H_m), 7.37 (s,

1H, N*H*CO), 2.54 (dt, J = 8.0 Hz, J = 7.2 Hz, 2H, -C*H*$_2$-SH), 2.28 (m, 2H, -C*H*$_2$-), 1.68 (m, 4H, -C*H*$_2$-), 1.51 (br, 6H, 2H$_2$O, -C*H*$_2$-), 1.37 (t, 1H, J = 8.0, S*H*). IR (KBr): ν_{CO} = 1656 cm^{-1} (broad). UV-vis (CH_2Cl_2, nm): 422 (Soret), 548, 586. MS{EI} Calcd. (found) m/e: 821.22 (821.2) $[M]^+$. Anal. Calcd. (found) for $C_{50}H_{32}N_5OSZn\cdot 2H_2O$: C, 69.88 (69.58), H, 5.04 (4.97), N, 8.15 (7.95).

Bis-[*o*-(3-bromopropionamido)]phenylporphyrin, H_2DPE-[NHC(O)$(CH_2)_2$Br]$_2$ (20). Compound **20** was synthesized from H_2DPE-$(NH_2)_2$, **2**, (330 mg, 0.500 mmol) and 3-bromopropionyl chloride (345 mg, 2.01 mmol) by a method similar to that used for the preparation of H_2TPP-NHC(O)$(CH_2)_4$Br, **4**. Yield: 440 mg (95%). Silica TLC analysis shows one spot in: CH_2Cl_2, $CHCl_3$ and CH_2Cl_2/hexane (1:1). ^{1}H NMR ($CDCl_3$, ppm): 10.29 (s, 2H, *meso*-H), 8.80 (d, 2H, J = 8.1 Hz, phenyl-H_6), 7.88-7.82 (m, 4H, phenyl-$H_{5,3}$), 7.54 (t, 2H, J = 7.2 Hz, phenyl-H_4), 6.93 (s, 2H, N*H*CO), 4.02 (m, 8H, -C*H*$_2$-CH$_3$), 3.05 (t, 4H, J = 6.3 Hz, -C*H*$_2$-), 2.53 (s, 12H, -C*H*$_3$), 1.85 (t, 4H, J = 6.3 Hz, -C*H*$_2$-), 1.77 (t, 12H, J = 7.5 Hz, -CH$_2$-C*H*$_3$), -2.47 (s, 2H, internal N*H*). IR (KBr): ν_{CO} = 1675 cm^{-1} (broad). UV-vis (CH_2Cl_2, nm): 406 (Soret), 506, 542, 574, 626, 656.

5α,15α-Bis-[*o*-(6-bromohexanamido)]phenylporphyrin, H_2DPE-[NHC(O)$(CH_2)_5$Br]$_2$ (21). This compound was synthesized from H_2DPE-$(NH_2)_2$, **2**, (330 mg, 0.500 mmol) and 6-bromohexanoyl chloride (427 mg, 2.00 mmol) by a similar method as described for the preparation of H_2TPP-NHC(O)$(CH_2)_4$Br, **4**. Yield: 450 mg (89%). Silica TLC analysis shows one spot in: CH_2Cl_2, $CHCl_3$ and CH_2Cl_2/hexane (1:1). ^{1}H NMR ($CDCl_3$, ppm): 10.28 (s, 2H, *meso*-H), 8.75 (d, 2H, J = 8.4 Hz, phenyl-H_6),

7.88-7.82 (m, 4H, phenyl-$H_{5,3}$), 7.52 (t, 2H, J = 7.2 Hz, phenyl-H_4), 6.84 (s, 2H, N*H*CO), 4.04 (m, 8H, -CH_2-CH_3), 2.58 (t, 4H, J = 6.6 Hz, -CH_2-), 2.53 (s, 12H, -CH_3), 1.77 (t, 12H, J = 7.5 Hz, -CH_2-CH_3), 1.34 (t, 4H, J = 7.2 Hz, -CH_2-), 1.07 (m, 4H, -CH_2-), 0.85 (m, 4H, -CH_2-), 0.62 (m, 4H, -CH_2-), -2.48 (s, 2H, internal N*H*). UV-vis (CH_2Cl_2, nm): 408 (Soret), 506, 540, 574, 626, 658.

Bis-[*o*-(3-tritylthio)propionamido]phenylporphyrin, H_2DPE-[NHC(O)$(CH_2)_2$SCPh_3]$_2$ (22). This compound was prepared from H_2DPE-$(NH_2)_2$, **2**, (220 mg, 0.330 mmol) and 3-(tritylthio)propionyl chloride (730 mg, 2.00 mmol) by the same method used for the preparation of H_2TPP-NHC(O)$(CH_2)_2$SCPh_3, **3**. Yield: 385 mg (87%). Silica TLC analysis shows one spot in: CH_2Cl_2, $CHCl_3$ and CH_2Cl_2/hexane (1:1). ^{1}H NMR (CD_2Cl_2, ppm): 10.24 (s, 2H, *meso*-H), 8.74 (d, 2H, J = 8.1 Hz, phenyl-H_6), 7.78 (m, 4H, phenyl-$H_{5,3}$), 7.47 (t, 2H, J = 7.2 Hz, phenyl-H_4), 6.81 (m, 12H, trityl-H_o), 6.71 (s, 2H, N*H*CO), 6.57-6.42 (m, 18H, trityl-$H_{m,p}$), 4.00 (m, 8H, -CH_2-CH_3), 2.50 (s, 12H, -CH_3), 2.12 (t, 4H, J = 6.9 Hz, -CH_2-), 1.74 (t, 12H, J = 7.6 Hz, -CH_2-CH_3), 1.25 (br, 4H, -CH_2-), -2.35 (s, 2H, internal N*H*). IR (KBr): ν_{CO} = 1695 cm^{-1} (broad). UV-vis (CH_2Cl_2, nm): 402 (Soret), 508, 542, 574, 626, 656.

5α,15α-Bis-[*o*-(6-tritylthio)hexanamido]phenylporphyrin, H_2DPE-[NHC(O)$(CH_2)_5$SCPh_3]$_2$ (23). This compound was synthesized from H_2DPE-$(NH_2)_2$, **2** (220 mg, 0.330 mmol), and 6-(tritylthio)hexanoyl chloride (820 mg, 2.00) by a similar method as described for the preparation of H_2TPP-NHC(O)$(CH_2)_2$SCPh_3, **3**. Yield: 420 mg (90%). Silica TLC analysis shows one spot in: CH_2Cl_2, $CHCl_3$ and CH_2Cl_2/hexane

(1:1). ^{1}H NMR (CD_2Cl_2, ppm): 10.29 (s, 2H, *meso*-H), 8.74 (d, 2H, J = 8.4 Hz, phenyl-H_6), 7.84 (t, 2H, J = 8.1 Hz, phenyl-H_5), 7.81 (d, 2H, J = 7.5 Hz, phenyl-H_3), 7.52 (t, 2H, J = 7.2 Hz, phenyl-H_4), 7.30-7.04 (m, 30H, trityl-H), 6.88 (s, 2H, N*H*CO), 4.04 (m, 8H, -C*H*$_2$-CH$_3$), 2.53 (s, 12H, -C*H*$_3$), 1.77 (t, 12H, J = 7.5 Hz, -CH$_2$-C*H*$_3$), 1.57 (t, 4H, J = 7.2 Hz, -C*H*$_2$-), 1.19 (t, 4H, J = 7.2 Hz, -C*H*$_2$-), 0.60 (m, 8H, -C*H*$_2$-), 0.45 (m, 4H, -C*H*$_2$-), -2.48 (s, 2H, internal N*H*). IR (KBr): ν_{CO} = 1696 cm^{-1} (broad). UV-vis (CH_2Cl_2, nm): 408 (Soret), 506, 540, 574, 626, 658.

5α,15α-Bis-[*o*-(6-mercaptohexanamido)]phenylporphyrin, H_2DPE-[NHC(O)(CH$_2$)$_5$SH]$_2$ (24). Compound **24** was synthesized from H_2DPE-[NHC(O)(CH$_2$)$_5$SCPh$_3$]$_2$, **23** (150 mg, 0.110 mmol) and mercuric acetate (220 mg, 0.680 mmol) by a similar method as described for the preparation of H_2TPP-NHC(O)(CH$_2$)$_2$SH, **8**. Yield: 60 mg (60%). Silica TLC analysis shows one spot in: CH_2Cl_2, $CHCl_3$ and CH_2Cl_2/hexane (1:1). ^{1}H NMR ($CDCl_3$, ppm): 10.28 (s, 2H, *meso*-H), 8.74 (d, 2H, J = 7.8 Hz, phenyl-H_6), 7.81 (m, 4H, phenyl-$H_{5,3}$), 7.52 (t, 2H, J = 7.2 Hz, phenyl-H_4), 6.85 (s, 2H, N*H*CO), 4.02 (m, 8H, -C*H*$_2$-CH$_3$), 2.53 (s, 12H, -C*H*$_3$), 1.77 (t, 12H, J = 6.6 Hz, -CH$_2$-C*H*$_3$), 1.57 (t, 4H, J = 6.0 Hz, -C*H*$_2$-), 1.36 (m, 4H, -C*H*$_2$-), 0.80-0.40 (m, 12H, -C*H*$_2$-), -2.48 (s, 2H, internal NH). IR (KBr): ν_{CO} = 1694 cm^{-1} (broad). UV-vis (CH_2Cl_2, nm): 408 (Soret), 506, 540, 574, 626, 658. MS{FAB} Calcd. (found) m/e: 920.5 (919.5) [M-H]$^+$.

{5α,15α-Bis-[*o*-(6-tritylthio)hexanamido]phenylporphyrinato}cobalt(II), Co{DPE-[NHC(O)(CH$_2$)$_5$SCPh$_3$]$_2$} (25). H_2DPE-[NHC(O)(CH$_2$)$_5$SCPh$_3$]$_2$, **23** (280 mg,

0.200 mmol) was dissolved in $CHCl_3$ (50 mL) and MeOH (5 mL). A solution of $Co(OAc)_2 \cdot 4H_2O$ (200 mg, 0.800 mmol) and NaOAc (33 mg, 0.40 mmol) in 5 mL MeOH was added and the reaction was stirred at ambient temperature. After 4 hours, the mixture was washed with water (3 x 100 mL) and dried over $MgSO_4$. The solution was concentrated to 2 mL under reduced pressure. Hexane was layered over the solution and the mixture was cooled to -20 °C for 6 hours to yield red crystals (175 mg, yield = 60%). Silica TLC analysis shows one spot in: CH_2Cl_2, $CHCl_3$ and $CHCl_3$/ethyl acetate (5:1). UV-vis (CH_2Cl_2, nm): 404 (Soret), 532, 560.

{5α,15α-Bis-[*o*-(6-tritylthio)hexanamido]phenylporphyrinato}zinc(II), Zn{DPE-[NHC(O)$(CH_2)_5$SCPh$_3$]$_2$} (26). This complex was prepared from H_2DPE-[NHC(O)$(CH_2)_5$SCPh$_3$]$_2$, **23** (280 mg, 0.200 mmol) and $Zn(OAc)_2 \cdot 2H_2O$ (176 mg, 0.800 mmol) by the same method used for the preparation of Co{DPE-[NHC(O)$(CH_2)_5$SCPh$_3$]$_2$}, **25**. Red crystals (275 mg, 94%) were isolated. Silica TLC analysis shows one spot in: CH_2Cl_2, $CHCl_3$ and $CHCl_3$/ethyl acetate (5:1). ^{1}H NMR (CD_2Cl_2, ppm): 10.24 (s, 2H, *meso*-H), 8.65 (d, 2H, J = 8.7 Hz, phenyl-H_6), 7.81 (t, 2H, J = 8.1 Hz, phenyl-H_5), 7.64 (d, 2H, J = 7.5 Hz, phenyl-H_3), 7.47 (t, 2H, J = 8.0 Hz, phenyl-H_4), 7.02-6.90 (m, 30 H, trityl-H), 6.79 (s, 2H, N*H*CO), 4.00 (m, 8H, -C*H*$_2$-CH$_3$), 2.49 (s, 12H, -C*H*$_3$), 1.75 (t, 12H, J = 7.5 Hz, -CH$_2$-C*H*$_3$), 1.53 (s, 2H, *H*$_2$O), 1.25 (m, 4H, -C*H*$_2$-), 0.94 (m, 8H, -C*H*$_2$-), 0.49 (m, 4H, -C*H*$_2$-), 0.26 (br, 4H, -C*H*$_2$-). IR (KBr): ν_{CO} = 1663 and 1696 cm^{-1}. UV-vis (CH_2Cl_2, nm): 412 (Soret), 540, 576. Anal. Calcd. (found) for $C_{94}H_{94}N_6O_2S_2Zn \cdot H_2O$: C, 75.91 (75.54), H, 6.51 (6.41), N, 5.65 (5.99).

{5α,15α-Bis-[*o*-(6-mercaptohexanamido)]phenylporphyrinato}cobalt(II), Co{DPE-[NHC(O)(CH_2)$_5$SH]$_2$} (27). This complex was prepared from Co{DPE-[NHC(O)(CH_2)$_5$SCPh$_3$]$_2$}, **25** (150 mg, 0.100 mmol) and $Hg(OAc)_2$ (210 mg, 0.660 mmol) by the same route used for the preparation of H_2DPE-[NHC(O)(CH2)$_5$SH]$_2$, **24**. Yield: 60 mg (61%). Silica TLC analysis shows one spot in: CH_2Cl_2, $CHCl_3$ and $CHCl_3$/ethyl acetate (5:1). IR (KBr): ν_{CO} = 1694 cm^{-1} (broad). UV-vis (CH_2Cl_2, nm): 402 (Soret), 528, 562. MS{FAB} Calcd. (found) m/e: 977.40 (975.4) $[M-2H]^+$.

{5α,15α-Bis-[*o*-(6-mercaptohexanamido)]phenylporphyrinato}zinc(II), Zn{DPE-[NHC(O)(CH_2)$_5$SH]$_2$} (28). Compound **28** was synthesized by the same method used for preparing H_2DPE-[NHC(O)(CH_2)$_5$SH]$_2$, **24** except Zn{DPE-[NHC(O)(CH_2)$_5$SCPh$_3$]$_2$}, **26** (60 mg, 0.040 mmol) replaced DPE-[NHC(O)(CH_2)$_5$SCPh$_3$]$_2$, **23**. Yield: 30 mg (74%). Silica TLC analysis shows one spot in: CH_2Cl_2, $CHCl_3$ and $CHCl_3$/ethyl acetate (5:1). ^{1}H NMR (CD_2Cl_2, ppm): 10.21 (s, 2H, *meso*-H), 8.66 (d, 2H, J = 8.4 Hz, phenyl-H_6), 7.82 (m, 4H, phenyl-$H_{5,3}$), 7.50 (t, 2H, 7.5 Hz, phenyl-H_4), 6.90 (s, 2H, N*H*CO), 4.00 (m, 8H, -C*H*$_2$-CH$_3$), 2.48 (s, 12H, -C*H*$_3$), 1.76 (t, 12H, J = 7.1 Hz, -CH$_2$-C*H*$_3$), 1.51 (s, 2H, *H*$_2$O), 1.30 (t, 4H, J = 6.6 Hz, -C*H*$_2$-), 1.12 (t, 4H, J = 6.6 Hz, -C*H*$_2$-), 0.84 (m, 4H, -C*H*$_2$-), 0.56 (m, 4H, -C*H*$_2$-), 0.29 (m, 4H,-C*H*$_2$-). IR (KBr): ν_{CO} = 1663 and 1696 cm^{-1}. UV-vis (CH_2Cl_2, nm): 412 (Soret), 542, 576. Anal. Calcd. (found) for $C_{56}H_{66}N_6O_2S_2 \cdot H_2O$: C, 67.08 (67.11), H, 6.85 (7.10), N, 8.38 (8.36). MS{FAB} Calcd. (found) m/e: 982.40 (982) $[M]^+$.

Results

Synthesis and characterization of mono thiol-derivatized porphyrins

Porphyrins with a single thiol-appendage can be synthesized readily from 5-(*p*-aminophenyl)-10,15,20-triphenylporphyrin (H_2TPP-NH_2), **1**. Two convenient synthetic routes are shown in Scheme 1. Alkylation of H_2TPP-NH_2 with $Ph_3CS(CH_2)_nC(O)Cl$ produces an appended porphyrin with the thiol protected by a trityl group. Removal of the trityl group by treatment with $Hg(OAc)_2$ and H_2S generates the final mono thiol-derivatized porphyrin in good yields (60-85 % isolated yields). Alternatively, the treatment of aminophenylporphyrin, **1**, with $Br(CH_2)_nC(O)Cl$ produced bromo-tailed porphyrins which could be converted into the trityl-protected thiol porphyrins with Ph_3CSH in the presence of K_2CO_3.

The resulting mono thiol-derivatized porphyrins were characterized by ^{1}H NMR, UV-vis (Table 1), and MS. The free base porphyrins H_2TPP-$NHC(O)(CH_2)_nSH$ (n = 2, **8**; n = 4, **9**; n =5, **10**; n = 10, **11**) and Zn(II) metalloporphyrin, Zn[TPP-$NHC(O)(CH_2)_5SH$], **19**, have easily assignable proton NMR spectra. The β-pyrrole protons are split into multiplets and appear at 8.8 to 9.0 ppm. The phenyl protons appears at 7.5 to 8.3 as doublets and multiplets, and the methylene proton signals resonate at 1.0 to 4.0 ppm. The thiol proton is observed by ^{1}H NMR in many of these compounds. Assignments of these resonances were confirmed with D_2O-exchange experiments. For example, in H_2TPP-$NHC(O)(CH_2)_2SH$, **8**, the thiol proton appears as a triplet at 1.84 ppm. On treatment with D_2O, this signal, as well as peaks at 7.57 ppm (N*H*CO) and -2.81 ppm

(internal N*H*) disappear. The corresponding Co(II) metalloporphyrins **16**, **17**, **18** have very broad NMR resonances which are difficult to assign because of the paramagnetism of the complex. The solid state IR spectrum of H_2TPP-NHC(O)$(CH_2)_n$SH (n = 4, **9**; n = 5, **10**) exhibits an amide carbonyl stretch at 1660 cm^{-1} (broad) for **9**, and 1695 cm^{-1} (broad) for **10**. The Co(II) complex Co[TPP-NHC(O)$(CH_2)_5$SH], **17** shows a carbonyl stretch at 1694 cm^{-1} (broad), and the Zn(II) complex Zn[TPP-NHC(O)$(CH_2)_5$SH], **19**, exhibits a carbonyl stretch at 1656 cm^{-1} (broad). Satisfactory parent ions in the MS were observed for all the thiol-derivatized porphyrins.

Changing the number of methylene units in the alkyl linkage from two to ten results in insignificant electronic perturbation on the porphyrin ring. In the UV-vis spectra, all the free base mono thiol-derivatized porphyrins have very similar absorption bands compared to that of the parent aminophenylporphyrin **1**. The Soret bands for H_2TPP-NHC(O)$(CH_2)_n$-SH range from 418 nm (n = 2, 10) to 420 nm (n = 4, 5).

Pure mono thiol-tail porphyrins are odorless brown-purple solids, and are soluble in organic solvents such as CH_2Cl_2, $CHCl_3$, acetone, C_6H_6, and toluene, but are not soluble in MeOH, EtOH, ether and hexane. They are mildly sensitive to the combination of light and air. When organic solutions of these compounds are exposed to air, decomposition occurs over a period of a few months. Thus, these thiol-tail porphyrins are best stored in the solid state under an inert atmosphere in the dark. Under these conditions, they are stable for years.

Scheme 1

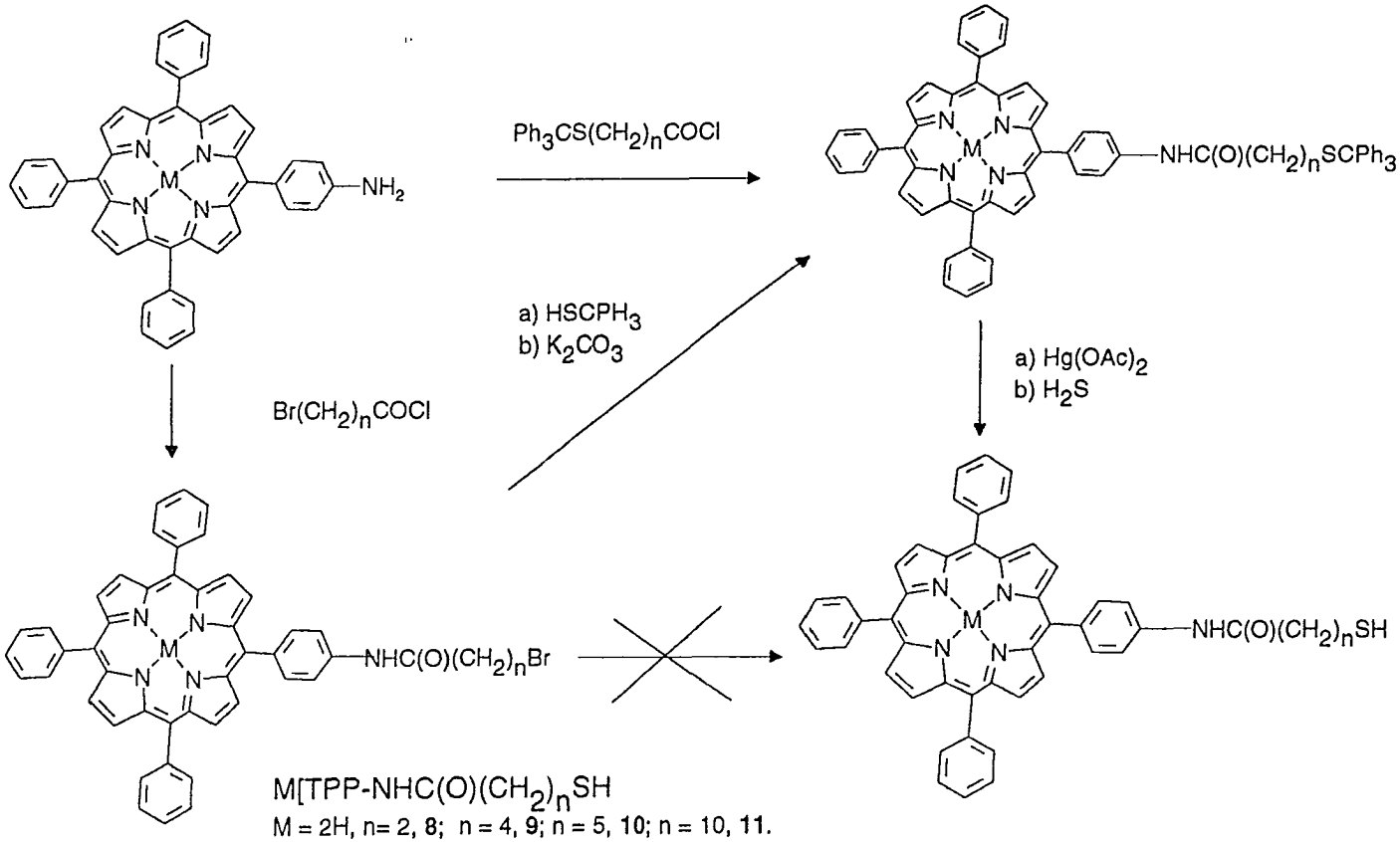

M = 2H, n= 2, **8**; n = 4, **9**; n = 5, **10**; n = 10, **11**.
M= Co, n = 2, **16**; n = 5 , **17**; n = 10, **18**. M = Zn, n = 5, **19**.

Table 1. UV for mono thiol-derivatized porphyrins (nm)

Porphyrin	UV-Vis nm
$H_2TPP\text{-}NH_2$, **1**	418 (Soret), 516, 552, 592, 648
$H_2TPP\text{-}NHC(O)(CH_2)_2SCPh_3$, **3**	420 (Soret), 516, 552, 592, 648
$H_2TPP\text{-}NHC(O)(CH_2)_4Br$, **4**	420 (Soret), 516, 552, 592, 648
$H_2TPP\text{-}NHC(O)(CH_2)_4SCPh_3$, **5**	420 (Soret), 516, 552, 592, 648
$H_2TPP\text{-}NHC(O)(CH_2)_5SCPh_3$, **6**	420 (Soret), 516, 552, 592, 646
$H_2TPP\text{-}NHC(O)(CH_2)_{10}SCPh_3$, **7**	418 (Soret), 514, 550, 590, 646
$H_2TPP\text{-}NHC(O)(CH_2)_2SH$, **8**	418 (Soret), 514, 550, 588, 644
$H_2TPP\text{-}NHC(O)(CH_2)_4SH$, **9**	420 (Soret), 516, 552, 588, 646
$H_2TPP\text{-}NHC(O)(CH_2)_5\text{-}SH$, **10**	420 (Soret), 516, 552, 588, 646
$H_2TPP\text{-}NHC(O)(CH_2)_{10}\text{-}SH$, **11**	418 (Soret), 514, 550, 592, 646
$Co[TPP\text{-}NHC(O)(CH_2)_2SCPh_3]$, **12**	412 (Soret), 528
$Co[TPP\text{-}NHC(O)(CH_2)_5SCPh_3]$, **13**	410 (Soret), 528
$Co[TPP\text{-}NHC(O)(CH_2)_{10}SCPh_3]$, **14**	412 (Soret), 526, 580
$Zn[TPP\text{-}NHC(O)(CH_2)_5SCPh_3]$, **15**	420 (Soret), 548, 592
$Co[TPP\text{-}NHC(O)(CH_2)_2SH]$, **16**	412 (Soret), 526
$Co[TPP\text{-}NHC(O)(CH_2)_5SH]$, **17**	412 (Soret), 526, 580
$Co[TPP\text{-}NHC(O)(CH_2)_{10}SH]$, **18**	412 (Soret), 528, 580
$Zn[TPP\text{-}NHC(O)(CH_2)_5\text{-}SH]$, **19**	422 (Soret), 548, 586

Synthesis and characterization of bis thiol-derivatized porphyrins

Bis thiol-derivatized porphyrins were prepared from bis(*o*-aminophenyl)porphyrin H_2(DPE-$(NH_2)_2$), **2**, by utilizing the same procedure used for the preparation of mono thiol-derivatized porphyrins. The purified α,α-atropisomers were used. The synthesis of α,α-bis thiol-derivatized porphyrins is shown in Scheme 2. The treatment of α,α-H_2DPE-$(NH_2)_2$ with excess 6-(tritylthio)hexanoyl chloride produced the bis acylated product, H_2DPE-[NHC(O)$(CH_2)_5$S$CPh_3]_2$, **23**. The corresponding Co(II) and Zn(II) complexes, Co{DPE-[NHC(O)$(CH_2)_5$S$CPh_3]_2$}, **25** and Zn{DPE-[NHC(O)$(CH_2)_5$S$CPh_3]_2$}, **26**, were prepared from **23** by treatment with Co(II) and Zn(II) acetate, respectively. UV-vis spectra of the reaction mixtures showed that the four Q bands of **23** collapsed to a two-band pattern (Table 2). Removal of the trityl group by treatment with $Hg(OAc)_2$ and H_2S generated the bis thiol-derivatized porphyrins H_2DPE-[NHC(O)$(CH_2)_5$SH$]_2$, **24**, Co{DPE-[NHC(O)$(CH_2)_5$SH$]_2$} **27**, and Zn{DPE-[NHC(O)$(CH_2)_5$SH$]_2$}, **28**.

Compounds **24** and **28** have easily assignable proton NMR spectra. The *meso*-protons appear at 10.20 to 10.30 ppm as a singlet. The phenyl protons appear at 7.5 to 8.8 ppm as doublets and multiplets. The amide protons resonate at 6.8 to 6.9 ppm and the methylene proton exhibit signals at 0.2 to 1.6 ppm. IR spectra (KBr) of H_2DPE-[NHC(O)$(CH_2)_5$SH$]_2$, **24** and Cn{DPE-[NHC(O)$(CH_2)_5$SH)$]_2$}, **27** present an amide carbonyl stretch at 1694 cm^{-1} (broad). Zn{DPE-[NHC(O)$(CH_2)_5$SH$]_2$}, **28**, shows amide stretches at 1663 and 1696 cm^{-1}. The expected molecular ion peaks are observed in the FAB mass spectra of these three complexes.

Scheme 2

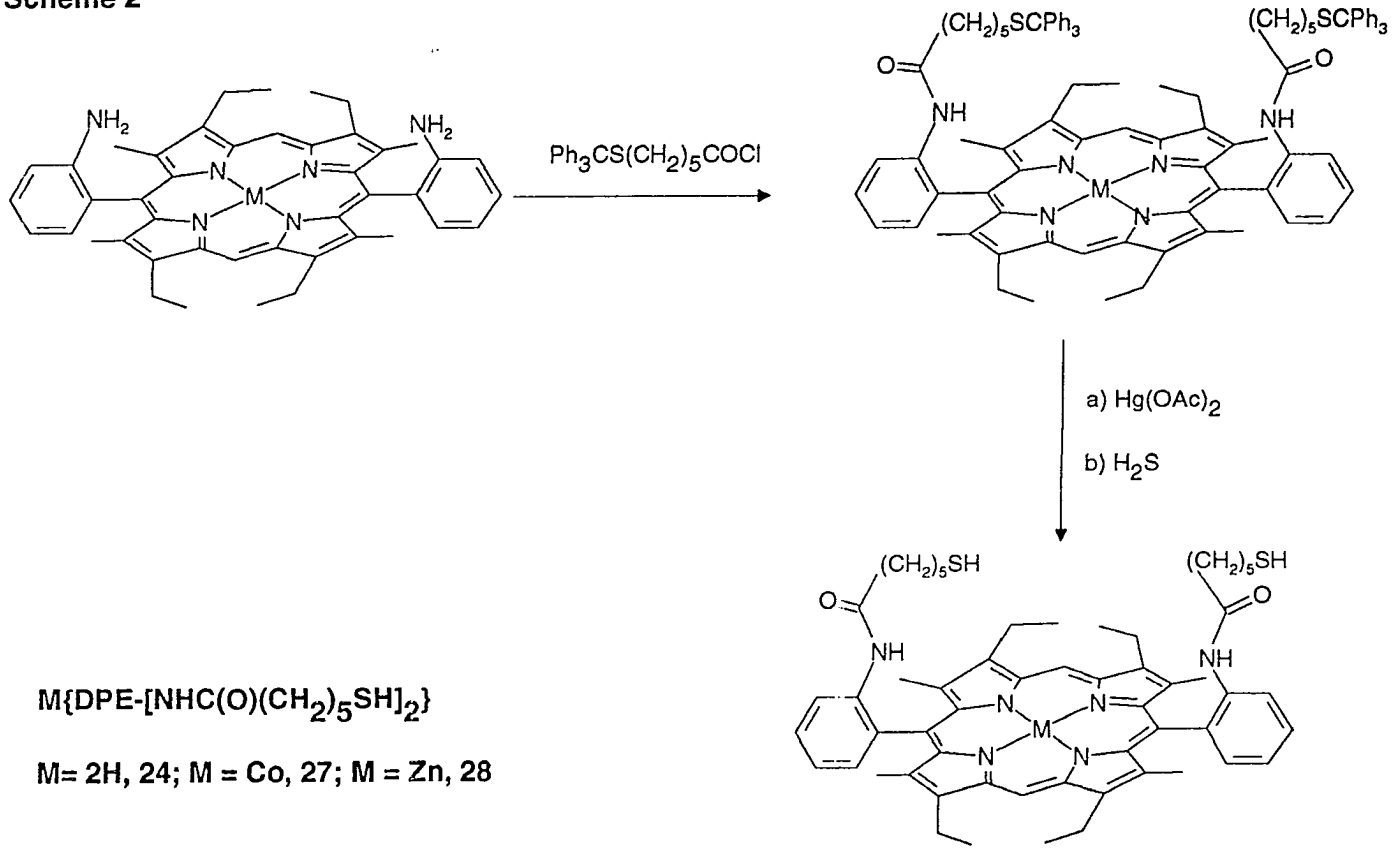

M{DPE-[NHC(O)$(CH_2)_5$SH]$_2$}

M= 2H, 24; M = Co, 27; M = Zn, 28

Table 2. UV for bis and tetra thiol-derivatized porphyrins (nm)

Porphyrin	UV-Vis nm
H_2DPE-$(NH_2)_2$, **2**	408 (Soret), 506, 540, 574, 626, 654
H_2DPE-$[NHC(O)(CH_2)_2Br]_2$, **20**	406 (Soret), 506, 542, 574, 626, 656
H_2DPE-$[NHC(O)(CH_2)_5Br]_2$, **21**	406 (Soret), 506, 540, 574, 626, 658
H_2DPE-$[NHC(O)(CH_2)_2SCPh_3]_2$, **22**	402 (Soret), 508, 542, 574, 626, 656
H_2DPE-$[NHC(O)(CH_2)_5SCPh_3]_2$, **23**	408 (Soret), 506, 540, 574, 626, 658
H_2DPE-$[NHC(O)(CH_2)_5SH]_2$, **24**	408 (Soret), 506, 540, 576, 626, 658
Co{DPE-$[NHC(O)(CH_2)_5SCPh_3]_2$}, **25**	404 (Soret), 532, 560
Zn{DPE-$[NHC(O)(CH_2)_5SCPh_3]_2$}, **26**	410 (Soret), 540, 576
Co{DPE-$[NHC(O)(CH_2)_5SH]_2$}, **27**	402 (Soret), 528, 562
Zn{DPE-$[NHC(O)(CH_2)_5SH]_2$}, **28**	410 (Soret), 540, 578

These bis thiol-tail porphyrins have higher solubility than the mono thiol-tail porphyrins in common organic solvents such as CH_2Cl_2, $CHCl_3$, acetone, C_6H_6, and toluene. They also have limited solubility in ether, hexane and MeOH. The bis thiol-tail porphyrins are less robust than the mono tail analogues. They gradually decompose in solution in a few weeks on exposure to air and light.

Discussion

Self-assembled alkanethiolate monolayers on gold surfaces provide an important method for the modification of electrode surfaces.[9] Studies of electroactive monolayers may lead to the discovery of new catalysts, information storage devices and bio-sensors. We have examined thiol-derivatized porphyrin monolayers on gold[3] and found thiol-derivatized porphyrins form oriented monomolecular coatings on gold surfaces. Gold electrodes that have been chemically modified with cobalt thiol porphyrin exhibit electrocatalytic potencies for the reduction of O_2 which vary as a function of the number and location of the thiol appendages.

For controlling the porphyrin monolayer architecture on the gold surface, we have synthesized mono-, and bis-thiol-tailed porphyrins from 5-(*p*-aminophenyl)-10,15,20-triphenylporphyrin **1** and 5α,15α-bis(*o*-aminophenyl)-porphyrin **2**. The structural integrity of the latter porphyrin is particularly important. The α,α-atropisomer of H_2DPE-$(NH_2)_2$ is nonfluxional and only under prolonged heating at > 100 °C could atropisomerization be observed.[7] The activation energy needed for thermal interconversion of the two isomers

was measured to be 26.2 kcal/mol for the α,α-bis(*o*-aminophenyl)porphyrin, **2**. Consequently, all reactions employed for the preparation of thiol-tailed porphyrins from α,α-DPE-$(NH_2)_2$ were performed at ambient temperature to prevent atropisomerism.

Only a few methods exist for the synthesis of alkyl thiols.[10] Nucleophilic substitution of an alkyl halide by HS^- or H_2S results in the formation of alkane thiols (Scheme 3). Alkane thiols can also be prepared from the treatment of an alkyl halide with thiourea, followed by alkaline workup (Scheme 3).

Scheme 3

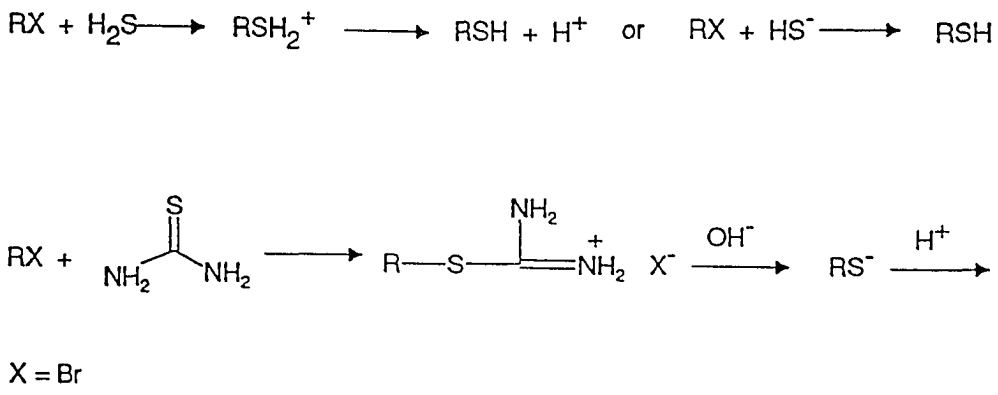

Murray *et al.* reported[4] that the treatment of 5,10,15,20-tetrakis[*o*-(2-bromoethoxy)phenyl]porphyrin with sodium thioacetate in refluxing $CHCl_3/CH_3CH_2OH$ yielded 5,10,15,20-tetrakis[*o*-[(s-acetyl-2-thio)ethoxy]phenyl]porphyrin. Conversion to

5,10,15,20-tetrakis[*o*-(2-thioethoxy)phenyl]porphyrin was accomplished by acidic hydrolysis in CH_3OH/HCl followed by $NaHCO_3$ workup. However, this tetra-thiol tailed product is a mixture of atropisomers.

Attachment of bromo appendages to the aminophenylporphyrins **1** and **2** was accomplished with $Br(CH_2)_nC(O)Cl$ (for mono(*p*-aminophenyl)porphyrin **1**: n = 4; for bis(*o*-aminophenyl)porphyrin **2**: n = 2, 5). However, attempts at converting these bromo-tailed porphyrins to the thiol analogues using methods shown in Scheme 3 resulted in the cleavage of the amide linkages. Consequently, we sought other methods for the preparation of thiol-tailed porphyrins.

In order to circumvent amide cleavage problems, attachment of protected thiol appendages was examined. The trityl group was found to be a good protecting agent for thiols by Hiskey *et al.*[11] Heavy-metal ions such as Hg(II) are efficient regents for removal of this protecting group. Attachment of S-trityl appendages to the aminophenylporphyrins (**1**, and **2**) was accomplished with $Ph_3CS(CH_2)_nC(O)Cl$ under ambient temperature. Alternatively, the treatment of bromo-tailed porphyrins with Ph_3CSH in the presence of K_2CO_3 also produced the trityl-protected thiol porphyrins Detritylation was initiated by treatment of the trityl-protected thiol-tailed porphyrin with Hg(II), which results in the formation of a Hg-SR complex. Subsequent treatment with H_2S gave the desired thiol-tail porphyrin.

For the bis(*o*-aminophenyl)porphyrin thiol derivatives, H_2DPE-$[NHC(O)(CH_2)_5SH]_2$ **24** and Zn{DPE-$[NHC(O)(CH_2)_5SH]_2$} **28**, purity is readily

ascertained by the presence of a single meso-proton resonance in the NMR spectrum. In H_2DPE-[NHC(O)$(CH_2)_5$SH]$_2$ **24**, this signal appears at 10.28 ppm. For the corresponding Zn complex **28**, it occurs at 10.21 ppm. The Co(II) complex **27** is paramagnetic. However, TLC analysis of **27** shows that only the α,α-atropisomer was present in the final product.

The treatment of bis-(*o*-aminophenyl) porphyrin **2** with 3-(tritylthio)propionyl chloride at room temperature under prolonged stirring produced the desired bis acylated product. However, we found that it is very difficult to remove the two trityl protecting groups in this compound. A possible explanation for this observation derives from spectroscopic information. The UV-vis spectrum for H_2DPE-[NHC(O)$(CH_2)_2$SC$Ph_3]_2$, **22**, exhibits a slight blue shifting of the Soret band relative to that in DPE-$(NH_2)_2$, **2** and H_2DPE-[NHC(O)$(CH_2)_5$SC$Ph_3]_2$, **23** (Table 2). In addition, the ^{1}H NMR signals for the trityl group in **22** are shifted significantly upfield about 0.6 ppm relative to $Ph_3CS(CH_2)_2COOH$. In H_2DPE-[NHC(O)$(CH_2)_5$SC$Ph_3]_2$, **23**, the upfield shift of the trityl resonance is only about 0.2 ppm relative to $Ph_3CS(CH_2)_5COOH$. Trityl group resonances in $Ph_3CS(CH_2)_2COOH$ and $Ph_3CS(CH_2)_5COOH$ are almost identical and appear at 7.42-7.14 ppm. This suggests that the trityl groups in compound **22** are much closer to the porphyrin ring and this proximity may block Hg(II) attack at the sulfur atom.

Standard procedures were employed to metalate the porphyrin core with Co(II) and Zn(II). In order to eliminate complications from the presence of thiol groups, the

trityl-protected precursors were used. Subsequent deprotection produced the desired thiol-tailed metal complexes.

Conclusion

We have synthesized a series of thiol-derivatized porphyrins which have different numbers of thiol appendages which are located at different positions of the porphyrin. By utilizing the trityl protecting group, a series mono- and bis-thiol-derivatized porphyrins have been prepared. These thiol-derivatized porphyrins have been used to construct porphyrin monolayers and should have important applications in the area of new bio-sensors and catalysts.

References

1. Presidential Young Investigator, 1990-1995: Camille and Henry Dreyfus Teacher-Scholar 1993-1998.
2. Collman, J. P.; Groh, S. E. *J. Am. Chem. Soc.* **1982**, *104*, 1391-1403.
3. Zak, J. Yuan, H.; Ho, M.; Woo, L. K.; Porter, M. D. *Langmuir*, **1993**, *9*, 2772-2774.
4. Hutchison, J. E.; Postlethwaite, T. A.; Murray, R. W. *Langmuir*, **1993**, *9*, 3277-3283.
5. (a) Lindsey, J. S.; Schreiman, I. C.; Hsu, H. C.; Hearney, P. C.; Marguerettaz,

A. M. *J. Org. Chem.* **1987**, *52*, 827-836. (b) Lindsey, J. S.; Wagner, R,. W. *J. Org. Chem.* **1989**, *54*, 828-836. (c) Adler, A. D.; Longo, F. R.; Finarelli, J. D.; Goldmacher, J.; Assour, J.; Korsakoff, L. *J. Org. Chem.* **1967**, *32*, 476.

6. Kruper, W. J. Jr.; Chamberlin, T. A.; Kochanny, M. *J. Org. Chem.* **1989**, *54*, 2753.

7. Young, R; and Chang, C. K. *J. Am. Chem. Soc.* **1985**, *107*, 898.

8. *Vogel's Textbook of Practical Organic Chemistry*, Vogel, A. I., 5th ed.; Longman Scientific & Technical, London, **1989**, pp. 692-693.

9. Ulman, A. *An Introduction to Ultrathin Organic Films*; academic Press, Inc.: Boston, 1991.

10. Patai, S. *The Chemistry of the Thiol Group*, part 1, pp. 179-211, Wiley, New York, **1974**.

11. (a) Hiskey, R. G.; Mizoguchi, T.; Igeta, H. *J. Org. Chem.* **1966**, *31*, 1188. (b) Hiskey, R. G.; Adams, J. B. *J. Org. Chem.* **1966**, *31*, 2178.

CHAPTER 3. THIOL-DERIVATIZED METALLOPORPHYRINS: MONOMOLECULAR FILMS FOR THE ELECTROCATALYTIC REDUCTION OF DIOXYGEN AT GOD ELECTRODES

A paper published in Langmuir[1]

Jerzy Zak, Hongping Yuan, Mankit Ho, L. Keith Woo, and Marc D. Porter

Abstract

This paper describes preliminary results in the design, construction, and characterization of cobalt(II) porphyrins derivatized with alkanethiol appendages. The use of the thiol appendages leads to the formation of a chemisorbed monolayer of the corresponding thiolate at gold electrodes. Our findings suggest that this approach may serve as a beginning for fabricating electrocatalytic monolayers with a preselected architecture through the manipulation of the number and location of the appendages. Voltammetric data indicate that monolayers from both **I(Co)** and **II(Co)** catalyze the two-electron reduction of O_2 to H_2O_2. The monolayer from **I(Co)**, however, has a lower electrocatalytic activity. Infrared, X-ray photoelectron, and visible spectroscopic data are presented that argue the difference in reactivity arises from a difference in interfacial architecture. The results from attempts to metalate monolayers from **I(H_2)** and **II(H_2)** support this interpretation. Findings are also reported that indicate the preparation of

mixed monolayers (e.g., two-component monolayers from **I(Co)** and $CH_3(CH_2)_3SH$) may prove valuable to this area of research.

Introduction

Recent findings point to the electrocatalytic reduction of O_2 via immobilized metallomacrocycles as an attractive reaction for use in fuel cells.[2,3] We report herein the creation and characterization of monolayers formed by chemisorption[4] of the thiol-derivatized cobalt(II) porphyrins **I(Co)** and **II(Co)** at gold electrodes. A key feature of **I(Co)** and **II(Co)** is the number and location of the thiol-containing "legs". Our findings suggest that this approach can serve as an effective starting point for controlling systematically the spatial orientation and coverage of the adsorbate (Chart I). We show that monolayers from **I(Co)** and **II(Co)** exhibit different electrocatalytic activities. Results from infrared (IRS), X-ray photoelectron (XPS), and visible (VS) spectroscopic data as well as from various chemical manipulations of the surface structure indicate that the differences in activity arise from differences in interfacial architecture.

Experimental

Preparation of the free-base thiol-derivatized porphyrins **I(H_2)** and **II(H_2)** followed modifications of earlier procedures.[5] Of paramount importance is the placement of both thiol appendages of **II(H_2)** on the same side of the porphyrin plane. This was achieved using the *cis*-amine isomer of 5,15-bis[*o*-aminophenyl]etioporphyrin as the precursor,

Chart I

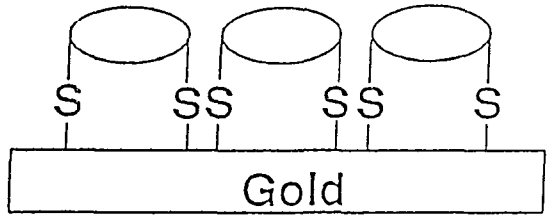

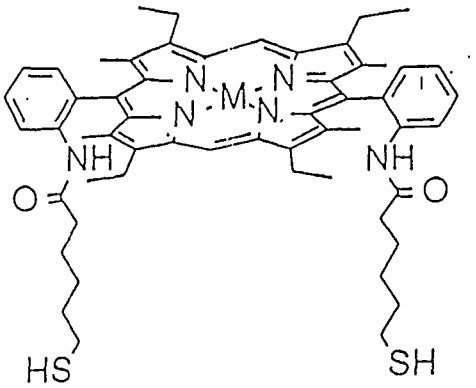

II(H_2) M = H_2

II(Co) M = Co

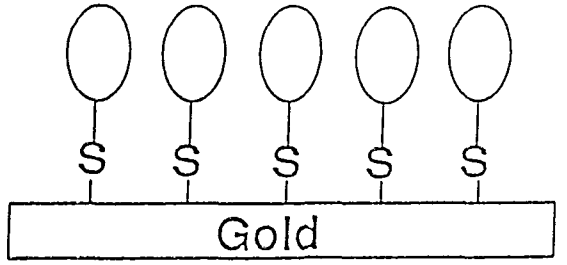

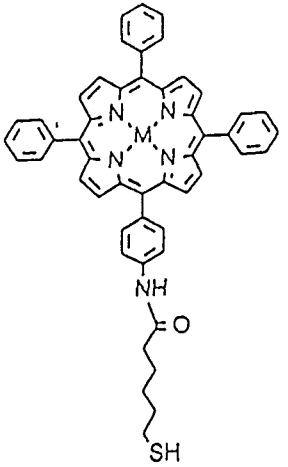

I(H_2) M = H_2

I(Co) M = Co

which was chromatographically separated from its *trans*-amine isomer.[6] Alkylation of the *cis*-amine isomer with 6-(tritylthio)hexanoyl chloride, followed by removal of the trityl protecting groups with $Hg(OAc)_2$ and H_2S,[7] produced 5α,15α-bis[*o*-(6-mercaptohexylamido)phenyl]-etioporphyrin, **II(H_2)**. The meso-[*p*-(6-mercaptohexylamido)phenyl]triphenylporphyrin, **I(H_2)**, was prepared in a similar manner from (*p*-aminophenyl)triphenylporphyrin.[8] The metal complexes, **I(Co)** and **II(Co)**, were synthesized by insertion of Co(II) before removal of the trityl groups.[9] Monolayers were constructed by the immersion of annealed mica-supported gold[10] into 10 μM CH_2Cl_2 solutions of the thiol derivatives for ~ 12 h. Samples were rinsed extensively with CH_2Cl_2 and CH_3CH_2OH upon emersion. The subsequent findings are representative of the testing of more than ten samples of each type of monolayer.

Results and Discussion

Evidence of the reactivities of the monolayers from **I(Co)** and **II(Co)** is provided by the voltammograms in O_2-saturated solutions of 0.1 M $HClO_4$ in Figure 1. Curve a is for uncoated gold. Curves b and c are for **I(Co)** and **II(Co)**, respectively, as chemisorbed monolayers at gold. A comparison of the positions and magnitudes of the curves reveals that the monolayer from **II(Co)** is a more effective electrocatalyst for the reduction of O_2 to H_2O_2.[11] Control experiments,[12] which used analogs of **I(Co)** and **II(Co)** in which all the SH groups are replaced by CH_3 groups, indicate that the differences in curves b and c do not arise from differences in the electronic structures of the absorbate precursors. We

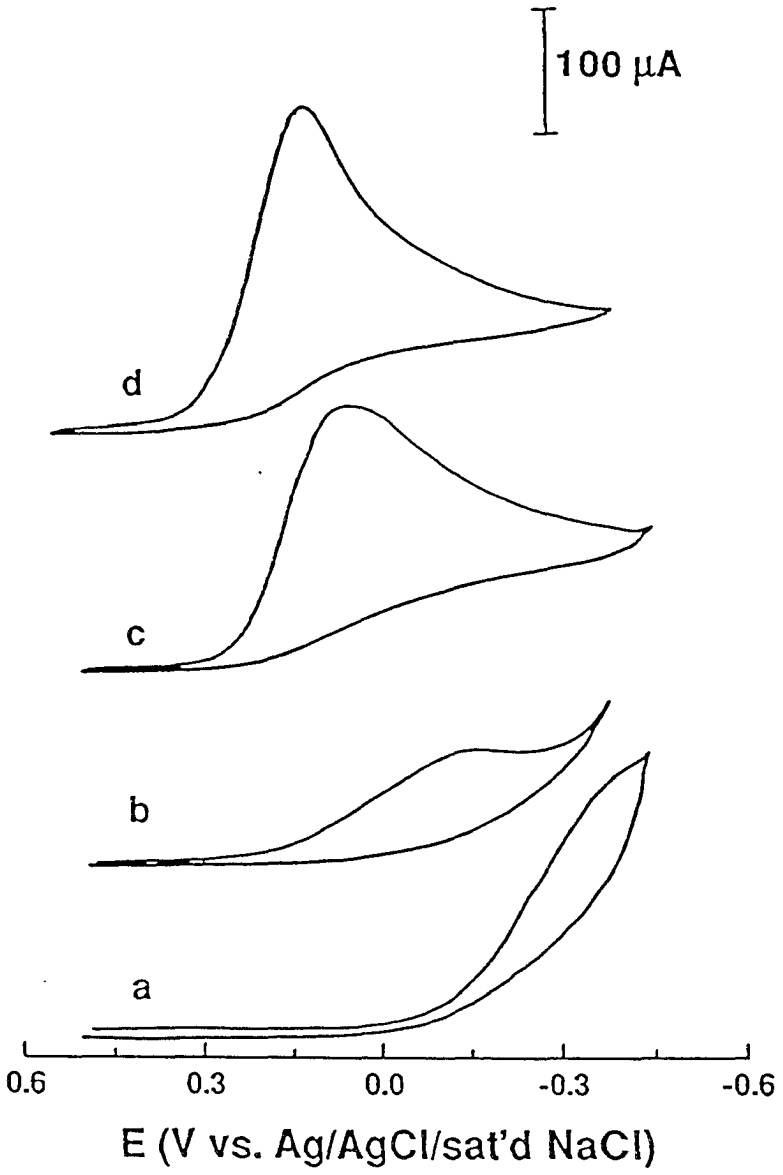

Figure 1. Voltammetric curves obtained for different Au electrodes: (a) uncoated Au; (b) I(Co) chemisorbed at Au; (c) II(Co) chemisorbed at Au; (d) mixed monolayer from $CH_3(CH_2)_3SH$ and I(Co) chemisorbed at Au. The supporting electrolyte was an O_2-saturated solution of 0.1 M $HClO_4$. The scan rate was 50 mV/s geometric electrode area was of 0.63 cm^2.

therefore attribute our observations to differences in the architecture of the two monolayers as directed by the chemisorption at gold via the thiol-containing appendages.

Figure 2 presents IRS[9] data that provides insight into the structures of the two monolayers. The absolute magnitudes of the bands for **I(Co)** and **II(Co)** at gold and the similarities of their positions with respect to the precursors in KBr point to the formation of a monomolecular film of each complex. In addition, these data reveal general *qualitative* details about the architecture of the two monolayers.[13] The details develop from considerations of the infrared surface selection rule which results from a preferential excitation of vibrational modes with dipoles normal to a highly reflecting metal surface.[14] Thus, the differences in the relative absorbances of the bands for **I(Co)** and **II(Co)** at gold relative to in KBr are diagnostic of a preferentially as opposed to randomly oriented surface structure for both types of monolayers. At this time, however, an analysis of the orientation of the porphyrin ring from these data awaits completion of an in-depth band assignment study.[15]

Characterizations using XPS, in addition to substantiating the composition of both types of monolayers, confirm chemisorption at gold through sulfur. For **I(Co)** at gold, bands only for sulfur as a gold-bound thiolate were observed: $S(2p_{1/2})$ at 163.1 eV and $S(2p_{3/2})$ at 161.9 eV.[16] Features diagnostic of unreacted SH groups as well as the more highly oxidized forms of sulfur (e.g., disulfides and sulfonates), which are all found at higher binding energies,[17] were not detected. The XPS data for **II(Co)** are in agreement with the data for **I(Co)** at gold, though we are unable in this case to rule out the presence

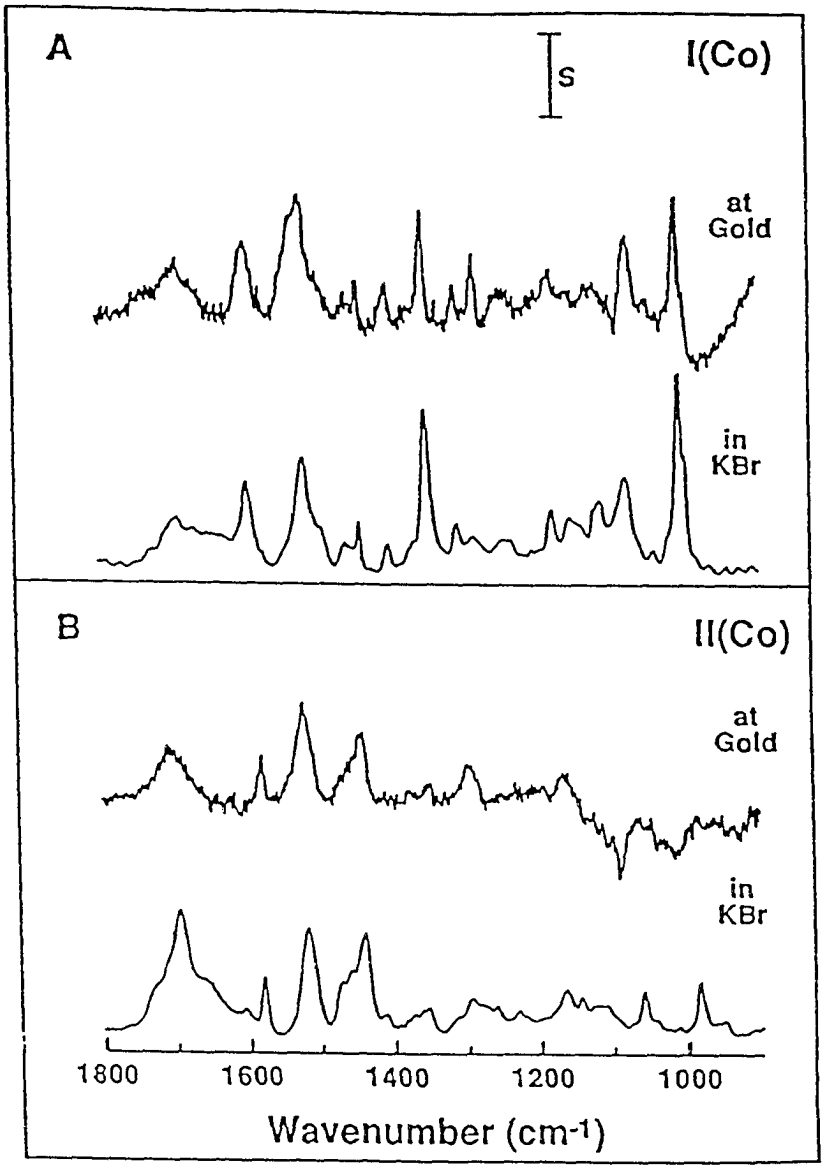

Figure 2. Infrared spectra for I(Co) (A) and II(Co) (B) in KBr and at gold. S is 4.0 x 10^{-2} and 4.0 x 10^{-4} AU for the KBr and the monolayers spectra, respectively. The reflection spectra were collected using p-polarized light incident at 82° with respect to the surface normal.

of a trace amount of polysulfide.[18]

The VS data reveal another feature of the two monolayers. Upon chemisorption, the B band of **I(Co)** undergoes an exitonic splitting to yield a doublet with blue- (394nm) and red-shifted (448 nm) components (Figure 3, spectrum e), as also found at related Langmuir-Blodgett films.[19] On the other hand, only a weakly absorbing red-shifted (436 nm) B band was observed upon chemisorption of **II(Co)**. The positions of the B bands in CH_2Cl_2 are 412 and 402 nm for **I(Co)** and **II(Co)**, respectively. These spectral changes suggest a difference in the electronic dipolar interactions between the adsorbates in the two monolayers. The red shift for the monolayer from **II(Co)** is typical of head-to-tail dipolar interactions between the π-systems of neighboring adsorbates.[19] In contrast, the spectrum for the monolayer from **I(Co)** reveals the presence of coplanar, inclined[19a] (as opposed to face-to-face[20]) π-π electronic interactions between neighboring adsorbates. Based on these data, we infer that the structure of the monolayer from **II(Co)** is in-line with that depicted in Chart I, whereas that from **I(Co)** is more consistent with representation in Chart II.

Chart II

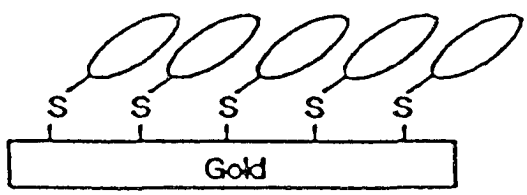

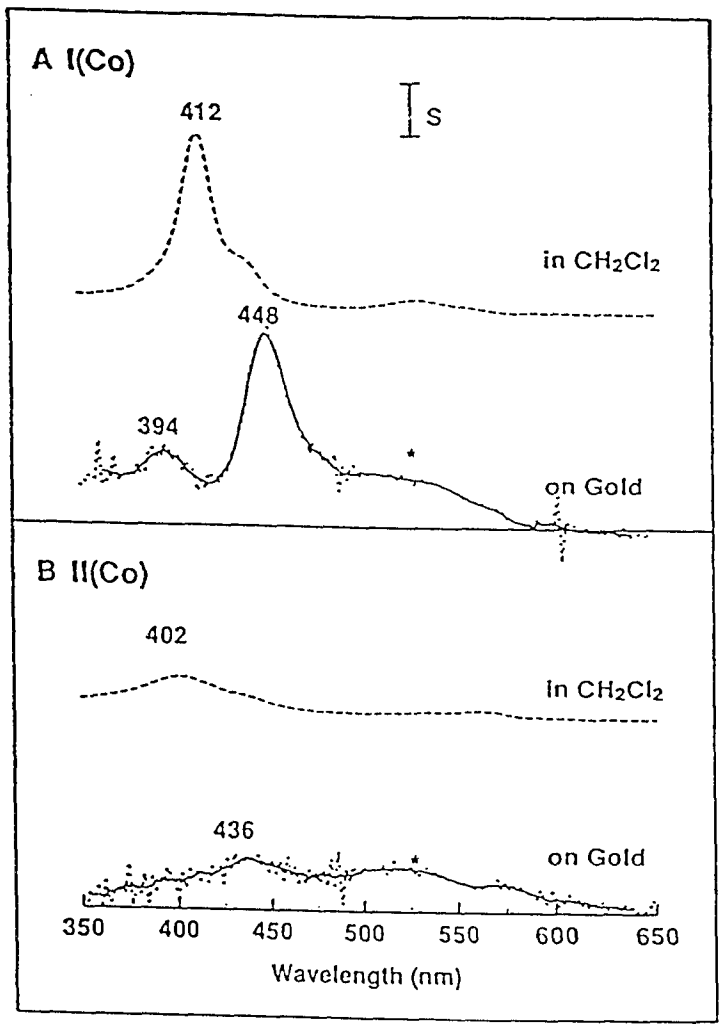

Figure 3. Visible spectra for **I(Co)**. (a) **I(Co)** in CH_2Cl_2. (b-d) mixed monolayers formed by exchanging a butanethiolate monolayer at gold with 10 μM of **I(Co)** in CH_2Cl_2: (b) butanethiolate only; (c) 2 h exchange; (d) 18 h exchange. (e) **I(Co)** at gold as a pure monolayer. S is 0.1 AU for (a) and 0.01 AU for (b-e). The VS measurements were made using a Hewlett-Packard 8452A diode array spectrometer. The reflection spectra were collected using p-polarized light incident at 60° with respect to the surface normal. An uncoated gold substrate served as a reference. The spectra in (b-e) were smoothed using an 11-point Savitsky-Golay algorithm.

To assess the influence of the π-π interactions for the monolayer from **I(Co)**, a mixed monolayer was prepared by a partial exchange with **I(Co)** at a previously formed monolayer from $CH_3(CH_2)_3SH$.[21] Curve d in Figure 1 exemplifies the improvement in the electrocatalytic response. We attribute the improvement to an isolation of porphyrin moieties within the matrix of the short chain thiolate. The VS data in Figure 3 confirm the effect of the short chain thiolate on the coplanar, inclined π-stacking of the monolayer from **I(Co)**. Spectrum b is for the monolayer from $CH_3(CH_2)_3SH$. The spectra in c and d are for exchange times of 2 and 18 h, respectively. Exitonic splitting of the B band is detectable only at long exchange times, consistent with the general architecture in Chart II. Voltammetric experiments revealed that the electrocatalytic potency of these samples decreased upon extensive exchange. These findings argue that the lower electrocatalytic current for the monolayer from **I(Co)** results from the coplanar, inclined π-π interactions between adsorbates, which hinders accessibility to catalytic sites.

Support of our interpretation is provided by the results of attempts to metalate **I(H_2)** and **II(H_2)** using $Co(OAc)_2$ (~ 2 mM in CH_3OH, 1 h immersion) after monolayer formation. With such treatment, monolayers from **II(H_2)** displayed a response like curve c in Figure 1. Similarly treated monolayers from **I(H_2)** failed to catalyze O_2 reduction at a detectable level. Finally, $Co(OAc)_2$ treatment of a mixed monolayer from **I(H_2)** and $CH_3(CH_2)_3SH$ produced an electrode with an activity similar to that in Figure 1, curve d.

Work in progress is addressing further the fundamental aspects of these types of monolayers. The goal is to establish a clear connection between the molecular

architecture of the interfacial structures and electrocatalytic potency and to improve electrocatalytic performance. Of particular interest is unraveling how the interplay of the chemisorption of sulfur at gold and the π-π interactions between neighboring porphyrins controls the interfacial structure.

Acknowledgment

Insightful discussion with M. G. Finn and the expert assistance of J. Andregg on the XPS measurements are gratefully acknowledged. The valuable comments of one of the reviewers is also noted. L. K. W. is a NSF Presidential Young Investigator (CHE-9057752) and a 1993 Camille and Henry Dreyfus Teacher-Scholar. The Ames Laboratory is operated for the U.S. Department of Energy by Iowa State University under Contract W-7405-Eng-82. This work was supported by the Office of Basic Energy Sciences, Chemical Science Division.

References and notes

1. Reprinted with permission from *Langmuir* **1993**, *9*, 2772. Copyright @ 1993 *Langmuir*.
2. Murray, R. W. *Electroanalytical Chemistry: A Series of Advances*; Bard, A. J., Ed.; Marcel Dekker: New York, 1984; Vol. 13, p 191.
3. (a) Forshey, P. A.; Kuwana, T. *Inorg. Chem.* **1983**, *22*, 699. (b) Durand, R. R.;

Bencosme, C.S.; Collman, J. P.; Anson, F. C. *J. Am. Chem. Soc.* **1983**, *105*, 2710. (c) Ni, C.-L.; Abdalmuhdi, I.; Chang, C. K.; Anson, F. C. *J. Phys. Chem.* **1987**, *91*, 1158. (d) Bettelheim, A.; White, B.A.; Murray, R. W. *J. Electroanal. Chem.* **1987**, *217*, 271. (e) Van Galen, D. A.; Majda, M. *Anal. Chem.* **1988**, *60*, 1549. (f) Hutchison, J. E.; Postlethwaite, T.A.; Murray, R. W. J. *Electroanal. Chem.*, submitted.

4. For overviews of the chemisorption of thiol-containing compounds, see: (a) Ulman, A. *An Introduction to Ultrahigh Organic Films: From Langmuir-Blodgett to Self-Assembly,* Academic Press: Boston, **MA**, 1991. (b) Whitesides, G. M.; Laibinis, P. E. *Langmuir*, 1990, *6*, 87. (c) Dubios, L. H.; Nuzzo, R. G. *Annu. Rev. Phys. Chem.* **1992**, *42*, 437.

5. (a) Woo, L. K.; Maurya, M. R.; Tolpppi, C. J.; Jacobson, R. A.; Yang, S.; Rose, E. *Inorg. Chim. Acta* **1991**, *182*, 41. (b) Woo, L. K.; Maurya, M. R.; Jacobson, R. A.; Yang, S.; Ringrose, S. L. *Inorg, Chem.* **1992**, *31*, 913.

6. Young, R.; Chang, C. K. *J. Am. Chem. Soc.* **1985**, *107*, 898.

7. Collman, J. P.; Groh, S. E. *J. Am. Chem. Soc.* **1982**, *104*, 1391.

8. Further details of the synthetic and other preparative procedures will appear in a manuscript in preparation.

9. Fuhrhop, J.; Smith, K. M. *Laboratory Methods in Porphyrin and Metalloporphyrin Research*; Elsevier: New York, 1975; p 42.

10. (a) Widrig, C. A.; Chung, C.; Porter, M. D. *J. Electroanal. Chem.* **1991**, *310*, 335. (b) Walczak, M. M.; Popenone, D. D.; Deinhammer, R. S.; Lamp, B.D.; Chung, C.; Porter, M. D. *Langmuir* **1991**, *7*, 2687.

11. Data confirming H_2O_2 as the product of the electrolysis of dioxygen at monolayers from both **I(Co)** and **II(Co)** were obtained spectroscopically using a long optical path length thin-layer spectroelectrochemical cell (J. Zak, Iowa State University, unpublished results).

12. Electrodes prepared by the chemisorption of the alkyl analogs of **I(Co)** and **II(Co)** at gold exhibited similar voltammetry in O_2-saturated solutions of 0.1 M $HClO_4$: peak potentials of the **I(Co)** and **II(Co)** analogs are +0.07 and +0.04 V (vs Ag/AgCl (saturated NaCl), respectively.

13. The voltammetry of the metal centers for **I(Co)** and **II(Co)** in deoxygenated solutions is poorly defined and difficult to distinguish from the background current. This has hindered attempts to determine the surface coverage by the measurement of the charge required for the one-electron conversion of the metal centers. We are presently devising a spectrophotometric assay for collecting such information.

14. (a) Greener, R. G. *J. Chem. Phys.* **1969**, *50*, 310. (b) Porter, M. D. Anal. Chem. **1988**, *60*, 1143A. (c) McIntyre, J. D. E. Advances in Electrochemistry and Electrochemical Engineering; Delahay, P., Tobias, C. W., Eds.; Wiley: New York, 1973

15. Leading references for the assignments of the vibrational modes of porphyrins include: (a) Nakanishi, K.: Solomon, P. H. *Infrared Absorption Spectroscopy*, Holden-Day, Inc.: Oakland, CA 1977. (b) Spiro, T. G.; Czernuszewicz, R. S.; Li, X.-Y. *Coord. Chem. Rev.* **1990**, *100*, 541, and references therein. However, we have as yet to translate these findings confidently to our structures, especially to **II(H_2)** and **II(Co)**.

16. (a) Nuzzo, R.G.; Zegarski, B. R.; Dubois, L. H. *J. Am. Chem. Soc.* **1987**, *109*, 733. (b) Bain, C. D.; Biebuyck, H. A.; Whitesides, G. M. *Langmuir*, **1989**, *5*, 723. (c) Laibinis, P. E.; Whitesides, G. M.; Allara, D. L.; Tao, Y.-T.; Parik, A. N.; Nuzzo, R. G. *J. Am. Chem. Soc.* **1991**, *113*, 7152. (d) Weisshaar, D. E.; Walczak, M. M.; Porter, M. D. *Langmuir* **1993**, *9*, 323.

17. Lindberg, B. J.; Hamrin, K.; Johansson, G.; Gelius, U.; Fahlman, A.; Nordling, C.; Siegbahn, K. *Phys. Scr.* **1970**, *1*, 286.

18. A slight broadening at the low energy side of the S(2p3/2) band for **II(Co)** suggests the possible presence of polysulfide. However, this feature is barely detectable above the noise of the measurement, indicating that only trace amounts of these impurities are present.

19. (a) Schick, G. A.; Schreiman, I. C.; Wagner, R. W.; Lindsey, J. S.; Bocian, D. F. *J. Chem. Soc.* **1989**, *111*, 1344. (b) Bulkowski, J. E.; Bull, R. A.; Sauerbrunn, S. R. *ACS Symp. Ser.* **1981**, No. *146*, 279. (c) Bull, R. A.; Bulkowski, J. E.; *J.*

Colloid Interface Sci. **1983**, *92*, 1. (d) Cantor, C. R.; Schimmel, P. R. *Biophysical Chemistry*, W. H. Freeman: San Francisco, CA, 1980; Part II, p395.

20. Face-to-face π-π electronic interactions between porphyrins exhibit only a blue-shifted B band (see, for example, Gouterman, M.; Hanson, L. K.; Khalil, G.-E.; Buchler, J. W.; Rohbock, K.; Dolphin, D. *J. Am. Chem. Soc.* **1975**, *97*, 3142).

21. The mixed monolayer structure was prepared by forming a layer from 1 mM $CH_3(CH_2)_3SH$ in ethanol, followed by a partial exchange with 10 μM of **I(Co)** in CH_2Cl_2 for ~ 4 h.

CHAPTER 4: PORPHYRIN-CONTAINING MULTI-COMPONENT SYSTEMS AS MODELS FOR PHOTOSYNTHESIS REACTION CENTER: A LITERATURE REVIEW

Overview

Photosynthesis is a key process in biological energy transduction that converts sunlight into stored chemical energy. Recorded scientific studies on natural photosynthetic systems date as far back as 1772[1] and interest in photosynthesis remains at an extremely high level as exemplified by several recent reviews.[2] It is clear that the ability to mimic this natural process in the laboratory would have great technological significance in terms of solar energy conversion and storage. Despite intensive efforts and dramatic progress in the past decade, the goal of achieving artificial photosynthesis remains elusive. Nonetheless, vital aspects of our knowledge of photosynthesis on a fundamental level has increased tremendously as a result of new investigations over the past few years. Important findings have evolved from the advancement of photochemistry from the "molecular" level to the "supramolecular" level.

The reaction centers that are responsible for the conversion of light energy into chemical potential in plants and other photosynthetic organisms consist of several molecular components held together in a protein environment in a well-organized macromolecular structure. Verification of the intricate structural features of bacterial photosynthetic reaction centers has been achieved through single crystal X-ray diffraction studies.[3] Unfortunately, it is difficult to obtain detailed information on this system in its

natural environment because it is a complex structure that can not be easily subjected to chemical and environmental modification to methodically examine energetics, nuclear, and electronic factors that contribute to determining rates of electron transfer. As a means of understanding the function of this macromolecular assembly, a great deal of effort has been directed towards copying structural features of natural reaction centers with small molecule analogues. Many elegant models have been devised for photoinduced electron transfer between covalently linked subunits in arrangements related to those found in bacterial photosynthetic centers. These studies have shown that the molecular components must be arranged precisely in order to exhibit the desired properties.

Porphyrin derivatives have found notable and extensive use as components for the energy and electron transfer subunits in artificial photosynthesis constructs. The types of supramolecular assemblies that have appeared in the literature now span a large range of sophistication and complexity. The simplest of these model systems contain two covalently linked donor/acceptor chromophores. Significant examples include porphyrin dimers,[4] porphyrin-quinone systems,[5] or chlorophyll-porphyrin molecules.[6] A number of approaches and types of spacers have been used to link the subunits together in these two-component arrays (dyads). The spacers perform a structural function as well as serve as an intervening medium through which the subunits interact. Thus, the spacers partially fulfill the role of the protein in natural reaction centers. Noteworthy spacers include phenylene,[7] vinyl,[8] spirocyclic,[9] naphthyl,[10] as well as direct linkage of the two

subunits with a single bond.[6] Porphyrin-based structures constructed in this manner have been found to be valid in modelling primary processes involved in natural photosynthetic reaction centers.

In the dyad assemblies, the geometrical relationship of the two components has been varied from linear (edge-to-edge),[7] stacked (face-to-face),[11] as well as intermediate arrangements.[12] Studies of molecular dyads have increased the knowledge of the distance and orientation factors that influence photoinduced electron transfer.[10, 12,13] In general, molecules that exhibit a better defined structural relationship between the donor and acceptor subunits yield more intricate insights into the photoinduced electron transfer process. However, the two-component models suffer from short lifetimes of the charge-separated states as the factors that favor efficient photoinduced electron transfer also result in extremely facile charge recombination.

The problem of rapid charge recombination is minimized in nature by the utilization of a sequence of multi-step electron transfer reactions that eventually result in charge separation over long distances. A similar strategy in artificial systems is successful in producing longer lived charge-separated states. For example, in multi-component models containing linearly linked carotene-porphyrin-quinone (C-P-Q) subunits, two tandem electron transfer steps occur after photoexcitation to produce a charge-separated state, C^{+}-P-Q^{-}. Subsequent lifetimes of this state as long as 2 μs have been observed.[10,12,14] This is in comparison to the 100 ms lifetimes achieved by bacterial reaction centers[15] and the 100 ps lifetimes in two-component assemblies.

Unfortunately, the increases in lifetimes in three-component systems over those observed in two-component assemblies is realized at the expense of quantum yields (eg. about 4%). Clearly, subtle factors are involved. An important aspect involves the efficiency of electron transfer processes to the final charge-separated state relative to the rates of charge recombination. Incorporation of additional electron acceptors that effectively compete with recombination has been shown to improve quantum yields. Thus, in a carotene-porphyrin-quinone$_a$-quinone$_b$ tetrad (C-P-Q_a-Q_b), the final charge separated state forms with a quantum yield of 0.5 at 240 K and has a lifetime of 460 ns.[16]

Although many clever and ingenious models have been prepared, the maximum efficiencies for charge separation and the lifetimes of the charged-separated states obtained to date are still well below those achieved by green plants and photosynthetic bacteria. Nonetheless, remarkable progress has been made in achieving these objectives. For example, in an amine/zinc porphyrin/quinone three-component assembly, a quantum yield of 675 and a lifetime of 4 ms has been realized in generating a charge-separated state that stores 1.85 eV of energy.[17]

It is clear that the sophistication of synthetic multi-component species that mimic primary events of natural photosynthesis has increased tremendously. Although impressive progress has been made towards assembling efficient artificial reaction center models, this field has still not reached maturity. Greater variability is still possible by changing the number and nature of subunits and spacers, distances, and orientations.

Thus, it is should be feasible to tailor systems with desired properties. This should allow closer mimicking of natural photosynthesis and in addition, investigating cooperative and competitive processes. However, as the types and numbers of components are increased, the level of complexity also expands and model systems become more difficult to prepare. To a large extent, progress in this area is still significantly synthesis limited. Nonetheless, previous studies indicate that new strategies for designing sequential multi-step electron transfer processes will continue to be a fruitful area of study.

Non-covalent bond linkage: hydrogen-bonded model systems

To avoid the difficulty of synthesis and separation of multi-component photosynthesis reaction center models, new strategies have been developed for the preparation of donor-acceptor model systems. One alterative employs hydrogen bonds to link photoactive chromophore subunits together in a self-assembled multi-chromophore structure.

Hamilton and coworkers[18] have used this strategy to make porphyrin-electron acceptor assemblies. A barbiturate moiety, attached to the porphyrin through a peptide linkage, was used as a hydrogen-bonding site to link the porphyrin with an electron acceptor. One of the complexes they prepared was the porphyrin-dansyl complex shown in Figure 1.

The distance between the chromophore centers in this assembly is estimated to be 23 Å. The association constant for formation of this complex is $K_a = 1.0 \times 10^6\ M^{-1}$.

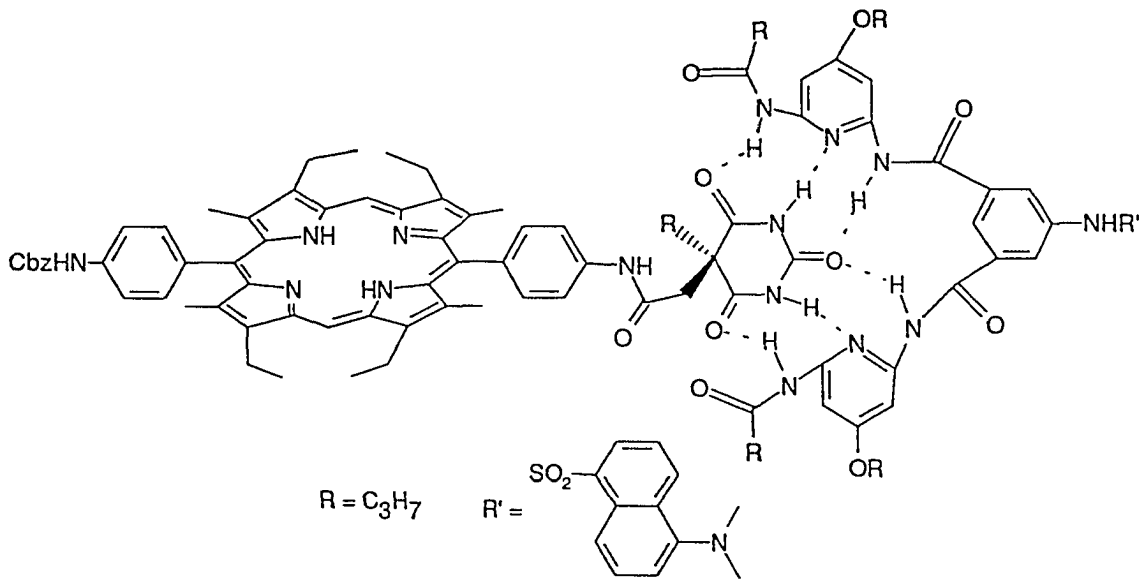

Figure 1. Porphyrin-danyl receptor assembly

Time resolved fluorescence measurements using single photon counting detection shows that the excited state of this complex decays with a lifetime of $\tau = 0.4$ ns. The fluorescence lifetime of the dansyl receptor by itself is $\tau = 16.3$ ns. The fluorescence study indicates that the porphyrin and dansyl receptor do communicate through the hydrogen-bonding.

Nocera *et al.*[19] has studied photoinduced electron transfer kinetics for the hydrogen-bonded complex **2** (Figure 2) which was formed from Zn^{II}PCOOH porphyrin (PCCOH = 13,17-diethyl-3,7,8,12,18-pentamethylporphin-2-acetic acid) and 3,4-dinitrobenzoic acid (DNBCOOH). The association constant for complex **2** is 552 M^{-1}.

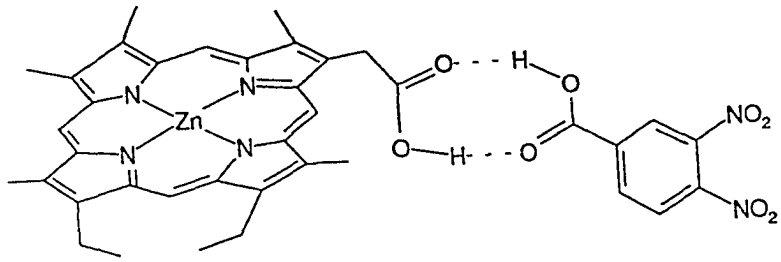

Figure 2. Complex 2 ZnPCOOH-DNBCOOH

In complex 2, electron transfer (ET) is channeled through a dicarboxylic acid interface from a photoexcited Zn^{II}PCOOH porphyrin donor to the electron acceptor 3,4-dinitrobenzoic acid. Photoexcitation of ZnPCOOH produces an emissive $^1\pi\pi^*$ excited state with a characteristic absorption band at 660 nm. The singlet decays to form a long-lived triplet state (τ_0 = 40 μs). The ZnPCOOH donor is a powerful one-electron reductant from its $^1\pi\pi^*$ state and is capable of reacting with the organic acceptor DNBCOOH. The driving forces for forward and back electron transfer are -0.73 and -1.37 V, respectively. Experimental observations show that ET through hydrogen-bonded interfaces is fast. The forward electron transfer rate constant is 5.0 x 10^{10} s^{-1} and the rate constant for charge recombination is 1.0 x 10^{10} s^{-1}. These rates are slightly slower than those of covalently linked Zn(II) porphyrin/acceptor systems of similar separation and driving force (k_{cs} = 2.5 x 10^{11} s^{-1}, k_{cr} = 1.2 x 10^{11} s^{-1}).[20] Nonetheless the ET rates are of

similar orders of magnitude, thereby establishing that hydrogen-bonded ET pathways can be competitive with ET through covalently bonded linkages. The deuterium isotope effect for the charge separation (CS) and recombination (CR) rates of complex **2** is k_H/k_D = 1.7 and 1.6, respectively. This study shows that hydrogen-bonding interfaces not only are important in the supramolecular preorganization of the acceptor/donor pair for energy and electron transfer but also may directly mediate the electron-transfer event.

Ogoshi *et al.* reported the construction of face-to-face porphyrin-quinone architectures by utilizing a hydrogen-bonding strategy.[21] They have synthesized 5α,15α-bis(2-hydroxynaphthyl)octaethylporphyrin and *meso*-tetra(α,α,α,α)-2-hydroxy-1-naphthyl)-porphyrin. These porphyrins form face-to-face complexes with variety of *p*-quinones through hydrogen-bonding in a host-guest arrangement. The binding constants range from 10^2 to 10^4 M^{-1}. The stability of an adduct is determined not only by the strength of hydrogen bonds involved but also by porphyrin-quinone electrostatic or charge-transfer interactions. Thus, electron donating or electron-withdrawing substituents in a guest quinone promote host-guest complexation. Furthermore, the enforced proximity of the porphyrin and quinone rings in the complexes results in significant π-π electronic interactions. Fluorescence quenching studies on these complexes show that the porphyrin fluorescence of the adducts is completely quenched by an efficient, intracomplex electron transfer from the excited host porphyrin to the bound quinone.

Sessler and coworkers have developed a novel approach to the assembly of supramolecular donor-acceptor systems.[22] In these systems, nucleic acid bases

(nucleobases) have been covalently bound to porphyrins and self-association of nucleic acid base pairs via multiple hydrogen-bonding generates a macromolecular ensemble upon mixing in aportic solvents. Several different supramolecular assemblies have been reported and are shown in Figure 3.

In ensemble **3** (Figure 3), the supramolecular complexes were constructed from Watson-Crick-type nucleobase pairing interactions between guanine and cytosine. The association constant for complex **3** is 1220 M^{-1}. Photoinduced triplet-triplet energy transfer was observed within the hydrogen-bonded complex following illumination. However, because of the high flexibility of this complex, no singlet-singlet energy transfer was observed. Also, the mechanistic details of the energy-transfer process remained indeterminate because an intracomplex diffusional encounter between the donor and acceptor, rather than through hydrogen bond energy-transfer process, could account for the observed triplet-triplet energy transfer.

In ensembles **4** and **5** (Figure 3), the donor (zinc(II) porphyrin) and acceptor (a free-base porphyrin) are connected *via* a phenyl ring to guanosine and cytidine, respectively. The two porphyrins are arranged in a side-by-side orientation with an interplanar dihedral angle of *ca.* 90°. The porphyrin-to-porphyrin center-to-center distance was estimated to be *ca.* 22.5 Å from CPK models. The association constants are around 2.2 x 10^4 M^{-1}. In these model systems, singlet energy transfer occurs with a rate constant of *ca.* 9 x 10^8 s^{-1} and with 60% efficiency. Triplet energy transfer from the zinc porphyrin to the free-base porphyrin in the guanosine-cytidine base-paired linked

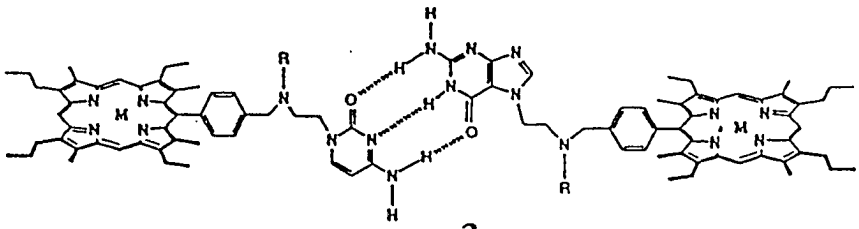

3

R, R' = $-CH_2CH_2OCH_2CH_2OCH_3$ or 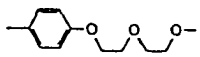 or porphyrinyl

M = Zn or H_2

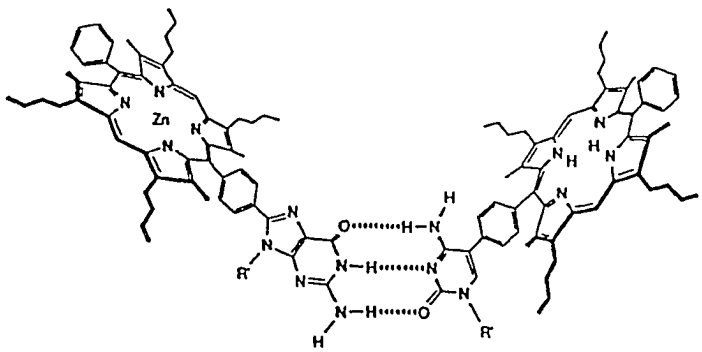

4

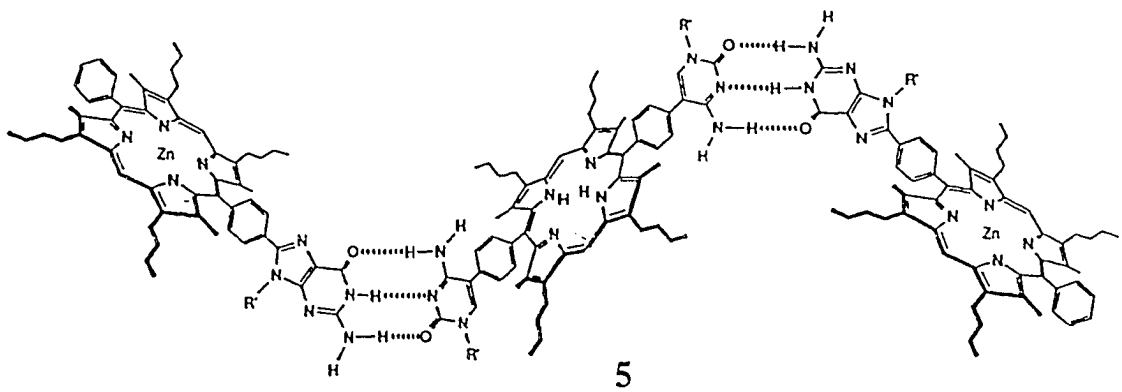

5

R' = 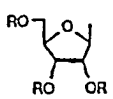 , R = $SiMe_2Bu^t$

Figure 3. Porphyrin ensembles via multiple hydrogen bonding (Reprinted with permission from *J. Am. Chem. Soc.* **1995**, *117*, 704. Copyright © 1995 ACS).

assembly needs *ca.* 1 μs to cross the hydrogen-bonded network in an unimolecular processes, and occurs with almost quantitative efficiency.

These studies demonstrate that hydrogen-bonding interactions can be used both to generate photoactive aggregates that are different from traditional systems and to provide an effective pathway for mediating donor-to-acceptor triplet-energy transfer. This non-covalent approach to constructing donor-acceptor model systems could also be used to assemble higher-order arrays without lengthy synthetic procedures.

Porphyrin assemblies organized by metal ion templates

Another strategy for the synthesis of supramolecular arrays was developed in recent years. In this strategy, the key aspect is using metal coordination environments as a structural feature that serves to organize the entire assembly.

Sauvage *et al.* has designed a bis-porphyrin system which uses 1,10-phenanthroline as a spacer.[23] In these bis-porphyrin phenanthroline systems, either gold(III) or zinc(II) cations have been inserted into each porphyrin cavity. This arrangement holds the porphyrin rings at an average center-to-center separation distance of 13.4 Å and an approximate interplanar angle of 77°.[24] The photophysical properties of an assembly containing gold(III) and zinc(II) porphyrins (Figure 4), have been studied.[25] Upon selective excitation of either porphyrin, the system undergoes rapid intramolecular electron transfer between the zinc porphyrin and the appended gold porphyrin. Return to the ground-state occurs by a relatively slow reverse electron

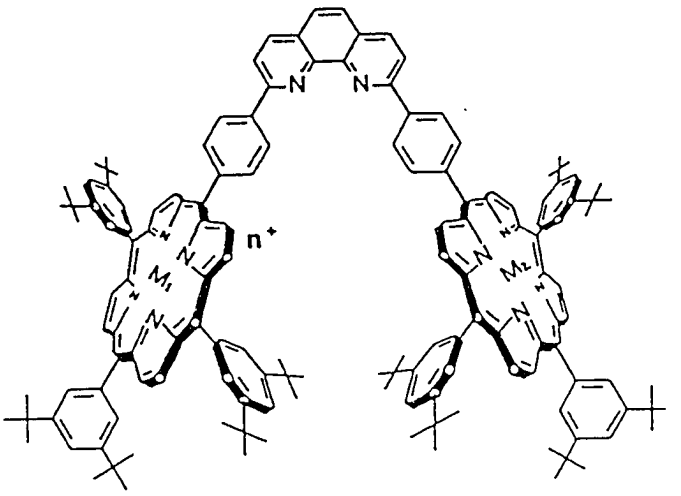

M_1 = Au ; n = 1 ; M_2 = Zn

Figure 4. Zinc(II)-gold(III) bisporphyrin (adapted from *Tetrahedron* **1991**, *47*, 5123).

transfer process. Both the zinc porphyrin excited singlet and triplet states transfer an electron to the appended gold porphyrin. Excitation of the gold(III) porphyrin generates a triplet excited state which abstracts an electron from the zinc(II) porphyrin (77%) or transfers electronic energy to it (15%). The rates of various electron transfer steps correlate with reaction exergonicity and temperature, but only poorly with the solvent polarity. The magnitude of electronic coupling between the reactants depends on the energy gap between relevant orbitals on the porphyrin and the spacer group, in agreement with through-bond interaction.[26] The process involving the zinc porphyrin excited singlet and triplet states proceeds via electron transfer through the LUMO of the spacer, while the gold porphyrin triplet excited states reacts via hole transfer through the HOMO

of the spacer moiety. The reverse electron transfer shows no preferred pathway and may involve through-space electron transfer.[27]

Two of these bis-porphyrins phenanthroline units coordinate to a single copper(I) cation through the 1,10-phenanthroline spacer groups to form a robust tetrameric porphyrin ensemble.[28] In the tetra gold(III) porphyrin ensemble, triplet excition annihilation is accomplished with electron transfer from the copper(I) complex to a gold porphyrin triplet. A mixed multicomponent array, comprised of gold(III) and zinc(II) bisporphyrins covalently-linked to a copper(I) bis(1,10-phenanthroline) complex, undergoes a variety of electron-transfer reactions depending on which porphyrin absorbs the photon energy. The copper(I) complex participates in these electron-transfer processes via both direct (redox) and indirect (superexchange) mechanisms. The complexes and the results of photophysical studies are shown in Figures 5 and 6.

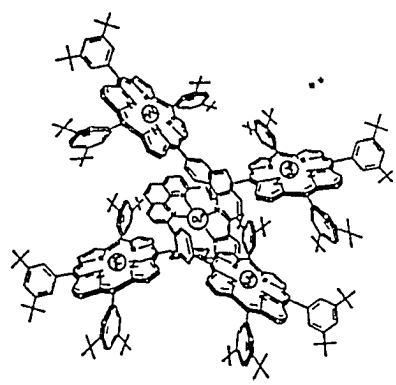

$M_1 = M_2 = Au$: n = 5
$M_1 = Au$: $M_2 = Zn$: n = 3

Figure 5. Cu-porphyrin tetramer (adapted from *Tetrahedron Lett.* **1991**, 197).

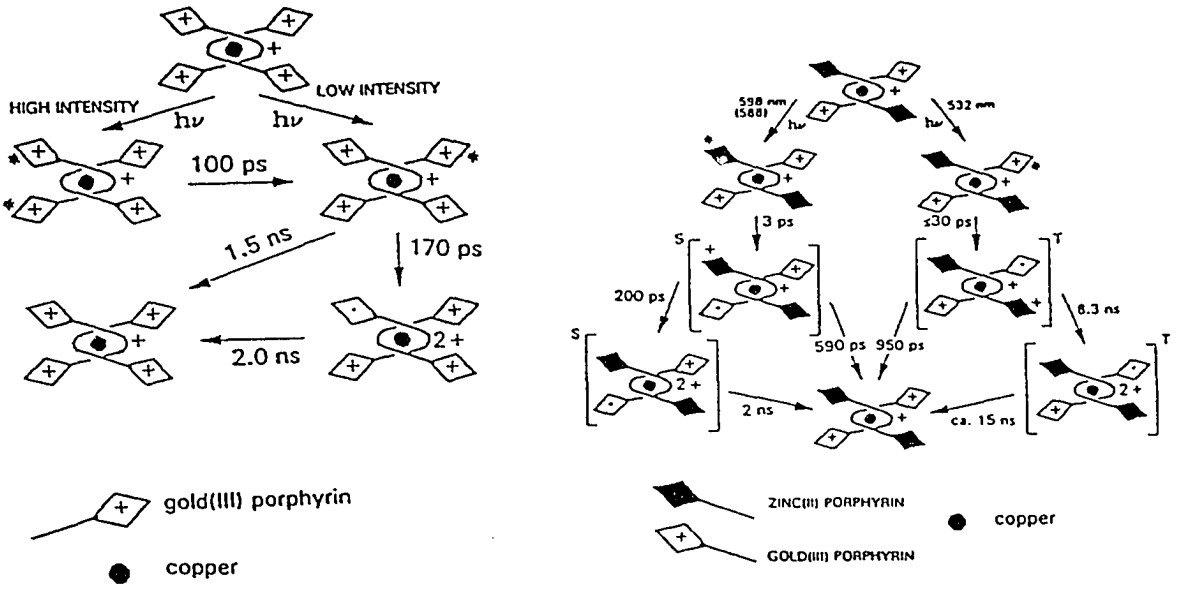

Figure 6. a) Cu-tetra gold porphyrin; b) Cu-gold porphyrin-zinc porphyrin (adapted from *J. Am. Chem. Soc.* 1992, *114*, 4632).

In these multicomponent systems, the central copper(I) complex plays an active role in: 1) assembling the tetrameric porphyrin ensemble, 2) catalyzing the forward electron transfer steps, and 3) functioning as an electron donor.

The bis-porphyrin 1,10-phenanthroline ligand has been used to synthesize rotaxanes built around copper(I) or zinc(II) cations or with no metal template as shown in Figure 7.[29] The photoinduced electron transfer between porphyrinic subunits in these rotaxanes has been studied.[30] Upon selective excitation of either porphyrin, rapid

electron transfer occurs from the zinc(II) porphyrin to the appended gold(III) porphyrin, generates zinc porphyrin π-radical cation and gold porphyrin neutral radical. In the copper(I) rotaxane, the copper(I) complex donates an electron to the resultant zinc porphyrin π-radical cation. The ground-state system is restored by relatively slow electron transfer from the gold porphyrin neutral radical to the copper(II) complex. The copper(I) complex mediates photoinduced electron transfer between the terminal porphyrinic subunits but not the reverse reaction. The coordinating cation modifies the energy of the orbitals on the spacer and affects the rate of electron transfer. The central Cu ion may be involved as a real intermediate in the electron-transfer pathway. Compared to the corresponding bis-porphyrin, rates of electron transfer and the magnitude of electronic coupling between the porphyrins are significantly lower in the rotaxanes.

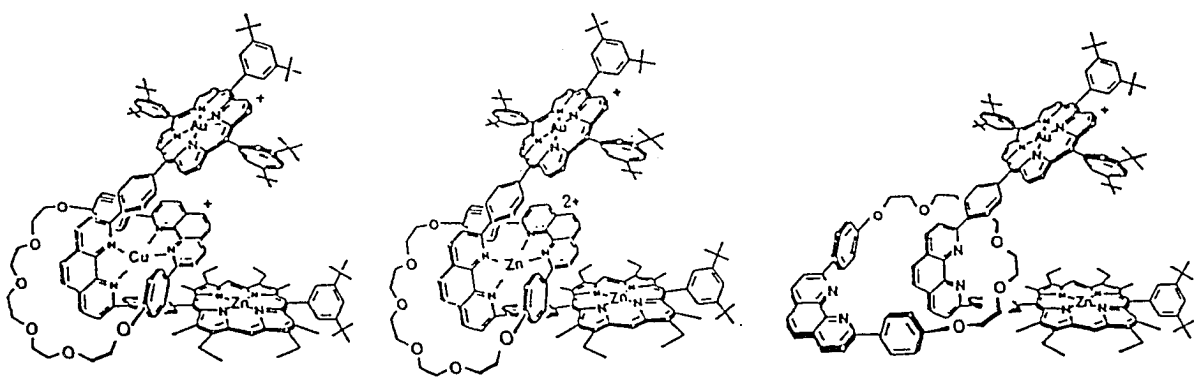

Figure 7. Structures of the rotaxane (reprinted with permission from *J. Am. Chem. Soc.* **1993**, *115*, 7419. Copyright © 1993 ACS)

Sauvage *et al.* have also prepared 5-(terpyridine)-10,15,20-triarylporphyrin and 5,15-bis(terpyridine)porphyrin. By using the coordinating properties of the terpy group towards transition metal like Rh and Ru, multicomponent systems with geometrically controlled linear arrays could be formed.[31] The photophysical properties of these systems have been studied.[32]

One of the linear arrays is a triad in which a central ruthenium(II) bis(terpy) complex is used as spacer for a zinc(II)-gold(III) bisporphyrin (Figure 8).[30a] In this complex, the center-to-center distance of the two porphyrin subunits is about 30 Å. Selective excitation of the zinc porphyrin subunit results in rapid electron transfer, first to the adjacent ruthenium(II) bisterpy complex and subsequently to the distant gold(III) porphyrin. The ruthenium(II) bisterpy complex is a real intermediate in the electron-transfer pathway. The ultimate charge-separated state, which is formed with a quantum yield of 0.6, retains approximately 1.2 eV of the photonic energy input of 2.1 eV. The system exhibits a relatively small reorganization energy (0.45 eV). Electron transfer occurs at relatively low thermodynamic driving force and favors rapid forward but slow reverse electron-transfer steps. The central ruthenium(II) bisterpy complex does not appear to enhance the rate of charge recombination between the final redox pairs, hence helping to ensure a long-lived charge-separated state.

The above examples show that assembling porphyrin subunits around a central metal ions is an attractive method for designing photosynthetic reaction center model systems. This method merits further exploration.

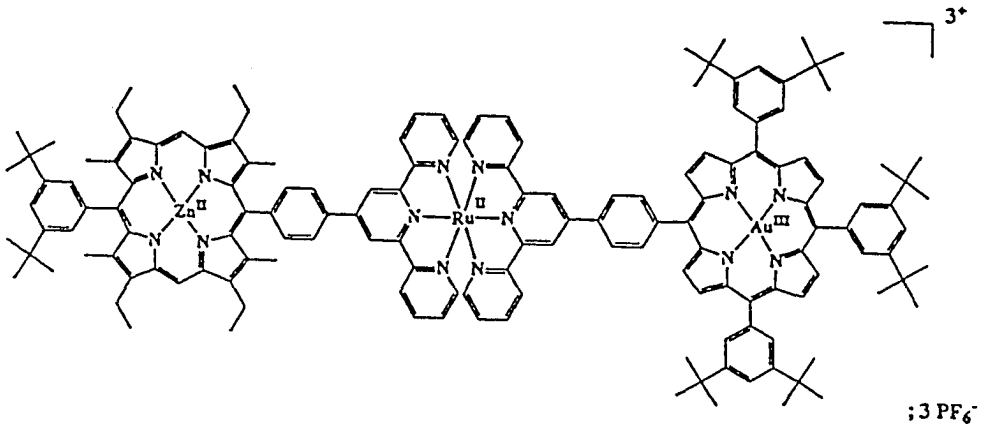

Figure 8. Zinc(II) porphyrin-Ru(II)-gold(III) porphyrin triad (reprinted with permission from *J. Am. Chem. Soc.* **1994**, *116*, 5481. Copyright © 1994 ACS).

The following chapter presents our research involving the synthesis, characterization, and molecular structure of Pd(II)- and Pt(II)-linked multi-porphyrin assemblies.

References

1. Priestly, J. *Phil. Trans. Roy. Soc. (London)* **1772**, *62*, 147.

2. (a) Gust, D.; Moore, T. A. *Adv. Photochem.* **1991**, *16*, 1. (b) Gust, D.; Moore, T. A. in *The Photosynthetic Reaction Center*, Deisenhofer, J.; Norris, J. R., Eds.;

Academic Press: San Diego, CA, **1993**, Chap. 14, pp. 419-464. (c) Wasielewski, M. R. in *The Photosynthetic Reaction Center*, Deisenhofer, J.; Norris, J. R., Eds.; Academic Press: San Diego, CA, **1993**, Chap. 15, pp. 465-511. (d) Wasielewski, M. R. *Chem. Rev.* **1992**, *92*, 435-461. (e) Harry, K.; Huber, M. *Angew. Chem.* **1995**, *107*, 927-947.

3. (a) Deisenhofer, J.; Epp, O.; Miki, K.; Huber, R.; Michel, H. *J. Mol. Biol.* **1984**, *180*, 385. (b) Chang, C. H.; Tiede, D. M.; Tang, J.; Norris, J. R.; Schiffer, M. *FEBS Lett.* **1986**, *205*, 82. (c) Allen, J. P.; Feher, G.; Yeates, T. O.; Deisenhofer, J.; Huber, R. *Proc. Natl. Acad. Sci. USA* **1986**, *83*, 8589.

4. Schwarz, F. P.; Gouterman, M.; Muljani, Z.; Dolphin, D. H. *Bioinorg. Chem.* **1972**, *1*, 1-32.

5. (a) Kong, J. L. Y.; Loach, P. A. In *Frontiers of Biological Energetics*; Dutton, P. L.; Leigh, J. S.; Scarpa, A., eds.; Academic Press: New York, **1978**; p 73. (b) Tabushi, I.; Koga, N.; Yanagita, M. *Tetrahedron Lett.* **1979**, 257.

6. Wasielewski, M. R.; Johnson, D. G.; Niemczyk, M. P.; Gaines, G. L.; O'Neil, M. P.; Svec, W. A. *J. Am. Chem. Soc.* **1990**, *112*, 6482-6488.

7. Heiler, D.; McLendon, G.; Rogalskyj, P. *J. Am. Chem. Soc.* **1987**, *109*, 604-606.

8. Johnson, D. G.; Svec, W. A.; Wasielewski, M. R. *Israel. J. Chem.* **1988**, *28*, 193.

9. Osuka, A.; Maruyama, K. *Chem. Lett.* **1987**, 825-828.

10. Osuka, A.; Maruyama, K. *J. Am. Chem. Soc.* **1988**, *110*, 4454-4456.

11. Lindsey, J. S.; Delaney, J. K.; Mauzerall, D. C.; Linschitz, H. *J. Am. Chem. Soc.* **1988**, *110*, 3610-3621.

12. Cowan, J. A.; Sanders, J. K. M.; Beddard, G. S.; Harrison, R. J. *J. Chem. Soc., Chem. Comm.* **1987**, 55-57.

13. (a) Osuka, A.; Morikawa, S.; Maruyama, K.; Hirayama, S.; Minami, T. *J. Chem. SOC., Chem. Comm.* **1987**, 359-361. (b) Sessler, J. L.; Johnson, M. R.; Lin, T.-Y. *Tetrahedron* **1989**, *45*, 4767-4784. (c) Sessler, J. L.; Johnson, M. R.; Creager, S. E.; Fettinger, J. C.; Ibers, J. A. *J. Am. Chem. Soc.* **1990**, *112*, 9310-9329. (d) Wasielewski, M. R.; Niemczyk, M. P.; Johnson, D. G.; Svec, W. A.; Minsek, D. W. *Tetrahedron* **1989**, *45*, 4785-4806. (e) Sakata, Y.; Nakashima, S.; Goto, Y.; Tatemitsu, H.; Misumi, S.; Asahi, T.; Hagihara, M.; Nishikawa, S.; Okada, T.; Mataga, N. *J. Am. Chem. Soc.* **1989**, *111*, 8979-8981. (f) Sakata, Y.; Tsue, H.; Goto, Y.; Misumi, S.; Asahi, T.; Nishikawa, S.; Okada, T.; Mataga, N. *Chem. Lett.* **1991**, 8979-8981.

14. (a) Gust, D.; Moore, T. A.; Liddell, P. A.; Nemeth, G. A.; Makings, L. R.; Moore, A. L.; Barrett, D.; Pessiki, P. J.; Bensasson, R. V.; Rougee, M.; Chachaty, C.; De Schryver, F. C.; Van der Auweraer, M.; Holzwarth, A. R.; Connolly, J. S. *J. Am. Chem. Soc.* **1987**, *109*, 846-856. (b) Chachaty, C.; Gust, D.; Moore, T. A.; Nemeth, G. A.; Liddell, P. A.; Moore, A. L. *Org. Magn. Reson.* **1984**, *22*, 39-46. (c) Gust, D.; Moore, T. A. *J. Photochem.* **1985**, *29*, 173-184. (d) Seta, P.;

Bienvenue, E.; Moore, A. L.; Mathis, P.; Bensasson, R. V.; Liddell, P. A.; Pessiki, P. J.; Joy, A.; Moore, T. A.; Gust, D. *Nature (london)* **1985**, *316*, 653-655. (e) Gust, D.; Moore, T. A.; Makings, L. R.; Liddell, P. A.; Nemeth, G. A.; Moore, A. L. *J. Am. Chem. Soc.* **1986**, *108*, 8028-8031. (f) Moore, T. A.; Gust, D.; Moore, A. L.; Bensasson, R. V.; Seta, P.; Bienvenue, e. In *Supramolecular photochemistry;* Balzani, V.; Ed.; D. Reidel: Boston, MA, **1987**, p 267. (h) Land, E. J.; Lexa, D.; Bensasson, R. V.; Gust, D.; Moore, T. A.; Moore, A. L.; Liddell, P. A.; Nemeth, G. *J. Phys. Chem.* **1987**, *91*, 4831-4835. (i) Moore, T. A.; Gust, D. In *Protein Structure, Molecular and Electronic Reactivity*; Austin, R.; Buhks, E.; Chance, B.; De Vault, D.; Dutton, P. L.; Frauenfelder, H.; Gol'danskii, V. I., Eds.; Springer: Berlin, Heidelberg, New York, **1987**; p 389. (j) Hung, S.-C.; Macpherson, A. N.; Lin, S.; Liddell, P. A.; Seely, G. R.; Moore, A. L.; Moore, T. A.; Gust, D. *J. Am. Chem. Soc.* **1995**, *117*, 1657-1658.

15. Parson, W. W. *Ann. Rev. Biophys. Bioeng.* 1982, *11*, 57.

16. (a) Gust, D.; Moore, T. A.; Moore, A. L.; Barrett, D.; Harding, L. O.; Makings, L. R.; Liddell, P. A.; De Schryver, F. C.; Van Der Auweraer, M.; Bensasson, R. V.; Rougee, M. *J. Am. Chem. Soc.* **1988**, *110*, 321-323. (b) Gust, D.; Moore, T. A.; Moore, A. L.; Seely, G.; Liddell, P.; Barrett, D.; Harding, L. O.; Ma, X. C.; Lee, S.-J.; Gao, F. *Tetrahedron* **1989**, *45*, 4867-4891.

17. Wasielewski, M. R.; Gaines, III, G. L.; O'Neil, M. P.; Niemczyk, M. P.; Svec, W.

A. In *Supramolecular Chemistry*; Balzani, V.; De Cola, L.; Eds.; Kluwer Academic: Boston, MA, **1991**; pp 201-218.

18. Tecilla, P.; Dixon, R. P.; Slobodkin, G.; Alavi, D. S.; Waldeck, D. H.; Hamilton, A. D. *J. Am. Chem. Soc.* **1990**, *112*, 9408-9410.

19. Turro, C.; Chang, C. K.; Leroi, G. E.; Cukier, R. I.; Nocera, D. G. *J. Am. Chem. Soc.* **1992**, *114*, 4013-4015.

20. Wasielewski, M. R.; Niemczyk, M. P.; Svec, W. A.; Pewitt, E. B. *J. Am. Chem. Soc.* **1985**, *107*, 1080.

21. (a) Aoyama, Y.; Asakawa, M.; Matsui, Y.; Ogoshi, H. *J. Am. Chem. Soc.* **1991**, *113*, 6233-6240. (b) Hayashi, T.; Miyahara, T.; Hashizume, N.; Ogoshi, H. *J. Am. Chem. Soc.* **1993**, *115*, 2049-2051.

22. (a) Harriman, A.; Magda, D.J.; Sessler, J. L. *J. Chem. Soc., Chem. Commun.* **1991**, 345-348. (b) Harriman, A.; Magda, D. J.; Sessler, J. L. *J. Phys. Chem.* **1991**, *95*, 1530-1532. (c) Harriman, A.; Kubo, Y.; Sessler, J. L. *J. Am. Chem. Soc.* **1992**, *114*, 388-390. (d) Harriman, A.; Wang, B.; Sessler, J. L. *J. Am. Chem. Soc.* **1993**, *115*, 10418-10419. (e) Sessler, J. L., Wang, B. Harriman, A. *J. Am. Chem. Soc.* **1995**, *117*, 704-714.

23. (a) Noblat, S.; Dietrich-Buchecher, C. O.; Sauvage, J.-P. *Tetrahedron Lett.* **1987**, *28*, 5829-5832. (b) Chardon-Noblat, S.; Sauvage, J.-P. *Tetrahedron* **1991**, *47*, 5123-5132. (c) Chardon-Noblat, S.; Sauvage, J.-P.; Mathis, P. *Angew. Chem., Int. Ed. Engl.* **1989**, *28*, 593.

24. Chardon-Noblat, S.; Guilhem, J.; Mathis, P.; Pascard, C.; Sauvage, J.-P.; In *Photoconversion Processes for Energy and Chemicals*; Hall, D. O, Grassi, G., Eds.; Elsevier: London, **1989**; p 90.

25. (a) Brun, A. M.; Harriman, A.; Heitz, V.; Sauvage, J.-P. *J. Am. Chem. Soc.* **1991**, *113*, 8657-8663. (b) Harriman, A.; Heitz, V.; Sauvage, J.-P. *J. Phys. Chem.* **1993**, *97*, 5940-5946.

26. (a) Closs, G. L.; Miller, J. R. *Science* **1988**, *240*, 440. (b) Miller, J. R. *Nouv. J. Chim.* **1987**, *11*, 83.

27. Miller, J. R.; Beitz, J. V.; Huddleston, R. K. *J. Chem. Phys.* **1984**, *106*, 5057.

28. (a) Heitz, V.; Chardon-Noblat, S.; Sauvage, J.-P. *Tetrahedron Lett.* **1991**, *32*, 197. (b) Brun, A. M.; Atherton, S. J.; Harriman, A.; Heitz, V.; Sauvage, J.-P. *J. Am. Chem. Soc.* **1992**, *114*, 4632-4639.

29. (a) Chambron, J.-C.; Heitz, V.; Sauvage, J.-P. *J. Chem. Soc., Chem. Commun.* **1992**, 1131-1133. (b) Chambron, J.-C.; Heitz, V.; Sauvage, J.-P. *J. Am. Chem. Soc.* **1993**, *115*, 12378-12384.

30. (a) Chambron, J.-C.; Harriman, A.; Heitz, V.; Sauvage, J.-P. *J. Am. Chem. Soc.* **1993**, *115*, 6109-6114. (b) Chambron, J.-C.; Harriman, A.; Heitz, V.; Sauvage, J.-P. *J. Am. Chem. Soc.* **1993**, *115*, 7419-7425.

31. (a) Collin, J.-P.; Heitz, V.; Sauvage, J.-P. *Tetrahedron Lett.* **1991**, *32*, 5977-5980. (b) Odobel, F.; Sauvage, J.-P.; Harriman, A. *Tetrahedron Lett.* **1993**, *34*, 8113-8116.

32. (a) Harriman, A.; Odobel, F.; Sauvage, J.-P. *J. Am. Chem. Soc.* **1994**, *116*, 5481-5482. (b) Collin, J.-P.; Harriman, A.; Heitz, V.; Odobel, F.; Sauvage, J.-P. *J. Am. Chem. Soc.* **1994**, *116*, 5679-5690.

CHAPTER 5: SYNTHESIS AND CHARACTERIZATION OF MONO-PYRIDYL TRIARYLPORPHYRIN Pd(II) AND Pt(II) COMPLEXES. MOLECULAR STRUCTURE OF A Pd-LINKED BISPORPHYRIN ASSEMBLY[1]

A paper to be submitted to *J. Am. Chem. Soc.*

Hongping Yuan, Leonard Thomas and L. Keith Woo[2]

Abstract

A series of mono-, bis- and tetra-porphyrin assemblies was synthesized from 5-pyridyl-10,15,20-triphenylporphyrin (H_2pyPP), 5-pyridyl-10,15,20-tri(*p*-tolyl)porphyrin (H_2pyTP), Zn(pyPP), Zn(pyTP) and Pt(II) and Pd(II) complexes. Porphyrin subunits assemble around the central metal ions through the pyridyl group. Treating *trans*-$Pd(DMSO)_2Cl_2$ with two equivalents of the pyridyl porphyrins, results in the *trans*-bisporphyrin assemblies $Pd(H_2pyPP)_2Cl_2$, $Pd(H_2pyTP)_2Cl_2$, $Pd[Zn(pyPP)]_2$ and $Pd[Zn(pyTP)]_2$. Treating *cis*-$Pt(DMSO)_2Cl_2$ with one equivalent of each pyridyl porphyrin produced the *cis*-monoporphyrin complexes $Pt(DMSO)(H_2pyPP)Cl_2$, $Pt(DMSO)(H_2pyTP)Cl_2$, $Pt(DMSO)[Zn(pyPP)]Cl_2$ and $Pt(DMSO)[Zn(pyTP)]Cl_2$. The treatment of $Pt(DMSO)(pyPOR)Cl_2$ with one more equivalent of pyridyl porphyrin, results in the formation of *cis*-bisporphyrin assemblies, $Pt(H_2pyPP)_2Cl_2$, $Pt(H_2pyTP)_2Cl_2$, $Pt[Zn(pyPP)]_2Cl_2$ and $Pt[Zn(pyTP)]_2Cl_2$. Also, the reaction of $Pt(DMSO)(pyPOR)Cl_2$ and

4-pyridyl-4'-methyl pyridinium iodide (MQ) afforded *cis*-porphyrin-Pt-MQ assemblies. Treatment of $M(DPPP)(OTf)_2$ (M = Pt, Pd; DPPP = 1,3-bis(diphenylphosphino)propane; OTf = triflate anion) with two equivalents of pyridyl porphyrin, results in *cis*-bisporphyrin assemblies $M(DPPP)(H_2pyPOR)_2(OTf)_2$ and $M(DPPP)[Zn(pyPOR)]_2(OTf)_2$. Synthesis of tetraporphyrin assembles $M(H_2pyTP)_4X_2$ (M = Pt, Pd; X = BF_4, OTf), was accomplished by the reaction of $M(CH_3CN)_4X_2$ with H_2pyTP. Solution ^1H NMR studies show that the four porphyrins are equivalent and the central metals have square planar geometry. The crystal structure of $Pd(DPPP)(H_2pyTP)_2(OTf)_2$ was determined by single-crystal X-ray diffraction analysis (monoclinic, $P2_1/n$, a = 13.211(5) Å, b = 36.741(19) Å, c = 22.971(10) Å, $\alpha = 90°$, $\beta = 91.54(3)°$, $\gamma = 90°$, V = 11145.8(86) $Å^3$, Z = 4, R = 8.25%, Rw = 18.44%).

Introduction

Photosynthesis is a key process in biological energy transduction that converts sunlight into stored chemical energy. Interest in photosynthesis remains at an extremely high level as exemplified by several recent reviews.[3] Understanding photoinduced electron transfer is a major objective of photosynthesis research and is of technological importance for the design of synthetic molecular devices.[4] It is clear that the ability to mimic this natural process in the laboratory would have great technological significance in terms of solar energy conversion and storage. Synthetic porphyrin-based assemblies

have been extensively used as models for molecular organization and energy/electron transfer processes.[5,6,7,8,9]

Although many clever and ingenious models have been prepared, the maximum efficiencies for charge separation and the lifetimes of the charged-separated states obtained to date are still well below those achieved by green plants and photosynthetic bacteria. It is clear that the sophistication of synthetic multi-component species that mimic primary events of natural photosynthesis has increased tremendously. However, as the types and numbers of components are increased, the level of complexity also expands and model systems become more difficult to prepare. To a large extent, progress in this area is still significantly synthesis limited. Most of the existing model systems are linked through organic spacers.[2-7] The synthetic methods for these systems typically are multistep processes and yields are often extremely low. Recently some attempts have turned to developing new strategies for designing assemblies that can achieve sequential multi-step electron transfer processes. Sessler *et al.* have prepared model systems that linked donors and acceptors through hydrogen-bonds.[10] Sauvage *et al.* have designed bis(terpyridyl)porphyrins, and utilized the terpyridyl group to build donor-acceptor arrays.[11]

We have developed new methods for utilizing transition metal coordination properties to place subunits at designated positions and at fixed distances. We report herein the synthesis of porphyrin and porphyrin-viologen assemblies linked by Pd(II) or Pt(II) ions. The porphyrins used here are monopyridyltriarylporphyrins and the

corresponding Zn complexes. Starting with Pd(II) and Pt(II) complexes, a series of bis-porphyrin and tetra-porphyrin assemblies has been synthesized. With Pt(II), it is possible to replace labile ligands in a stepwise manner to form porphyrin-metal-viologen complexes. When 1,3-bis(diphenylphosphino)propane (DPPP) was employed as an ancillary ligand around Pd(II) and Pt(II), bisporphyrin assemblies with the composition $M(DPPP)(POR)_2(OTf)_2$ (M= Pt, Pd; POR = H_2pyTP, ZnpyTP), were synthesized. The molecular structure of $Pd(DPPP)(H_2pyTP)_2(OTf)_2$ has been determined. This is the first example of a porphyrin assembly linked by a metal ion which has been characterized structurally by single-crystal X-ray diffraction. However, a related series of compounds recently appeared.[12] In particular, the assemblies, $M(H_2pyPP)_2Cl_2$ and $M[Zn(PyPP)]_2Cl_2$ (M = Pd, Pt), prepared by Drain and Lehn were also reported by us.[1]

Experimental

General. All reagents were analytical grade. THF and toluene were freshly distilled from purple solutions containing sodium and benzophenone. CH_3CN, CH_2Cl_2 and $CHCl_3$ were distilled from CaH_2. 5-Pyridyl-10,15,20-triphenylporphyrin (H_2pyPP) and 5-pyridyl-10,15,20-tritolylporphyrin (H_2pyTP) were synthesized according to a method reported elsewhere.[13] The corresponding Zn metalloporphyrins were prepared by standard methods.[14] *Cis*-$Pt(DMSO)_2Cl_2$[15], *trans*-$Pd(DMSO)_2Cl_2$,[15] $Pt(DPPP)Cl_2$,[16] $Pd(DPPP)Cl_2$,[16] $Pt(DPPP)(OTf)_2$[16] and $Pd(DPPP)(OTf)_2$[16], $Pt(CH_3CN)_4(OTf)_2$ and $Pd(CH_3CN)_4(OTf)_2$[17] were prepared according to literature procedures.

UV-visble data were obtained using a Hewlett-Packard HP 8452A diode-array spectrophotometer. ^{1}H NMR spectra were recorded on a Nicolet NT300 spectrometer, on a Varian VXR 300-MHz spectrometer or on a Bruker DRX 400-MHz spectrometer. Proton peak positions are referenced to TMS and assignments were made with the aid of 2D-COSY experiments. ^{31}P NMR spectra were recorded on a Bruker AC 200-MHz spectrometer and all phosphorus chemical shifts are reported in ppm relative to the external 85% H_3PO_4. IR spectra were recorded from KBR pellets on a IBM/Bruker IR-98 or on a BIO-RAD Digilab FTS-7 spectrometer. Elemental analyses were performed by Atlantic Microlabs, Norcross, Georgia.

Preparations

5-Pyridyl-10,15,20-tritolylporphyrin (H_2pyTP). H_2pyTP was prepared according to a modified literature method[13] using *p*-tolualdehyde in place of benzaldehyde. Pyrrole (20.8 mL, 0.300 mol), *p*-tolualdehyde (23.6 mL, 0.200 mol), 4-pyridinecarboxaldehyde (6.6 mL, 0.080 mol) and 700 mL propionic acid were added to a two-liter 3-necked round bottom flask. The mixture was refluxed for 3 hours, cooled to ambient temperature, and allowed to sit over-night. Purple crystals (7.0 g) were filtered and washed with cold methanol. Two-gram batches of this mixture were loaded on a flash chromatography column packed with silica gel (30 x 5 cm). CH_2Cl_2 was used to remove H_2TTP. Chloroform was used next to wash H_2pyTP off the column. The combined yield of H_2pyTP was 1.26 g (2.4%). ^{1}H NMR ($CDCl_3$, 300 MHz, ppm): 9.00 (d, 2H, J = 5.7

Hz, py-H_o), 8.89 (d, 2H, J= 4.8 Hz, β-H), 8.85 (s, 4H, β-H), 8.75 (d, 2H, J = 4.8 Hz, β-H), 8.14 (d, 2H, J = 5.7 Hz, py-H_m), 8.07 (d, 6H, J = 7.5 Hz, phenyl-H_o), 7.54 (d, 6H, J = 7.5 Hz, phenyl-H_m), 2.69 (s, 9H, Me), -2.82 (s, 2H, internal N*H*). UV-vis (CH_2Cl_2, nm): 418 (Soret), 482(s), 514, 548, 588, 646.

5-Pyridyl-10,15,20-triphenylporphyrinato zinc(II), Zn(pyPP). To a solution of H_2pyPP (250 mg, 0.400 mmol) in chloroform (100 mL) was added a saturated solution of zinc acetate (175 mg, 0.800 mmol) in methanol (5.0 mL). After 30 min of heating at reflux, the mixture was concentrated to about 3 mL, diluted with 10 mL methanol, and cooled to -20 °C for 8 hours. Purple crystals were filtered and washed with cold methanol to afford 265 mg of product (yield = 96%). ^{1}H NMR ($CDCl_3$, 300 MHz, ppm): 8.93 (s, 2H, β-H), 8.85 (m, 4H, β-H), 8.52 (d, 2H, J = 4.5 Hz, β-H), 8.20 (m, 2H, py-H_o), 8.08 (d, 6H, J = 6.6 Hz, phenyl-H_o), 7.77-7.62 (m, 11H, py-H_m, phenyl-$H_{m,p}$), 7.42 (bs, py-H_o from coordination oligomers), 6.24 (bs, py-H_m from coordination oligomers). (C_5D_5N, 300 MHz, ppm): 9.13 (d, 2H, J = 4.8 Hz, β-H), 9.10 (s, 6H, β-H, py-H_o), 9.03 (d, 2H, J = 4.8 Hz, β-H), 8.34 (m, 6H, phenyl-H_o), 8.24 (d, 2H, J = 5.7 Hz, py-H_m), 7.74 (m, 9H, phenyl-H_m). UV-vis (CH_2Cl_2, nm): 418 (Soret), 560, 604.

5-Pyridyl-10,15,20-tritolylporphyrinato zinc(II), Zn(pyTP). The same procedure for making Zn(pyPP) was employed using H_2pyTP (265 mg, 0.400 mmol) in place of H_2pyPP. Yield: 275 mg (95%). ^{1}H NMR ($CDCl_3$, 400 MHz, ppm): 8.86 (m, 6H, β-H), 8.55 (d, 2H, J = 4.4 Hz, β-H), 8.06 (d, 2H, J = 8.4 Hz, py-H_o), 7.97 (d, 6H, J = 7.2 Hz, phenyl-H_o), 7.50 (d, 6H, J = 7.2 Hz, phenyl-H_m), 7.45 (d, 2H, J = 8.4 Hz, py-

H_m), 2.71 (s, 6H, 10,20-phenyl-Me), 2.63 (s, 3H, 15-phenyl-Me). (C_5D_5N, 400 MHz, ppm): 9.21 (s, 2H, β-H), 9.19 (s, 6H, β-H), 9.10 (d, 2H, J = 5.3 Hz, py-H_o), 9.04 (d, 2H, J = 5.3 Hz, py-H_m), 8.24 (d, 12 H, J = 6.9 Hz, phenyl-$H_{o,m}$), 2.54 (s, 9H, Me). UV-vis (CH_2Cl_2, nm): 422 (Soret), 562, 610.

***Trans*-Pd(H_2pyPP)$_2Cl_2$.** *Trans*-Pd(DMSO)$_2Cl_2$ (17 mg, 0.050 mmol) and H_2pyPP (62 mg, 0.10 mmol) were dissolved in 20 mL of $CHCl_3$ in a 50-mL round-bottom flask and heated at reflux for 4 hours. The mixture was cooled to ambient temperature and solvent was removed under reduced pressure. The residue was loaded on a silica column (25 x 2.5 cm), and eluted with $CHCl_3$. The first band was collected and solvent was removed under reduced pressure. The product was recrystallized from CH_2Cl_2/hexane, filtered, washed with hexane and air dried to give 70 mg (95% yield) of purple solid. R_f = 0.80 (on silica gel TLC, in $CHCl_3$). ^{1}H NMR ($CDCl_3$, 300 MHz, ppm): 9.39 (d, 4H, J = 6.3 Hz, py-H_o), 8.94 (d, 4H, J = 4.8 Hz, β-H), 8.86(s, 8H, β-H), 8.83 (d, 4H, J = 4.8 Hz, β-H), 8.29 (d, 4H, J = 6.3 Hz, py-H_m), 8.21 (d, 12H, J = 7.2 Hz, phenyl-H_o), 7.78 (m, 18H, phenyl-$H_{m,p}$), 1.51 (s, 2H, H_2O), -2.81 (s, 4H, internal N*H*). UV-vis (CH_2Cl_2, nm): 420 (Soret), 484(s), 516, 552, 592, 646. IR (KBr): $\nu_{Pd\text{-}Cl}$ = 367 cm^{-1}. Anal. Calcd. (found) for $C_{86}Cl_2H_{58}N_{10}Pd{\cdot}H_2O$: C, 72.40 (72.36), H, 4.24 (4.22), N, 9.82 (9.90).

***Trans*-Pd[Zn(pyPP)]$_2Cl_2$.** *Trans*-Pd(DMSO)$_2Cl_2$ (17 mg, 0.050 mmol) and Zn(pyPP) (68 mg, 0.10 mmol) were dissolved in 20 mL $CHCl_3$ in a 50-mL round-bottom flask and heated at reflux for 2 hours. The mixture was cooled to ambient temperature and solvent was removed under reduced pressure. The residue is not soluble in most

organic solvents except pyridine. The product was air dried to give 70 mg (91% yield) of purple solid. ^{1}H NMR (C_5D_5N, 300 MHz, ppm): 9.20-9.13 (m, 16H, β-H), 9.05 (d, 4H, J = 6.0 Hz, py-H_o), 8.37 (br, 12H, phenyl-H_o), 8.27 (d, 4H, J = 6.0 Hz, py-H_m), 7.76 (m, 18H, phenyl-$H_{m,p}$). UV-vis (pyridine, nm): 428 (Soret), 562, 602. MS {ESI} Calcd. (found) m/e: 1619.7 (1620.6) $[MH]^+$.

***Trans*-Pd(H_2pyTP)$_2Cl_2$.** A similar method for preparation of Pd(H_2pyPP)$_2Cl_2$ was used, replacing H_2pyPP with H_2pyTP (66 mg, 0.10 mmol). The product was isolated as a purple power (69 mg, 92%). ^{1}H NMR ($CDCl_3$, 300 MHz, ppm): 9.38 (d, 4H, J = 6.3 Hz, py-H_o), 8.96 (d, 4H, J = 5.0 Hz, β-H), 8.88 (s, 8H, β-H), 8.81 (d, 4H, J = 5.0 Hz, β-H), 8.28 (d, 4H, J = 6.4 Hz, py-H_m), 8.10 (d, 8H, J = 7.8 Hz, 10,20-phenyl-H_o), 8.08 (d, 4H, J = 7.8 Hz phenyl-H_o), 7.58 (d, 8H, J = 7.8 Hz, 10,20-phenyl-H_m), 7.55 (d, 4H, J = 7.8H, 15-phenyl-H_m), 2.72 (s, 12H, 10,20-phenyl-Me) 2.70 (s, 6H, 15-phenyl-Me), -2.79 (s, 4H, internal N*H*). UV-vis (CH_2Cl_2, nm): 422 (Soret), 484(s), 518, 554, 592, 648. MS {ESI} Calcd. (found) m/e: 1490.4 (1491.0) $[MH]^+$.

***Cis*-Pt(DMSO)(H_2pyPP)Cl_2.** *Cis*-Pt(DMSO)$_2Cl_2$ (42 mg, 0.10 mmol) and H_2pyPP (62 mg, 0.10 mmol) were dissolved in 20 mL CH_2Cl_2 in a 50-mL round-bottom flask and stirred for 4 hours at ambient temperature. The solvent was removed under reduced pressure and the solid residue was loaded on a silica column (25 x 2.5 cm) and eluted with $CHCl_3$/ethyl acetate (5:1). The second band was collected and taken to dryness under reduced pressure. The product was recrystallized from CH_2Cl_2/hexane to afford 92 mg (95% yield) of purple solid. R_f = 0.35 (silica gel TLC, in $CHCl_3$). ^{1}H NMR ($CDCl_3$,

300 MHz, ppm): 9.17 (d, 2H, J = 6.5 Hz, py-H_o), 8.91 (d, 2H, J = 4.8 Hz, β-H), 8.84 (s, 4H, β-H), 8.74 (d, 2H, J = 4.8 Hz, β-H), 8.28 (d, 2H, J = 6.5 Hz, py-H_m), 8.19 (d, 6H, J = 7.2 Hz, phenyl-H_o), 7.77 (m, 9H, phenyl-$H_{m,p}$), 3.60 (s, 6H, Me on DMSO), -2.83 (s, 2H, internal N*H*). UV-vis (CH_2Cl_2, nm): 420 (Soret), 484(s), 516, 552, 590, 646.

***Cis*-Pt(DMSO)(H_2pyTP)Cl_2.** H_2pyTP (66 mg, 0.10 mmol) was used in place of H_2pyPP, in a similar method for the preparation of *cis*-Pt(DMSO)(H_2pyPP)Cl_2. Yield: 90 mg (90%). ^{1}H NMR ($CDCl_3$, 300 MHz, ppm): 9.15 (d, 2H, J = 5.9 Hz, py-H_o), 8.92 (d, 2H, J = 4.5 Hz, β-H), 8.86 (s, 4H, β-H), 8.72 (d, 2H, J = 4.5 Hz, β-H), 8.26 (d, 2H, J = 5.9 Hz, py-H_m), 8.06 (d, 6H, J = 7.5 Hz, phenyl-H_o), 7.55 (d, 6H, J = 7.5 Hz, phenyl-H_m), 3.60 (s, 6H, DMSO), 2.69 (s, 9H, Me), 1.50 (s, 2H, H_2O), -2.82 (s, 2H, internal N*H*). UV-vis (CH_2Cl_2, nm): 422 (Soret), 484(s), 518, 554, 592, 648. Anal. Calcd. (found) for $C_{48}Cl_2H_{41}N_5OSPt{\cdot}H_2O$: C, 56.53 (56.25), H, 4.25 (4.20), N, 6.87 (6.86). MS {ESI} Calcd. (found) m/e: 1000.9 (1001.9) $[MH]^+$.

***Cis*-Pt(DMSO)[Zn(pyPP)]Cl_2.** A similar procedure for the preparation of Pt(DMSO)(H_2pyPP)Cl_2 was employed, using Zn(pyPP) (68 mg, 0.10 mmol) in place of H_2pyPP. Yield: 96 mg (93%). ^{1}H NMR ($CDCl_3$, 300 MHz, ppm): 9.14 (d, 2H, J = 6.8 Hz, py-H_o), 9.01 (d, 2H, J = 4.8 Hz, β-H), 8.94 (m, 4H, β-H), 8.84 (d, 2H, J = 4.8 Hz, β-H), 8.28 (d, 2H, J = 6.8 Hz, py-H_m), 8.19 (m, 6H, phenyl-H_o), 7.75 (m, 9H, phenyl-$H_{m,p}$), 3.56 (s, 6H, DMSO). UV-vis (CH_2Cl_2, nm): 420 (Soret), 548, 588.

***Cis*-Pt(DMSO)[Zn(pyTP)]Cl_2.** A similar procedure for the preparation of Pt(DMSO)(H_2pyPP)Cl_2 was employed, using Zn(pyTP) (72 mg, 0.10 mmol) in place of

H_2pyPP. Yield: 98 mg (92%). ^{1}H NMR ($CDCl_3$, 400 MHz, ppm): 9.14 (d, 2H, J = 5.8 Hz, py-H_o), 9.02 (d, 2H, J = 4.4, β-H), 8.96 (s, 4H, β-H), 8.82 (d, 2H, J = 4.4 Hz, β-H), 8.27 (d, 2H, J = 5.8 Hz, py-H_m), 8.07 (d, 6H, J = 7.4 Hz, phenyl-H_o), 7.55 (d, 6H, J = 7.4 Hz, phenyl-H_m), 3.58 (s, 6H, DMSO), 2.70 (s, 9H, Me), 1.50 (s, 2H, H_2O). UV-vis (CH_2Cl_2, nm): 420 (Soret), 548, 588. Anal. Calcd. (found) for $C_{48}Cl_2H_{39}N_5OSPtZn\cdot H_2O$: C, 53.22 (52.98), H, 3.81 (3.77), N, 6.40 (6.47). MS {ESI} Calcd. (found) m/e: 1065.3 (1066) $[MH]^+$.

***Cis*-Pt(H_2pyPP)$_2Cl_2$.** Method A. *Cis*-Pt(DMSO)$_2Cl_2$ (21 mg, 0.050 mmol) and H_2pyPP (62 mg, 0.10 mmol) were dissolved in 20 mL toluene in a 50-mL round-bottom flask and heated at reflux for 36 hours. The mixture was cooled to ambient temperature and solvent was removed under reduced pressure. The residue was loaded on a silica column (25 x 2.5 cm) and eluted with $CHCl_3$. The first band was collected and taken to dryness under reduced pressure. The product was recrystallized from CH_2Cl_2/hexane to afford 72 mg (96% yield) of purple solid. Method B. Pt(DMSO)(H_2pyPP)Cl_2 (50 mg, 0.050 mmol) was added to the solution of H_2pyPP (32 mg, 0.050 mmol) in toluene (20 mL) and heated at reflux for 36 hours. The product was isolated as described in method A to afford 65 mg (87% yield) of purple solid. R_f = 0.84 (silica gel TLC, in $CHCl_3$). ^{1}H NMR ($CDCl_3$, 300 MHz, ppm): 9.47 (d, 4H, J = 6.2 Hz, py-H_o), 8.96 (d, 4H, J = 4.8 Hz, β-H), 8.86 (m, 12H, β-H), 8.26 (d, 4H, J = 6.2 Hz, py-H_o), 8.22 (m, 12H, phenyl-H_o), 7.78 (m, 18H, phenyl-$H_{m,p}$), -2.80 (s, 4H, internal N*H*). UV-vis (CH_2Cl_2, nm): 420

(Soret), 484(s), 516, 552, 590, 646. IR (KBr): $\nu_{Pt\text{-}Cl}$ = 354, 324 cm^{-1}. MS {ESI} Calcd. (found) m/e: 1495.4 (1496) $[MH]^+$.

***Cis*-Pt(H_2pyTP)$_2Cl_2$.** Method A for the preparation of *Cis*-Pt(H_2pyPP)$_2Cl_2$ was used, except H_2pyTP (66 mg, 0.10 mmol) was substituted for H_2pyPP. Yield: 74 mg of purple product (93%). ^{1}H NMR ($CDCl_3$, 300 MHz, ppm): 9.46 (d, 4H, J = 6.3 Hz, py-H_o), 8.96 (d, 4H, J = 4.8 Hz, β-H), 8.87 (s, 8H, β-H), 8.83 (d, 4H, J = 4.8 Hz, β-H), 8.25 (d, 4H, J = 6.3 Hz, py-H_m), 8.08 (d, 12H, J = 7.8 Hz, phenyl-H_o), 7.57 (m, 12H, phenyl-H_m), 2.72 (s, 12H, 10,20-phenyl-Me), 2.70 (s, 6H, 15-phenyl-Me), -2.79 (s, 4H, internal N*H*). UV-vis (CH_2Cl_2, nm): 422 (Soret), 484(s), 518, 554, 592, 649. Anal. Calcd. (found) for $C_{92}Cl_2H_{70}N_{10}Pt$: C, 69.87 (69.38), H, 4.48 (4.38), N, 8.86 (8.58). MS{ESI} Calcd.(found) m/e: 1579 (1579) $[M]^+$.

***Cis*-Pt(H_2pyPP)(MQ)Cl_2.** *Cis*-Pt(DMSO)(H_2pyPP)Cl_2 (37 mg, 0.037 mmol) was added to a boiling solution of 4-pyridyl-4'-methyl pyridinium iodide (MQ) (45 mg, 0.15 mmol) in 25 mL of THF/EtOH (1:1 v/v). The mixture was heated at reflux under N_2 for 12 hours. After removing the solvent under reduced pressure, the residue was dissolved in CH_2Cl_2 and filtered to remove excess 4-pyridyl-4'-methyl pyridinium iodide. This process was repeated twice to produce a purple solid (30 mg, 70%). ^{1}H NMR ($CDCl_3$, 300 MHz, ppm): 9.51 (d, 2H, J = 5.4 Hz, py-H_o), 8.97 (d, 2H, J = 5.6 Hz, MQ-H_o), 8.86 (m, 2H, MQ-$H_{o'}$), 8.84 (m, 6H, β-H), 8.77 (d, 2H, J = 5.1 Hz, β-H), 8.19 (m, 8H, py-H_m, phenyl-H_o), 8.14 (d, 2H, J = 5.6 Hz, MQ-H_m), 7.76 (m, 9H, phenyl-$H_{m,p}$), 7.61 (d, 2H, J =

6.0 Hz, MQ-$H_{m'}$), 4.78 (s, 3H, MQ-Me), -2.84 (s, 2H, internal N*H*). UV-vis (CH_2Cl_2, nm): 418 (Soret), 514, 548, 588, 644.

***Cis*-Pt(H_2pyTP)(MQ)Cl_2.** A similar method for the preparation of Pt(H_2pyPP)(MQ)Cl_2 was employed, using Pt(DMSO)(H_2pyTP)Cl_2 (37 mg, 0.037 mmol) in place of Pt(DMSO)(H_2pyPP)Cl_2. Yield: 23 mg (51%). ^{1}H NMR ($CDCl_3$, 300 MHz, ppm): 9.42 (d, 2H, J = 6.3, py-H_o), 8.97 (d, 2H, J = 5.4 Hz, MQ-H_o), 8.89 (d, 2H, J = 5.6 Hz, MQ-$H_{o'}$), 8.85 (m, 6H, β-H), 8.75 (d, 2H, J = 4.5 Hz, β-H), 8.19 (d, 2H, J = 5.4 Hz, MQ-H_m), 8.14 (d, 2H, J = 6.3 Hz, py-H_m), 8.07 (d, 6H, J = 7.8 Hz, phenyl-H_o), 7.59 (d, 2H, J = 5.6 Hz, MQ-$H_{m'}$), 7.53 (d, 6H, J = 7.8 Hz, phenyl-H_m), 4.73 (s, 3H, MQ-Me), 2.69 (s, 9H, Me), -2.83 (s, 2H, internal N*H*). UV-vis (CH_2Cl_2, nm): 418 (Soret), 514, 548, 588, 644.

***Cis*-Pt[Zn(pyPP)](MQ)Cl_2.** This complex was prepared from Pt(DMSO)[Zn(pyPP)]Cl_2 (29 mg, 0.028 mmol) and 4-pyridyl-4'-methyl pyridinium iodide (34 mg, 0.12 mmol) by the same method used for the preparation of Pt(H_2pyPP)(MQ)Cl_2. Yield: 25 mg (72%). ^{1}H NMR ($CDCl_3$, 400 MHz, ppm): 9.37 (br, 2H, py-H_o), 8.85 (m, 6H, β-H), 8.54 (br, 2H, β-H), 8.37 (br, 2H, MQ-H_o), 8.18 (d, 2H, J = 6.8 Hz, MQ-$H_{o'}$), 8.09 (d, 8H, J = 6.4 Hz, py-H_m, phenyl-H_o), 7.74-7.65 (m, 11H, MQ-$H_{m'}$, phenyl-$H_{m,p}$), 7.43 (d, 2H, J = 4.8 Hz, MQ-H_m), 4.67 (s, 3H, MQ-Me). Peak assignments for MQ-H_o and MQ-H_m are less certain because cross peaks were too weak to be observed in the 2D-COSY experiment. UV-vis (CH_2Cl_2, nm): 418 (Soret), 550, 606.

***Cis*-Pt[Zn(pyTP)](MQ)Cl_2.** A similar method for the preparation of Pt[Zn(pyPP)](MQ)Cl_2 was employed, using Pt(DMSO)[Zn(pyTP)]Cl_2 (30 mg, 0.028 mmol) in place of Pt(DMSO)[Zn(pyPP)]Cl_2. Yield: 22 mg (60%). ^{1}H NMR ($CDCl_3$, 400 MHz, ppm): 9.10 (d, 2H, J = 6.2 Hz, py-H_o), 8.88 (m, 8H, MQ-H_o, β-H), 8.67 (d, 2H, J = 4.8 Hz, β-H), 8.60 (br, 2H, MQ-$H_{o'}$), 8.07 (d, 2H, J = 6.2 Hz, py-H_m), 8.04 (d, 6H, J = 7.6 Hz, phenyl-H_o), 7.98 (m, 2H, MQ-H_m), 7.50 (m, 8H, phenyl-H_m, MQ-$H_{m'}$), 4.55 (s, 3H, MQ-Me), 2.68 (s, 9H, phenyl-Me). Assignments for MQ-$H_{o'}$ and MQ-$H_{m'}$ are less certain because cross peaks in the 2D-COSY spectrum were too weak to be observed. UV-vis (CH_2Cl_2, nm): 418 (Soret), 552, 606. Anal. Calcd. (found) for $C_{57}Cl_2H_{44}IN_7PtZn$: C, 53.47 (53.92); H, 3.65 (3.99); N, 7.98 (8.44).

***Cis*-Pd(DPPP)(H_2pyTP)$_2$($OTf)_2$** Pd(DPPP)Cl_2 (60 mg, 0.10 mmol) and $Ag(OSO_2CF_3)$ (53 mg, 0.21 mmol) were dissolved in 50 mL CH_2Cl_2 and the mixture was stirred under argon in the dark for 3 hours. AgCl was removed by filtration and the filtrate was concentrated to 5 mL. H_2pyTP (135 mg, 0.210 mmol) and 50 mL acetone were added to the filtrate and the mixture was stirred at room temperature for 5 hours. Solvent was removed under reduced pressure and the residue was recrystallized from CH_2Cl_2/hexane. The production was a purple solid (196 mg, 92%). ^{1}H NMR ($CDCl_3$, 300 MHz, ppm): 9.61 (d, 4H, J = 6.6 Hz, py-H_o), 8.83 (d, 8H, J = 4.8 Hz, β-H), 8.75 (br, 4H, β-H), 8.22 (br, 4H, β-H), 8.08 (m, 24H, py-H_m, porphyrin phenyl-H_o, DPPP-phenyl-H_o), 7.63 (t, 12H, J = 7.4 Hz, DPPP-phenyl-$H_{m,p}$), 7.55 (d, 12H, J = 7.8 Hz, porphyrin phenyl-H_m), 3.47 (m, 4H, -CH_2-P), 2.70 (s, 18H, Me), 2.49 (m, 2H, -CH_2-), -

2.88 (s, 4H, internal N*H*). ^{31}P NMR (acetone-d_6, ppm): 6.91. UV-vis (CH_2Cl_2, nm): 420 (Soret), 518, 554, 592, 648.

***Cis*-Pd(DPPP)[Zn(pyTP)]$_2$(OTf)$_2$.** *Cis*-Pd(DPPP)[Zn(pyTP)]$_2$(OTf)$_2$ was prepared analogously to Pd(DPPP)(H_2pyTP)$_2$(OTf)$_2$, except that Zn(pyTP) (150 mg, 0.210 mmol) was added to the Pd(DPPP)(OTf)$_2$ solution. Yield: 203 mg of purple power (90%). ^{1}H NMR ($CDCl_3$, 400 MHz, ppm): 9.57 (d, 4H, J = 6.0 Hz, py-H_o), 8.96 (s, 8H, β-H), 8.84 (m, 4H, β-H), 8.54 (br, 4H, β-H), 8.11-7.90 (m, 24H, porphyrin phenyl-H_o, DPPP-phenyl-H_o, py-H_m), 7.66-7.35 (m, 24H, porphyrin phenyl-H_m, DPPP-phenyl-$H_{m,p}$), 3.45 (m, 4H, -C*H*$_2$-P), 2.70 (s, 12H, 10,20-phenyl-Me), 2.66 (br, 2H, -C*H*$_2$-), 2.63 (s, 6H, 15-phenyl-Me). ^{31}P NMR ($CDCl_3$, ppm): 5.28. UV-vis (CH_2Cl_2, nm): 422 (Soret), 550, 592. MS {ESI} Calcd. (found) m/e: 2261.1 (2262) $[MH]^+$.

***Cis*-Pt(DPPP)(H_2pyTP)$_2$(OTf)$_2$.** *Cis*-Pt(DPPP)(H_2pyTP)$_2$(OTf)$_2$ was prepared analogously to Pd(DPPP)(H_2pyTP)$_2$(OTf)$_2$. However, Pt(DPPP)Cl_2 (68 mg, 0.10 mmol) was used. Yield: 195 mg of purple powder (86%). ^{1}H NMR ($CDCl_3$, 400 MHz, ppm): 9.68 (d, 4H, J = 4.6 Hz, py-H_o), 8.86 (m, 8H, β-H), 8.75 (br, 4H, β-H), 8.24 (br, 4H, β-H), 8.15 (d, 4H, J = 4.6 Hz, py-H_m), 8.07 (d, 20H, PPh_2-H_o, porphyrin phenyl-H_o), 7.64 (t, 12H, J = 7.2 Hz, PPh_2-$H_{m,p}$), 7.54 (m, 12 H, porphyrin-phenyl H_m), 3.54 (m, 4H, -C*H*$_2$-P), 2.70 (s, 18H, Me), 2.47 (m, 2H, -C*H*$_2$-), -2.87 (s, 4H, interal N*H*). ^{31}P NMR (acetone-d_6, ppm): -15.00 ($J_{Pt\text{-}P}$ = 3235 Hz). UV-vis (CH_2Cl_2, nm): 420 (Soret), 448, 518, 550, 592, 650. MS {ESI} Calcd. (found) m/e: 960.8 (961) $[(M\text{-}2OTf)]^{2+}$.

***Cis*-Pt(DPPP)[Zn(pyTP)]$_2$(OTf)$_2$.** *Cis*-Pt(DPPP)[Zn(pyTP)]$_2$(OTf)$_2$ was synthesized analogously to Pt(DPPP)(H$_2$pyTP)$_2$(OTf)$_2$, except that Zn(pyTP) (150 mg, 0.210 mmol) was added to the Pt(DPPP)(OTf)$_2$ solution. Yield: 213 mg of purple powder (90%). ^{1}H NMR ($CDCl_3$, 400 MHz, ppm): 9.63 (d, 4H, J = 6.0 Hz, py-H$_o$), 8.94 (br, 8H, β-H), 8.80 (m, 4H, β-H), 8.54 (m, 4H, β-H), 8.15 (d, 4H, J = 6.0 Hz, py-H$_m$), 8.09 (d, 20H, J = 7.8 Hz, PPh$_2$-H$_o$, porphyrin phenyl-H$_o$), 7.66 (m, 12H, PPh$_2$-H$_{m,p}$), 7.49 (m, 12H, porphyrin H$_m$), 3.55 (m, 4H, -C*H*$_2$-P), 2.70 (s, 18H, Me), 2.63 (m, 2H, -C*H*$_2$-). ^{31}P NMR ($CDCl_3$, ppm): -16.47. UV-vis (CH_2Cl_2, nm): 422 (Soret), 552, 594.

Pd(H$_2$pyTP)$_4$(BF$_4$)$_2$. Pd(CH$_3$CN)$_4$(BF$_4$)$_2$ (20 mg, 0.045 mmol) and H$_2$pyTP (120 mg, 0.180 mmol) were refluxed in toluene for 2 days under Ar. Solvent was removed under reduced pressure and the residue was dissolved in minimum amount of C_6H_6. Diethyl ether and hexane were added and the mixture was cooled to -20 °C for eight hours. Filtration and washing the solid with diethyl ether produced a purple powder (112 mg, 85%). ^{1}H NMR (CD_2Cl_2, 400 MHz, ppm): 10.35 (d, 2H, J = 6.0 Hz, py-H$_o$), 8.89 (m, 6H, β-H), 8.81 (d, 2H, J = 6.0 Hz, py-H$_m$), 8.75 (d, J = 4.4, β-H), 8.11 (m, 4H, 10,20-phenyl-H$_o$), 7.87 (d, 2H, J = 7.5 Hz, 15-phenyl-H$_o$), 7.61 (m, 4H, 10,20-phenyl-H$_m$), 7.25 (d, 2H, J = 7.8 Hz, 15-phenyl-H$_m$), 2.71 (s, 6H, 10,20-phenyl-Me), 2.43 (s, 3H, 15-phenyl-Me), -2.78 (s, 2H, internal N*H*). UV-vis (CH_2Cl_2, nm): 420 (Soret), 484 (shoulder), 518, 556, 592, 650.

Pt(H$_2$pyTP)$_4$(OTf)$_2$ Pt(CH$_3$CN)$_4$(OTf)$_2$ (20 mg, 0.030 mmol) and H$_2$pyTP (82 mg, 0.12 mmol) were refluxed in toluene/CH_2Cl_2 (v/v: 1:1) for 12 hours under Ar. The

solvent was removed under reduced pressure and the residue was dissolved in minimum amount of CH_2Cl_2. Diethyl ether and hexane were added and the mixture was cooled to -20 °C for eight hours. Filtration and washing the solid with diethyl ether produced a purple powder (75 mg, 80%). ^{1}H NMR (CD_2Cl_2, 300 MHz, ppm): 10.52 (d, 2H, J = 6.0 Hz, py-H_o), 8.91 (m, 4H, β-H), 8.84 (d, 2H, J = 4.8 Hz, β-H), 8.79 (d, 4H, J = 6.0 Hz, py-H_m, β-H), 8.13 (d, 2H, J = 8.0 Hz, 15-phenyl-H_o), 7.91 (d, 4H, J = 7.7 Hz, 10,20-phenyl-H_o), 7.61 (d, 2H, J = 8.0 Hz, 15-phenyl-H_m), 7.28 (d, 4H, J = 7.7 Hz, 10,20-phenyl-H_m), 2.72 (s, 3H, Me on 15-phenyl), 2.45 (s, 6H, Me on 10,20-phenyl), 1.52 (s, 2H, H_2O), -2.76 (s, 2H, internal N*H*). UV-vis (CH_2Cl_2, nm): 422 (Soret), 518, 556, 592, 650. Anal. Calcd. (found) for $C_{186}F_6H_{140}N_{20}O_6S_2Pt{\cdot}H_2O$: C, 71.09 (70.89); H, 4.55 (4.45); N, 8.91 (8.67). MS {ESI} Calcd. (found) m/e: 1413 (1413) $[M\text{-}2OTf]^{2+}$.

Pt[Zn(pyPP)]$_4$(OTf)$_2$. $Pt(CH_3CN)_4(OTf)_2$ (20 mg, 0.030 mmol) and Zn(pyPP) (85 mg, 0.12 mmol) were refluxed in toluene for 2 days under argon. The solvent was removed under reduced pressure and the residue was dissolved in minimum amount of C_6H_6. Diethyl ether and hexane were added and the mixture was cooled to -20 °C for eight hours. Filtration and washing the solid with diethyl ether produced a purple powder (85 mg, 88%). ^{1}H NMR (CD_2Cl_2, 300 MHz, ppm): 10.48 (d, 2H, J = 6.3 Hz, py-H_o), 9.05 (d, 2H, J = 4.5 Hz, β-H), 9.00 (d, 2H, J = 4.5 Hz, β-H), 8.95 (d, 2H, J = 6.6 Hz, β-H), 8.93 (d, 2H, J = 6.6 Hz, β-H), 8.80 (d, 2H, J = 6.3 Hz, py-H_m), 8.26 (d, 2H, J = 6.3 Hz, 15-phenyl-H_o), 8.10 (m, 4H, 10,20-phenyl-H_o), 7.80 (m, 3H, 15-phenyl-$H_{m,p}$), 7.56 (m, 6H, 10,20-phenyl-$H_{m,p}$). UV-vis (CH_2Cl_2, nm): 420 (Soret), 552, 600.

X-Ray Crystal Structure Determination of $Pd(DPPP)(H_2pyTP)_2(OTf)_2$.

Crystals of $Pd(DPPP)(H_2pyTP)_2(OTf)_2$ suitable for single-crystal X-ray diffraction were grown by layering a $CHCl_3$ solution of $Pd(DPPP)(H_2pyTP)_2(OTf)_2$ with ethanol. A red-maroon crystal (0.20 x 0.10 x 0.075 mm) was mounted on a glass fiber on a Siemen P4 rotating anode diffractometer for data collection at 213 ± 2 K. The cell constants for the data collection were determined from reflections found from a 360° rotation photograph. Twenty-five reflections in the range of 20-25° θ were used to determine precise cell constants. Lorentz and polarization corrections were applied. A nonlinear correction based on the decay in the standard reflections was also applied to the data. A series of azimuthal reflections was collected. A semi-empirical absorption correction based on psi-scan data was applied to the data.

The space group $P2_1/n$ was chosen based on systematic absences and intensity statistics. This assumption proved to be correct as determined by a successful direct-methods solution[18] and subsequent refinement. All non-hydrogen atoms associated with the porphyrin rings along with Pd and P were found from the initial E-map. All subsequent non-hydrogen atoms were placed from successive difference fourier maps. All non-hydrogen atoms of the major molecule were refined with anisotropic displacement parameters. The SO_3 moiety of the triflate counter ions were refined anisotropically while the CF_3 moieties were refined isotropically. The C-F distances were also constrained. The ethanol and water solvate molecules were also refined isotropically. This refinement scheme was used due to the large amount of thermal

motion that the counter ion and solvent molecules exhibited. All hydrogens were treated as riding atoms with individual isotropic displacement parameters. Final refinements were done with SHELXL-93.[19,20]

Data collection and structure solution were conducted at the Iowa State Molecular Structure Laboratory. Refinement calculations were performed on a Digital Equipment Micro VAX 3100 computer using the SHELXTL-PLUS[18] and SHELXL-93[19] programs.

Results and Discussion

The use of Pd(II) and Pt(II) as a template provides a convenient means of fabricating multi-component assemblies. For example, the treatment of *trans*-$Pd(DMSO)_2Cl_2$ with two equivalent of 5-pyridyl-triphenylporphyrin (H_2pyPP) results in the formation of the di-substituted complex *trans*-$Pd(H_2pyPP)_2Cl_2$. If *trans*-$Pd(DMSO)_2Cl_2$ was treated with one equivalent of H_2pyPP, the di-substituted porphyrin-Pd assembly was formed in a 1:1 ratio with starting material *trans*-$Pd(DMSO)_2Cl_2$. The labile DMSO ligands can not be displaced in a stepwise manner in this Pd complex (Scheme I). The Zn porphyrin analog, $Pd[Zn(pyPP)]_2Cl_2$, has very low solubility in most organic solvents. However, it is soluble in the strongly coordinating solvent pyridine.

In contrast with $Pd(DMSO)_2Cl_2$, *cis*-$Pt(DMSO)_2Cl_2$ undergoes reaction with H_2pyPP in a 1:1 ratio at room temperature to produce the mono-substituted porphyrin-platinum complex *cis*-$Pt(DMSO)(H_2pyPP)Cl_2$ as shown in Scheme II. The mono-substituted porphyrin-Pt complexes were isolated in high yield (90-95%). Treatment of

Scheme I. *Trans*-Pd-bis-porphyrin assemblies

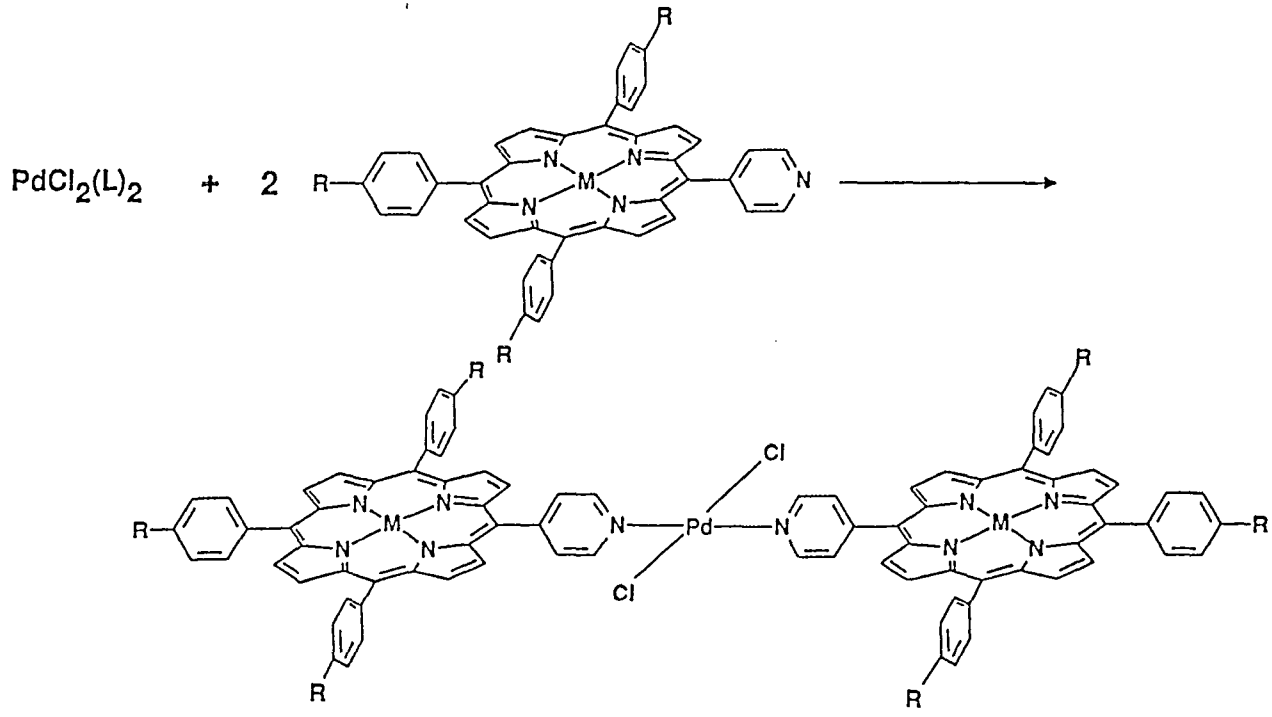

M= 2H, Zn; L= DMSO, CH_3CN

Scheme II. Mono-porphyrin-Pt assemblies

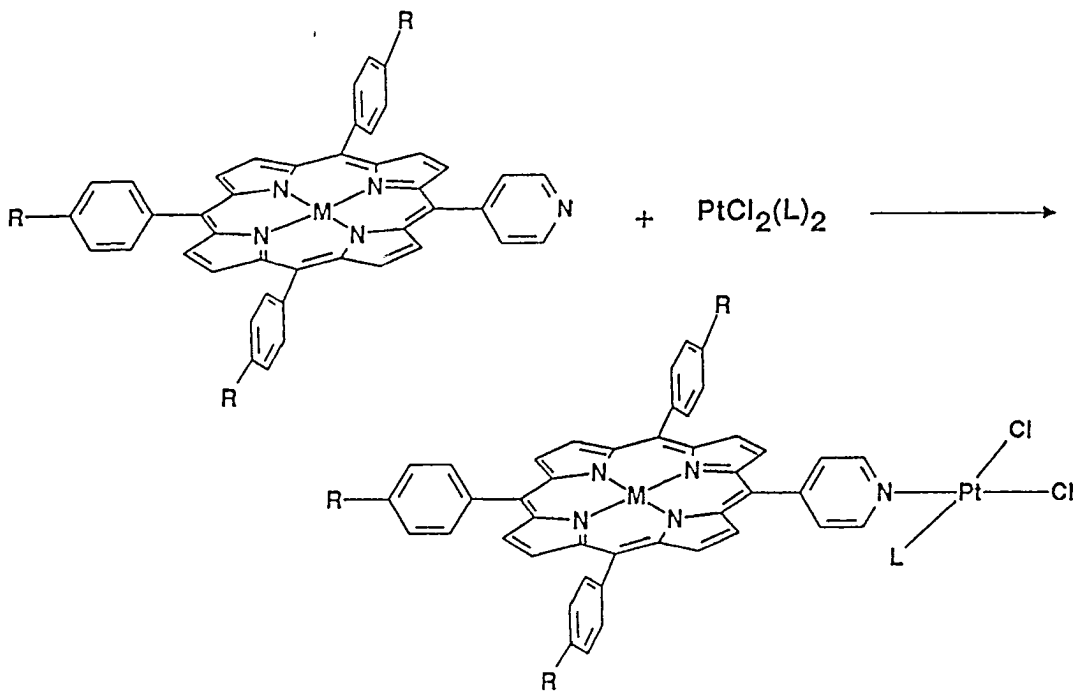

R = H, CH_3; M = 2H, Zn
L = DMSO, CH_3CN

cis-$Pt(DMSO)_2Cl_2$ with 2 equivalents of mono-pyridylporphyrin at higher temperatures and longer times (reflux in toluene for more than 48 hours), results the formation of *cis*-bis-porphyrin-Pt assemblies. Alternatively, treatment of the mono-substituted complex with an additional equivalent of mono-pyridyl porphyrin at higher temperature and longer time (reflux in toluene for more than 48 hours) results in the displacement of the second DMSO ligand to form the bisporphyrin-Pt-porphyrin assembly (Scheme III).

The substitution properties of Pt(II) allow stepwise displacement of ligands. If the mono-porphyrin substituted Pt complex was treated with excess 4-pyridyl-4'-methyl pyridinium iodide (monoquat, MQ) in refluxing THF/EtOH solution, DMSO could be displaced by MQ to form porphyrin-Pt-MQ assemblies (Scheme IV). With this strategy, it is possible to build multi-porphyrin assemblies around a metal ion in a relatively simple way with high yields. However, preparation of mixed porphyrin assemblies is more difficult. For example, treatment of $Pt(DMSO)(H_2pyPP)Cl_2$ with one equivalent Zn(pyTP) produced the three bis porphyrin complexes $Pt[Zn(pyTP)]_2Cl_2$, $Pt(H_2pyPP)_2Cl_2$and $Pt[Zn(pyTP)](H_2pyPP)Cl_2$. All these species have very similar mobility on chromatography supports and we have not been able to separate these three compounds. Metallation of the coordinated porphyrin can also be achieved from the multi-component assembly. Thus, treatment of $Pt(H_2pyPP)_2Cl_2$ with excess $Zn(OAc)_2$ produces $Pt[Zn(pyPP)]_2Cl_2$. When $Pt(H_2pyPP)_2Cl_2$ was treated with one equivalent of $Zn(OAc)_2$, amixture resulted which contained $Pt[Zn(pyPP)]_2Cl_2$, $Pt(H_2pyPP)_2Cl_2$ and $Pt[Zn(pyPP)](H_2pyPP)Cl_2$, as observed by ^1H NMR.

Scheme III. Pt-bis-porphyrin assemblies

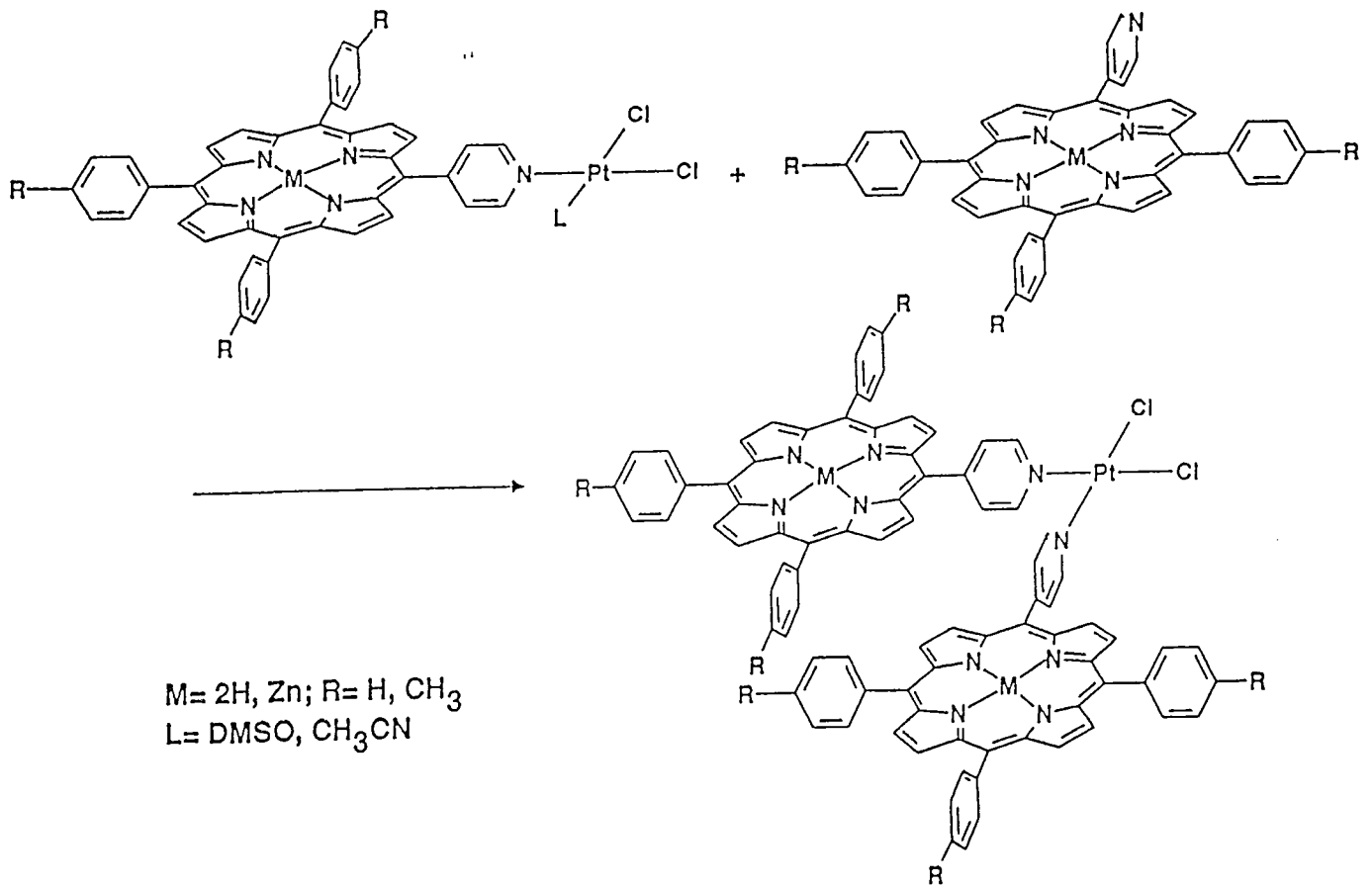

Scheme IV. Pt-porphyrin-viologen assemblies

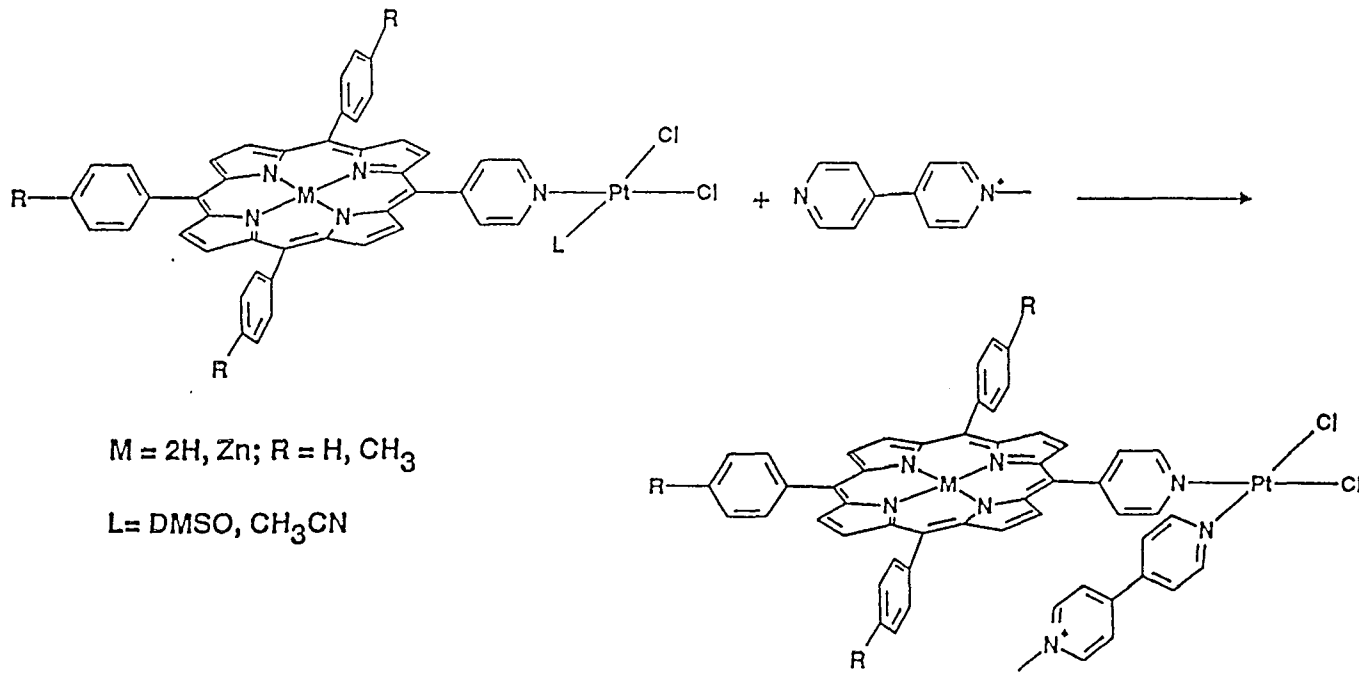

M = 2H, Zn; R = H, CH_3

L= DMSO, CH_3CN

The reaction of H_2pyTP or H_2pyPP with $M(CH_3CN)_4]X_2$ (M = Pt, Pd; X = BF_4, OTf) leads to the formation of a tetra substituted complex, $M(H_2pyPOR)_4^{2+}$ as shown in Scheme V. The ^1H NMR spectra of these complexes exhibit only one set of porphyrin resonances. This indicates that all four porphyrins around the metal ion are identical and that the Pt and Pd ions have square planar environments. The tetrapyridine Pd(II) analog, $[Pd(py)_4]^{2+}$ has a similar coordination geometry.[21] If $M(CH_3CN)_4]X_2$ (M=Pt, Pd; X=BF_4, OTf) was treated with 2 equivalent H_2pyTP or H_2pyPP, the resulting products are a mixture of di-substituted and tetra-substituted complexes, in a ratio of 3 to 1, as determined by ^1H NMR.

Because the dichloro Pt- and Pd-porphyrin assemblies have relatively low solubility in organic solvents, growing X-ray quality single-crystals was difficult. In general, these complexes precipitate as powers or as microcrystals. For achieving higher solubility, platinum and palladium compounds containing the chelate ligand 1,3-bis(diphenylphosphino)propane (DPPP), were employed as starting materials. Treating $Pt(DPPP)Cl_2$ and $Pd(DPPP)Cl_2$ with two equivalents of silver triflate generates $M(DPPP)(OTf)_2$. Substitution of the triflate ligands with mono-pyridylporphyrins produced only bis-porphyrin complexes. Treatment of $M(DPPP)(OTf)_2$ with one equivalent of mono-pyridyl porphyrin results in a mixture of bis-porphyrin complexes and unreacted starting material. Scheme VI illustrates the synthesis of DPPP bisporphyrin assemblies. The diphosphine complexes, $M(DPPP)(H_2pyTP)_2(OTf)_2$, are soluble in common organic solvents such as C_6H_6, toluene, acetone, CH_2Cl_2 and $CHCl_3$ and have

Scheme V. Pd, Pt-tetra porphyrin assemblies

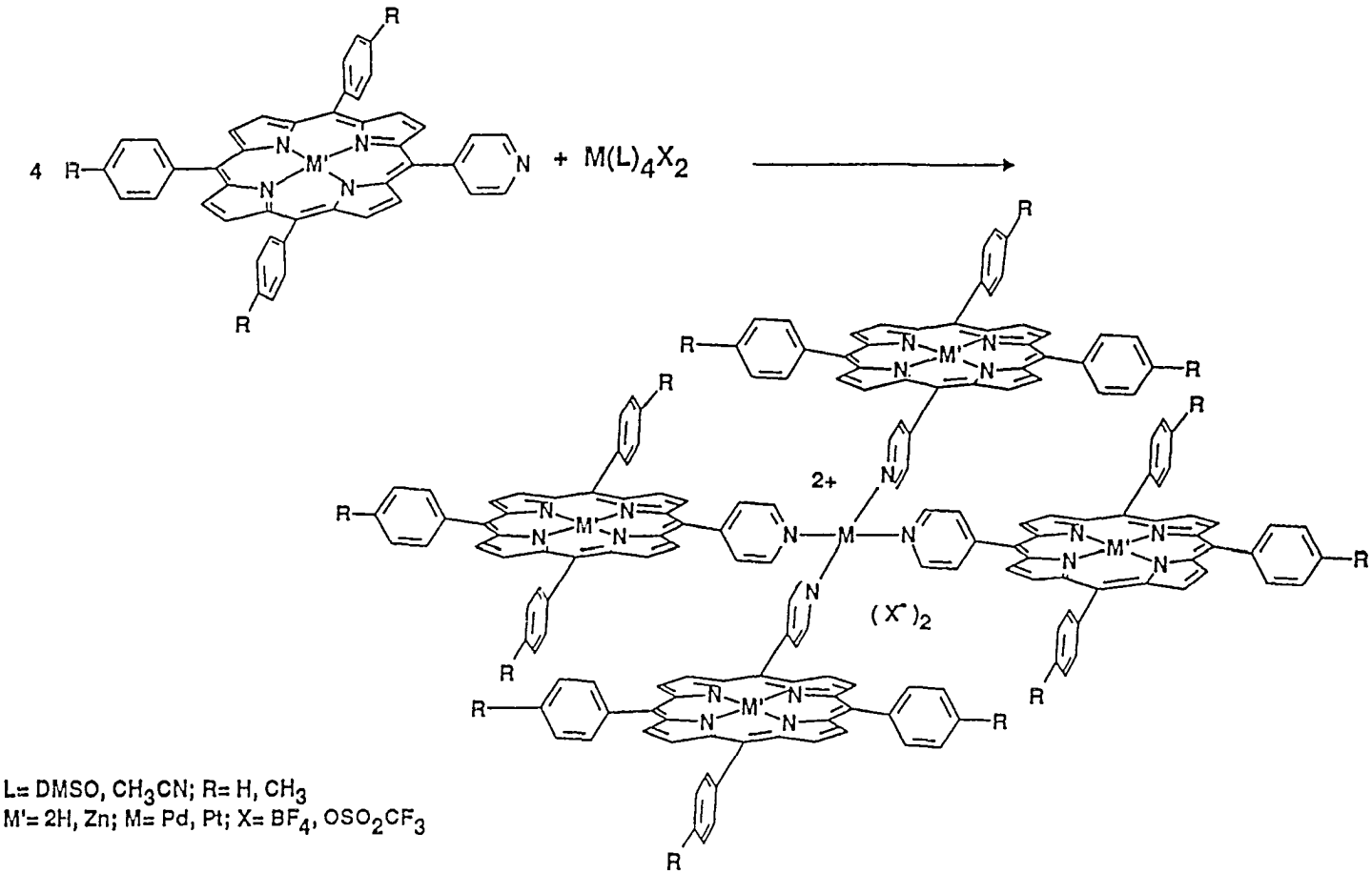

L= DMSO, CH_3CN; R= H, CH_3
M'= 2H, Zn; M= Pd, Pt; X= BF_4, OSO_2CF_3

Scheme VI. Pd, Pt-bis-porphyrin assemblies

$M(DMSO)_2Cl_2$ + DPPP ⟶ $M(DPPP)Cl_2$

2AgX, 2MpyTTP ⟶

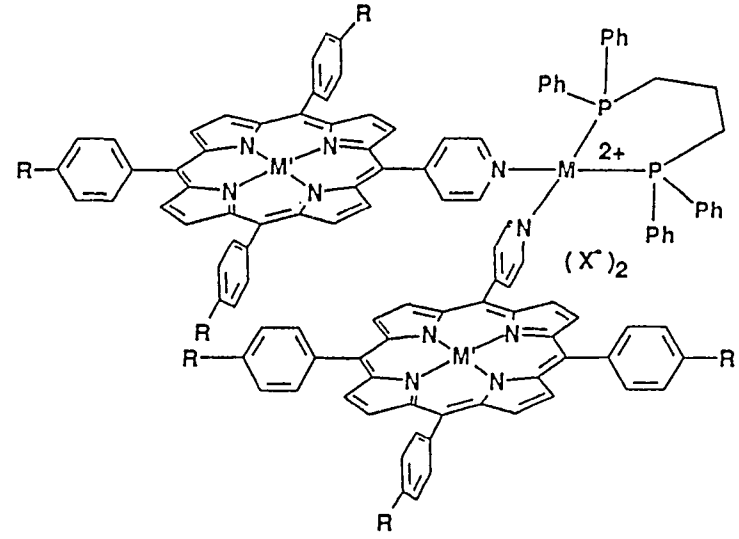

M= Pd, Pt; M'= 2H, Zn
R= H, CH_3; X= OSO_2CF_3

much higher solubility compared with the chloride analogues, $M(H_2pyPOR)_2Cl_2$. Crystals of $Pd(DPPP)(H_2pyTP)_2(OTf)_2$ suitable for single X-ray diffraction were prepared by layering ethanol on top of a $CHCl_3$ solution.

It is well known that $Pd(L)_2Cl_2$ complexes prefer *trans* configurations and that $Pt(L)_2Cl_2$ complexes prefer *cis* configurations.[15,22] The *trans* geometry for $Pd(H_2pyPOR)_2Cl_2$ was confirmed by far-IR studies. For example, $Pd(H_2pyPP)_2Cl_2$ has only one Pd-Cl stretch found at 368 cm^{-1}. The *cis* configuration for $Pt(H_2pyPP)_2Cl_2$ was established from two observed Pt-Cl vibrations found at 357 and 324 cm^{-1}.

^1H NMR is very useful tool for the identification these complexes. Chemical shifts for the protons in the pyridyl group are very sensitive to the coordination environment. In the free base porphyrin H_2pyTP, these protons show two signals at 9.00 (d) and 8.14 (d) ppm. When the pyridyl group is coordinated to metals, these two signals shift down field. In $Pt(DMSO)(H_2pyTP)Cl_2$, they appear at to 9.15 and 8.26 ppm, about 0.15 further down field. In $Pt(H_2pyTP)_2Cl_2$, the pyridyl proton H_o appears at 9.46 ppm. In the tetra-porphyrin complex $Pt(H_2pyTP)_4(OTf)_2$, H_o resonates at 10.53 ppm. The correspond Zn analogues follow a similar trend. The ^1H NMR chemical shifts of the porphyrin pyridyl protons (Table 1) indicate that properties of these complexes can be tuned.

The absorption (Table 2) and emission (Table 3) spectra of the porphyrin complexes show that there are only very limited changes between the porphyrin and the

Table 1. ^1H NMR chemical shifts of the porphyrin pyridyl protons (in $CDCl_3$)

Compound	H_o	H_m
H_2pyTP	9.00	8.14
$Pt(DMSO)(H_2pyTP)Cl_2$	9.15	8.26
$Pt(H_2pyTP)(MQ)Cl_2$	9.40	8.17
$Pt(H_2pyTP)_2Cl_2$	9.46	8.25
$Pd(H_2pyTP)_2Cl_2$	9.38	8.28
$Pt(H_2pyTP)_4(OTf)_2$	10.52	8.85
$Pt(DPPP)(H_2pyTP)_2(OTf)_2$	9.68	8.15
$Pd(DPPP)(H_2pyTP)_2(OTf)_2$	9.62	8.22
$Pd(H_2pyTP)_4(BF_4)_2$	10.36	8.75
$Pd(H_2pyTP)_4(OTf)_2$	10.53	8.84
$Zn(H_2pyTP)$	8.06	7.45
$Pt(DMSO)[Zn(pyTP)]Cl_2$	9.12	8.27
$Pt[Zn(pyTP)](MQ)Cl_2$	9.01	8.03
$Pt[Zn(pyPP)]_4(OTf)_2$	10.48	8.80
$Pt(DPPP)[Zn(pyTP)]_2(OTf)_2$	9.63	8.15
$Pd(DPPP)[Zn(pyTP)]_2(OTf)_2$	9.55	8.02

Table 2. UV Data for Pd, Pt Complexes

Complex	UV-vis, nm in CH_2Cl_2
H_2pyPP	418 (Soret), 482 (s), 514, 548, 588, 646
Pt(DMSO)(H_2pyPP)Cl_2	418 (Soret), 484 (s), 514, 550, 590, 646
Pt(H_2pyPP)$_2Cl_2$	422 (Soret), 482 (s), 516, 552, 590, 646
Pd(H_2pyPP)$_2Cl_2$	420 (Soret), 486 (s), 516, 552, 590, 646
Zn(pyPP)	418 (Soret), 560, 604
Pt(DMSO)[Zn(pyPP)]Cl_2	422 (Soret), 512 (s), 548, 588
Pt[Zn(pyPP)]$_2Cl_2$	420 (Soret), 548, 588
Pd[Zn(pyPP)]$_2Cl_2$	428 (Soret), 524 (s), 562, 602 in Py
Pt(H_2pyPP)(MQ)Cl_2	418 (Soret), 514, 548, 588, 644
Pt[Zn(pyPP)](MQ)Cl_2	418 (Soret), 550, 606
H_2pyTP	418 (Soret), 514, 550, 588, 646
Zn(pyTP)	422 (Soret), 562, 610
Pt(DMSO)(H_2pyTP)Cl_2	422 (Soret), 484 (s), 518, 554, 592, 648
Pd(H_2pyTP)$_2Cl_2$	422 (Soret), 484 (s), 518, 554, 592, 648
Pt(H_2pyTP)$_2Cl_2$	422 (Soret), 484 (s), 518, 554, 592, 646
Pt(H_2pyTP)(MQ)Cl_2	418 (Soret), 514, 548, 588, 644
Pt(H_2pyTP)$_4$(OTf)$_2$	422 (Soret), 518, 556, 592, 650
Pd(H_2pyTP)$_4$(OTf)$_2$	418 (Soret), 518, 554, 592, 650
Pd(DPPP)(H_2pyTP)$_2$(OTf)$_2$	420 (Soret), 518, 554, 592, 648
Pt(DPPP)(H_2pyTP)$_2$(OTf)$_2$	420 (Soret), 448 (s), 518, 550, 592, 650
Pt(DMSO)[Zn(pyTP)]Cl_2	422 (Soret), 548, 588
Pt[Zn(pyTP)](MQ)Cl_2	418 (Soret), 552, 606
Pd(DPPP)[Zn(pyTP)]$_2$(OTf)$_2$	422 (Soret), 550, 592
Pt(DPPP)[Zn(pyTP)]$_2$(OTf)$_2$	422 (Soret), 552, 594

Table 3. Emission Spectra of Pt, Pd Porphyrin Complexes

Name	Excitation (nm)	Crossover	Emission
H_2pyPP	510	629	652, 714
H_2pyTP	510	629	656, 717
Zn(pyPP)	540	584	604, 647
Zn(pyTP)	540	584	604, 648
Pt(DMSO)(H_2pyPP)Cl_2	510	636	652, 714
Pt(H_2pyPP)$_2Cl_2$	510	636	652, 714
Pt(H_2pyPP)(MQ)Cl_2	510	630	652, 714
Pt(DMSO)[Zn(pyPP)]Cl_2	540	586	610, 647
Pt[Zn(pyPP)](MQ)Cl_2	540	582	604, 717
Pt(DMSO)(H_2pyTP)Cl_2	510	639	654, 719
Pt(H_2pyTP)$_2Cl_2$	510	640	654, 718
Pt(DMSO)[Zn(pyTP)]Cl_2	540	602	613, 653
Pt[Zn(pyTP)]$_2Cl_2$	540	583	606, 648
Pt[Zn(pyTP)](MQ)Cl_2	540	583	606, 649
Pd(H_2pyTP)$_2Cl_2$	510	635	654, 717
Pd(H_2pyTP)$_4$(BF_4)$_2$	510	635	654, 717

porphyrin-metal assemblies. In the UV-vis spectra, the Soret band for H_2pyPP appears at 418 nm and the Q-bands occur at 514, 548, 588, and 646 nm. In the mono-porphyrin complex *cis*-Pt(DMSO)(H_2pyPP)Cl_2, the absorption bands are virtually unchanged and appear at 418 (Soret), 514, 550, 590, and 646 nm. The bis-porphyrin assembly, *cis*-Pt(H_2pyPP)$_2Cl_2$ showed a slight red-shift in absorption bands to 422 (Soret), 516, 552, 590, and 647 nm. In the emission spectra, H_2pyPP has peaks at 652, 714, while the Pt and Pd complexes Pt(DMSO)(H_2pyPP)Cl_2, Pt(H_2pyPP)$_2Cl_2$, Pt(H_2pyPP)(MQ)Cl_2 and Pd(H_2pyPP)$_2Cl_2$ essentially have the same emission peak positions. This observation is also true for the case of H_2pyTP and their Zn porphyrins Pd(II) and Pt(II) complexes. Consequently, the Pd and Pt centers do not strongly couple the subunits electronically and thus serve primarily as structural components.

X-ray Crystal structure of Pd(DPPP)(H_2pyTP)$_2$(OTf)$_2$. The molecular structure of Pd(DPPP)(H_2pyTP)$_2$(OTf)$_2$ was determined by single-crystal X-ray diffraction. The molecular structure and atom numbering scheme are shown in Figure 1. Crystallographicdata for the structure determination are listed in Table 4. Atomic positional parameters are given in Table 5. Bond distances and angles are listed in Tables 6 and 7.

Pd(DPPP)(H_2pyTP)$_2$(OTf)$_2$ crystallizes in the space group $P2_1/n$ with 4 molecules per unit cell. The Pd(II) ion has a distorted square-planar coordination. Two cis sites are occupied by the DPPP ligand and the remaining two sites are taken up by the pyridyl porphyrins. The bond angles around the palladium(II) ion are close to the expected value

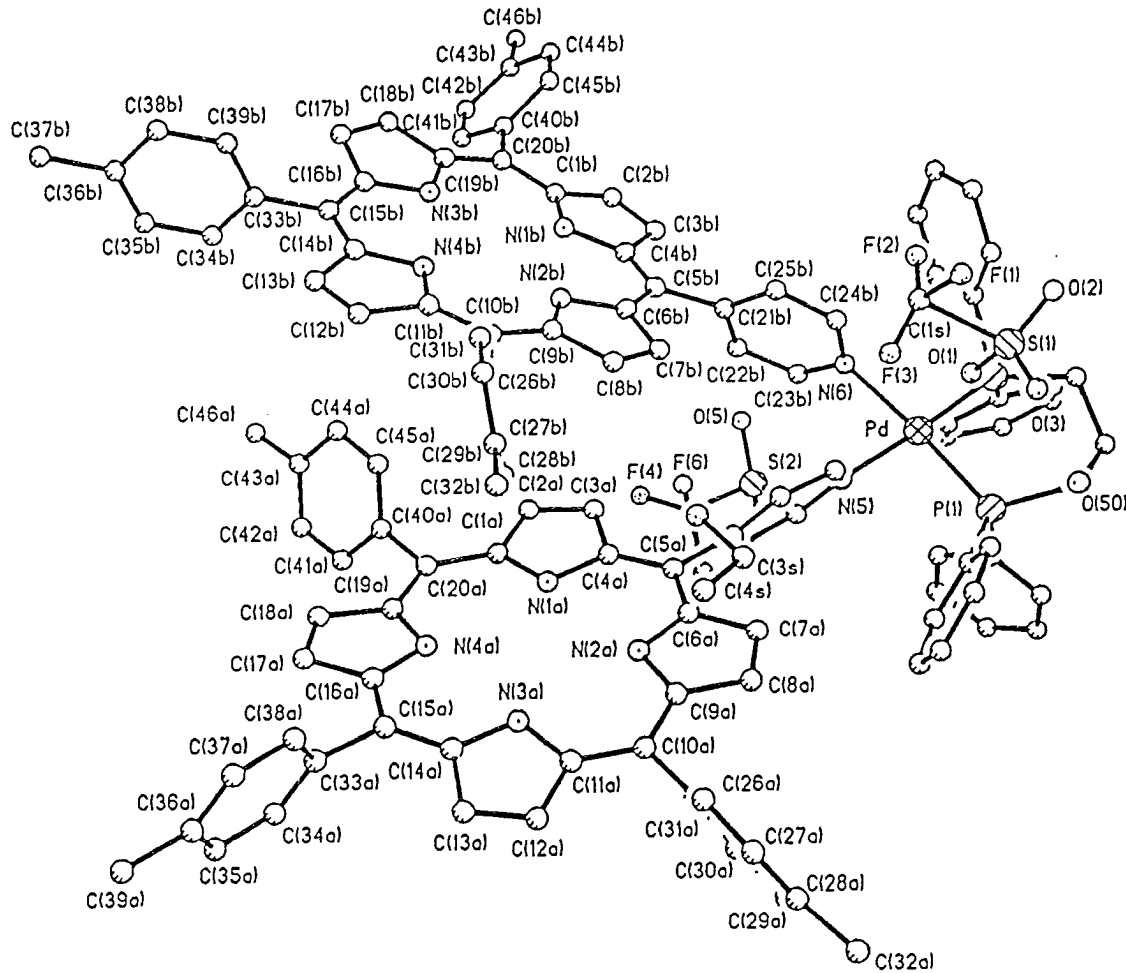

Figure 1. Molecular structure and atom numbering scheme for $Pd(DPPP)(H_2pyTP)_2(OTf)_2$

of 90°, ranging from 83.5(3)° to 94.3(3)°. The P-Pd-P chelate angle is 90.23° and the N-Pd-N angle is 83.5°. The Pd-N distances (2.095(9) Å and 2.114(9) Å) are in the range of those observed for other bispyridinepalladium(II) complexes.[23] The Pd-P distances (2.246(3) Å and 2.259(3) Å) are also in the normal range for *cis*-chelating phosphine Pd complexes.[24] The center-to-center distance between the two porphyrin rings is 8.69 Å and the dihedral angle between the two porphyrin mean planes is only 19.8°. The angle between the pyridyl ring and the Pd coordination plane is 88.3° and the angle between the pyridyl ring and the mean porphyrin plane is 28.5°. The two triflate counter ions are situated above and below the Pd coordination plane. The distance between O1 of the triflate and Pd is 2.86 Å.

CONCLUSION

We have utilized the well defined and versatile chemistry of square planar Pt(II) and Pd(II) complexes to synthesize a series of porphyrin-metal-porphyrin and porphyrin-metal-viologen assemblies. These are potentially new model systems for studying photoinduced electron and energy transfer. Because of the rigidity and structural constraints of Pt(II) and Pd(II) coordination, control of both the distance and the orientation of a donor and an acceptor are possible. This simple strategy may lead to the discovery of new synthetic models for the photosynthetic reaction center and may complement and supplement the important information gained from organically linked reaction center models.

Table 4. Structure determination summary for $Pd(DPPP)(H_2pyTP)_2(OTf)_2$

Crystal Data	
Empirical Formula	$C_{123}\ H_{104}\ F_6\ N_{10}\ O_8\ P_2\ Pd\ S_2$
Color, Habit	red-maroon, rectangular prism
Crystal Size (mm)	0.2 x 0.1 x 0.075
Crystal System	Monoclinic
Space Group	$P2_1/n$
Unit Cell Dimensions	a = 13.211(5) Å
	b = 36.741(19) Å
	c = 22.971(10) Å
	$\alpha = 90°$
	$\beta = 91.54(3)°$
	$\gamma = 90°$
Volume	11145.8(86) $Å^3$
Z	4
Formula Weight	2196.62
Density (calc.)	1.309 Mg/m^3
Absorption Coefficient	2.554 mm^{-1}
F(000)	4552

Table 4. (continued)

Data Collection	
Diffractometer Used	Siemens P4 Rotating Anode
Radiation	CuKaKα (λ = 1.54178 Å)
Temperature (K)	213(2)
Monochromator	graphite
θ Range	3.08 to 56.75°
Scan Type	2θ - θ
Standard Reflections	3 measured every 97 reflections
Index Ranges	$-1 \leq h \leq 14$ $-1 \leq k \leq 39$ $-24 \leq l \leq 24$
Reflections Collected	17837
Independent Reflections	14901 (R_{int} = 0.0826)
Observed Reflections	5252 ($I \geq 2\sigma(I)$)
Min./Max. Transmission	0.614/ 0.704
Absorption Correction	Semi-empirical from psi-scans

Table 4. (continued)

Solution and Refinement

System Used	SHELXL-93 (Sheldrick, 1993)
Solution	Direct
Refinement Method	Full-matrix least-squares on F^2
Extinction Correction	0.000057(12)
Extinction Expression	$Fc^* = kFc[1 + 0.001 \times Fc^2\lambda^3/\sin(2\theta)]^{-1/4}$
Hydrogen Atoms	Riding
Weighting Scheme	w = calc w = $1/[\sigma(Fo^2) + (0.0800\ P)^2 + 0.00$ where $P = (Fo^2 + 2Fc^2)/3$
Parameters Refined	1313
Final R Indices [$I \geq 2\sigma(I)$]	R1 = 0.0821, wR2 = 0.1844
R Indices (all data)	R1 = 0.1964, wR2 = 0.2183
GooF, Observed and All Data	1.269, 0.824
Largest and Mean Δ/σ	1.007, 0.018
Largest Difference Peak	0.877 e/Å^{-3}
Largest Difference Hole	-0.633 e/Å^{-3}

$R1 = \Sigma||Fo| - |Fc|| / \Sigma|Fo|$
$wR2 = [\Sigma[w(Fo^2 - Fc^2)^2] / \Sigma[w(Fo^2)^2]]^{0.5}$
where $w = 1/[\sigma^2(Fo^2) + (a*P)^2 + b*P + d + e*\backslash\sin\theta]$
$GooF = [\Sigma[w(Fo^2 - Fc^2)^2]/(n - p)]^{0.5}$

Table 5. Atomic coordinates (x 10^4) and equivalent isotropic displacement parameters ($Å^2$ x 10^3) for $Pd(DPPP)(H_2pyTP)_2(OTf)_2$

Atom	x	y	z	U(eq)
Pd	6960(1)	117(1)	7636(1)	36(1)
P(1)	5892(2)	403(1)	8236(1)	39(1)
P(2)	7461(2)	657(1)	7284(1)	40(1)
N(5)	6519(7)	-400(2)	7938(4)	37(2)
N(6)	7931(7)	-187(2)	7118(4)	37(2)
N(1A)	6348(7)	-2114(2)	8581(4)	40(3)
N(2A)	4310(7)	-1869(2)	8806(4)	44(3)
N(3A)	3762(7)	-2590(2)	9155(4)	45(3)
N(4A)	5784(7)	-2844(2)	8911(4)	39(3)
N(1B)	10468(7)	-1553(2)	6066(4)	45(3)
N(2B)	8451(7)	-1824(2)	6364(4)	40(3)
N(3B)	11006(7)	-2285(2)	5726(4)	40(3)
N(4B)	9001(7)	-2543(2)	6074(4)	39(3)
C(101)	5208(8)	786(3)	7935(5)	44(3)
C(102)	5904(9)	1087(3)	7715(5)	47(4)
C(103)	6459(9)	984(3)	7154(5)	50(4)
C(104)	6563(9)	5[illegible](3)	8874(5)	35(3)
C(105)	6169(9)	832(3)	9228(5)	39(3)
C(106)	6704(9)	936(3)	9718(5)	45(3)
C(107)	7613(10)	789(4)	9879(6)	62(4)
C(108)	7995(10)	510(3)	9532(6)	59(4)
C(109)	7479(9)	405(3)	9039(5)	46(3)

Table 5. (continued)

Atom	x	y	z	U(eq)
C(110)	4896(8)	106(3)	8493(5)	40(3)
C(111)	4992(9)	-57(3)	9025(6)	50(3)
C(112)	4202(10)	-273(3)	9226(6)	52(4)
C(113)	3346(11)	-318(3)	8893(7)	64(4)
C(114)	3284(10)	-160(4)	8368(6)	76(5)
C(115)	4038(10)	56(3)	8155(6)	63(4)
C(116)	8407(9)	887(3)	7697(5)	45(3)
C(117)	8536(11)	1267(3)	7673(6)	65(4)
C(118)	9330(14)	1429(4)	7977(8)	87(5)
C(119)	9957(13)	1234(5)	8343(8)	94(6)
C(120)	9898(13)	849(5)	8373(7)	91(5)
C(121)	9045(11)	694(4)	8053(6)	61(4)
C(122)	8012(11)	589(3)	6572(5)	46(3)
C(123)	7424(11)	566(3)	6080(6)	53(4)
C(124)	7853(10)	496(3)	5551(6)	54(4)
C(125)	8863(12)	439(3)	5512(7)	61(4)
C(126)	9462(12)	460(4)	6019(7)	73(5)
C(127)	9056(9)	536(3)	6551(6)	52(4)
C(1A)	7260(8)	-2289(3)	8481(5)	31(3)
C(2A)	7950(9)	-2030(3)	8255(5)	47(3)
C(3A)	7479(8)	-1709(3)	8209(5)	43(3)
C(4A)	6465(9)	-1754(3)	8419(5)	39(3)
C(5A)	5708(9)	-1491(3)	8439(5)	38(3)
C(6A)	4701(9)	-1542(3)	8614(5)	41(3)

Table 5. (continued)

Atom	x	y	z	U(eq)
C(7A)	3955(9)	-1265(3)	8661(5)	49(4)
C(8A)	3107(10)	-1421(3)	8878(5)	47(3)
C(9A)	3334(9)	-1795(3)	8978(5)	37(3)
C(10A)	2689(9)	-2048(3)	9236(5)	43(3)
C(11A)	2889(9)	-2413(3)	9323(6)	49(3)
C(12A)	2230(10)	-2673(3)	9583(6)	71(5)
C(13A)	2678(10)	-3004(3)	9565(6)	62(4)
C(14A)	3629(9)	-2952(3)	9286(5)	47(4)
C(15A)	4342(10)	-3219(3)	9213(5)	47(4)
C(16A)	5339(9)	-3175(3)	9039(5)	41(3)
C(17A)	6076(9)	-3462(3)	8973(5)	43(3)
C(18A)	6935(10)	-3299(3)	8813(5)	46(3)
C(19A)	6762(9)	-2918(3)	8776(5)	38(3)
C(20A)	7445(8)	-2661(3)	8572(5)	34(3)
C(21A)	5986(10)	-1110(3)	8254(5)	45(3)
C(22A)	6784(8)	-927(3)	8538(5)	38(3)
C(23A)	7027(9)	-572(3)	8358(5)	43(3)
C(24A)	5768(10)	-575(3)	7675(5)	50(4)
C(25A)	5478(9)	-935(3)	7807(5)	38(3)
C(26A)	1695(9)	-1913(3)	9436(6)	43(3)
C(27A)	1633(9)	-1688(3)	9909(6)	56(4)
C(28A)	683(10)	-1558(3)	10095(6)	56(4)
C(29A)	-172(10)	-1646(4)	9848(7)	61(4)
C(30A)	-134(10)	-1887(4)	9411(7)	85(5)

Table 5. (continued)

Atom	x	y	z	U(eq)
C(31A)	781(12)	-2015(4)	9190(7)	92(6)
C(32A)	-1206(9)	-1491(3)	10037(7)	88(5)
C(33A)	3999(9)	-3608(3)	9333(6)	45(3)
C(34A)	4289(10)	-3784(3)	9831(5)	53(4)
C(35A)	3885(10)	-4126(3)	9948(6)	53(4)
C(36A)	3233(9)	-4298(3)	9570(7)	53(4)
C(37A)	2948(10)	-4123(3)	9071(6)	57(4)
C(38A)	3333(9)	-3782(3)	8943(6)	56(4)
C(39A)	2834(10)	-4674(3)	9704(6)	73(4)
C(40A)	8473(9)	-2801(3)	8415(5)	37(3)
C(41A)	9129(9)	-2944(3)	8831(5)	47(3)
C(42A)	10061(9)	-3081(3)	8686(6)	53(4)
C(43A)	10351(10)	-3071(3)	8108(6)	55(4)
C(44A)	9716(9)	-2924(3)	7685(6)	52(4)
C(45A)	8777(9)	-2794(3)	7843(5)	47(3)
C(46A)	11383(9)	-3225(4)	7979(6)	85(5)
C(1B)	11451(9)	-1483(3)	5894(5)	42(3)
C(2B)	11652(9)	-1104(3)	6005(6)	51(4)
C(3B)	10804(9)	-952(3)	6219(6)	53(4)
C(4B)	10058(9)	-1234(3)	6275(5)	37(3)
C(5B)	9064(9)	-1188(3)	6448(5)	38(3)
C(6B)	8323(8)	-1456(3)	6490(5)	36(3)
C(7B)	7312(8)	-1401(3)	6701(5)	49(4)
C(8B)	6843(9)	-1726(3)	6688(5)	45(3)

Table 5. (continued)

Atom	x	y	z	U(eq)
C(9B)	7557(10)	-1985(3)	6479(5)	45(3)
C(10B)	7354(8)	-2358(3)	6434(5)	34(3)
C(11B)	8047(9)	-2619(3)	6250(5)	37(3)
C(12B)	7915(9)	-3011(3)	6251(5)	46(3)
C(13B)	8746(8)	-3163(3)	6082(5)	40(3)
C(14B)	9465(9)	-2875(3)	5955(5)	40(3)
C(15B)	10421(9)	-2918(3)	5740(5)	41(3)
C(16B)	11099(9)	-2652(3)	5606(5)	42(3)
C(17B)	12022(9)	-2690(3)	5292(5)	49(4)
C(18B)	12486(9)	-2366(3)	5267(5)	46(3)
C(19B)	11868(9)	-2106(3)	5551(5)	43(3)
C(20B)	12083(8)	-1736(3)	5643(5)	38(3)
C(21B)	8765(9)	-807(3)	6644(5)	39(3)
C(22B)	9201(10)	-648(3)	7121(5)	50(3)
C(23B)	8746(9)	-335(3)	7347(5)	42(3)
C(24B)	7563(9)	-320(3)	6616(5)	42(3)
C(25B)	7938(9)	-638(3)	6357(5)	43(3)
C(26B)	6327(9)	-2491(3)	6568(5)	39(3)
C(27B)	5945(9)	-2458(3)	7128(6)	52(4)
C(28B)	4950(11)	-2570(3)	7227(7)	60(4)
C(29B)	4328(10)	-2695(3)	6804(7)	56(4)
C(30B)	4674(9)	-2727(3)	6251(6)	51(4)
C(31B)	5667(9)	-2625(3)	6135(6)	46(3)

Table 5. (continued)

Atom	x	y	z	U(eq)
C(32B)	3264(9)	-2814(4)	6932(7)	94(6)
C(33B)	10777(9)	-3303(3)	5623(5)	37(3)
C(34B)	11349(9)	-3480(3)	6046(6)	45(3)
C(35B)	11716(9)	-3832(3)	5944(6)	52(4)
C(36B)	11548(9)	-4005(3)	5418(6)	49(4)
C(37B)	10943(10)	-3822(3)	4995(6)	56(4)
C(38B)	10592(9)	-3472(3)	5100(6)	50(4)
C(39B)	11961(11)	-4385(3)	5310(7)	92(5)
C(40B)	13108(9)	-1604(3)	5469(5)	39(3)
C(41B)	13986(10)	-1753(3)	5688(6)	53(4)
C(42B)	14894(10)	-1624(3)	5540(6)	57(4)
C(43B)	15015(9)	-1337(3)	5165(6)	49(4)
C(44B)	14138(9)	-1193(3)	4921(5)	50(4)
C(45B)	13191(9)	-1318(3)	5068(5)	49(3)
C(46B)	16040(8)	-1178(3)	5018(6)	63(4)
S(1)	4570(3)	168(1)	6387(2)	60(1)
O(1)	5395(6)	117(2)	6795(3)	64(2)
O(2)	4728(7)	437(3)	5970(4)	101(4)
O(3)	3593(7)	163(3)	6623(4)	97(3)
C(1S)	4757(15)	-347(6)	5955(9)	134(8)
F(1)	3924(9)	-272(3)	5610(5)	147(4)
F(2)	5504(11)	-248(4)	5704(6)	193(6)
F(3)	4499(11)	-533(4)	6362(7)	207(6)
S(2)	10246(4)	-325(2)	8749(3)	143(2)

Table 5. (continued)

Atom	x	y	z	U(eq)
O(4)	10861(10)	-183(4)	9256(5)	167(6)
O(5)	10735(9)	-350(5)	8180(5)	185(8)
O(6)	9247(7)	-157(3)	8750(6)	137(5)
C(2S)	9946(19)	-765(10)	8893(12)	238(14)
F(4)	10846(13)	-950(4)	8890(6)	217(6)
F(5)	9588(17)	-712(6)	9463(11)	351(11)
F(6)	9362(9)	-907(3)	8477(5)	162(5)
C(3S)	1819(16)	-1715(6)	7449(10)	192(10)
C(4S)	962(12)	-2045(4)	7474(7)	97(5)
O(23)	2932(10)	-1798(3)	7304(5)	139(5)
O(50)	1385(22)	-5(8)	7000(13)	420(16)

Equivalent isotropic U defined as one third of the trace of the orthogonalized U_{ij} tensor.

Table 6. Bond lengths (Å) for $Pd(DPPP)(H_2pyTP)_2(OTf)_2$

Pd-N(6)	2.095(9)	N(2B)-C(6B)	1.394(12)
Pd-N(5)	2.112(9)	N(3B)-C(16B)	1.381(12)
Pd-P(2)	2.247(3)	N(3B)-C(19B)	1.385(13)
Pd-P(1)	2.258(3)	N(4B)-C(11B)	1.362(13)
P(1)-C(104)	1.792(11)	N(4B)-C(14B)	1.395(13)
P(1)-C(101)	1.799(10)	C(101)-C(102)	1.533(13)
P(1)-C(110)	1.820(11)	C(102)-C(103)	1.547(14)
P(2)-C(116)	1.765(13)	C(104)-C(109)	1.387(14)
P(2)-C(103)	1.806(11)	C(104)-C(105)	1.390(13)
P(2)-C(122)	1.826(12)	C(105)-C(106)	1.367(14)
N(5)-C(24A)	1.315(14)	C(106)-C(107)	1.36(2)
N(5)-C(23A)	1.322(13)	C(107)-C(108)	1.40(2)
N(6)-C(23B)	1.303(13)	C(108)-C(109)	1.36(2)
N(6)-C(24B)	1.332(13)	C(110)-C(111)	1.364(14)
N(1A)-C(4A)	1.382(12)	C(110)-C(115)	1.37(2)
N(1A)-C(1A)	1.389(12)	C(111)-C(112)	1.401(14)
N(2A)-C(9A)	1.385(13)	C(112)-C(113)	1.36(2)
N(2A)-C(6A)	1.382(12)	C(113)-C(114)	1.34(2)
N(3A)-C(14A)	1.376(13)	C(114)-C(115)	1.37(2)
N(3A)-C(11A)	1.389(13)	C(116)-C(121)	1.36(2)
N(4A)-C(19A)	1.364(13)	C(116)-C(117)	1.41(2)
N(4A)-C(16A)	1.384(13)	C(117)-C(118)	1.38(2)
N(1B)-C(4B)	1.385(12)	C(118)-C(119)	1.37(2)
N(1B)-C(1B)	1.392(13)	C(119)-C(120)	1.42(2)
N(2B)-C(9B)	1.353(14)	C(120)-C(121)	1.45(2)

Table 6. (continued)

C(122)-C(123)	1.36(2)	C(16A)-C(17A)	1.446(14)
C(122)-C(127)	1.39(2)	C(17A)-C(18A)	1.343(14)
C(123)-C(124)	1.38(2)	C(18A)-C(19A)	1.419(14)
C(124)-C(125)	1.36(2)	C(19A)-C(20A)	1.396(14)
C(125)-C(126)	1.39(2)	C(20A)-C(40A)	1.504(14)
C(126)-C(127)	1.38(2)	C(21A)-C(25A)	1.37(2)
C(1A)-C(20A)	1.405(13)	C(21A)-C(22A)	1.40(2)
C(1A)-C(2A)	1.424(14)	C(22A)-C(23A)	1.409(13)
C(2A)-C(3A)	1.338(14)	C(24A)-C(25A)	1.412(14)
C(3A)-C(4A)	1.446(14)	C(26A)-C(31A)	1.37(2)
C(4A)-C(5A)	1.395(14)	C(26A)-C(27A)	1.37(2)
C(5A)-C(6A)	1.413(14)	C(27A)-C(28A)	1.42(2)
C(5A)-C(21A)	1.511(14)	C(28A)-C(29A)	1.29(2)
C(6A)-C(7A)	1.423(14)	C(29A)-C(30A)	1.34(2)
C(7A)-C(8A)	1.37(2)	C(29A)-C(32A)	1.55(2)
C(8A)-C(9A)	1.423(14)	C(30A)-C(31A)	1.40(2)
C(9A)-C(10A)	1.403(14)	C(33A)-C(34A)	1.36(2)
C(10A)-C(11A)	1.38(2)	C(33A)-C(38A)	1.40(2)
C(10A)-C(26A)	1.486(14)	C(34A)-C(35A)	1.393(14)
C(11A)-C(12A)	1.43(2)	C(35A)-C(36A)	1.36(2)
C(12A)-C(13A)	1.36(2)	C(36A)-C(37A)	1.36(2)
C(13A)-C(14A)	1.44(2)	C(36A)-C(39A)	1.513(14)
C(14A)-C(15A)	1.372(14)	C(37A)-C(38A)	1.39(2)
C(15A)-C(16A)	1.40(2)	C(40A)-C(41A)	1.38(2)
C(15A)-C(33A)	1.527(14)	C(40A)-C(45A)	1.383(14)

Table 6. (continued)

C(41A)-C(42A)	1.379(14)	C(17B)-C(18B)	1.341(14)
C(42A)-C(43A)	1.39(2)	C(18B)-C(19B)	1.425(14)
C(43A)-C(44A)	1.38(2)	C(19B)-C(20B)	1.405(14)
C(43A)-C(46A)	1.51(2)	C(20B)-C(40B)	1.503(14)
C(44A)-C(45A)	1.39(2)	C(21B)-C(22B)	1.36(2)
C(1B)-C(20B)	1.387(14)	C(21B)-C(25B)	1.41(2)
C(1B)-C(2B)	1.437(14)	C(22B)-C(23B)	1.404(14)
C(2B)-C(3B)	1.357(14)	C(24B)-C(25B)	1.406(13)
C(3B)-C(4B)	1.439(14)	C(26B)-C(27B)	1.40(2)
C(4B)-C(5B)	1.392(14)	C(26B)-C(31B)	1.40(2)
C(5B)-C(6B)	1.395(14)	C(27B)-C(28B)	1.40(2)
C(5B)-C(21B)	1.524(13)	C(28B)-C(29B)	1.34(2)
C(6B)-C(7B)	1.448(14)	C(29B)-C(30B)	1.37(2)
C(7B)-C(8B)	1.346(14)	C(29B)-C(32B)	1.51(2)
C(8B)-C(9B)	1.432(14)	C(30B)-C(31B)	1.40(2)
C(9B)-C(10B)	1.399(14)	C(33B)-C(38B)	1.370(14)
C(10B)-C(11B)	1.397(14)	C(33B)-C(34B)	1.38(2)
C(10B)-C(26B)	1.481(14)	C(34B)-C(35B)	1.402(14)
C(11B)-C(12B)	1.453(14)	C(35B)-C(36B)	1.38(2)
C(12B)-C(13B)	1.300(14)	C(36B)-C(37B)	1.41(2)
C(13B)-C(14B)	1.455(14)	C(36B)-C(39B)	1.523(14)
C(14B)-C(15B)	1.377(14)	C(37B)-C(38B)	1.388(14)
C(15B)-C(16B)	1.369(14)	C(40B)-C(41B)	1.37(2)
C(15B)-C(33B)	1.517(14)	C(40B)-C(45B)	1.403(14)
C(16B)-C(17B)	1.440(14)	C(41B)-C(42B)	1.34(2)

Table 6. (continued)

C(42B)-C(43B)	1.38(2)	C(1S)-F(1)	1.37(2)
C(43B)-C(44B)	1.38(2)	S(2)-O(6)	1.457(9)
C(43B)-C(46B)	1.521(14)	S(2)-O(5)	1.476(11)
C(44B)-C(45B)	1.382(14)	S(2)-O(4)	1.497(11)
S(1)-O(2)	1.397(9)	S(2)-C(2S)	1.70(3)
S(1)-O(3)	1.414(9)	C(2S)-F(6)	1.32(2)
S(1)-O(1)	1.429(8)	C(2S)-F(4)	1.37(2)
S(1)-C(1S)	2.15(2)	C(2S)-F(5)	1.42(2)
C(1S)-F(3)	1.21(2)	C(3S)-O(23)	1.55(2)
C(1S)-F(2)	1.21(2)	C(3S)-C(4S)	1.66(2)

Table 7. Bond angles (°) for $Pd(DPPP)(H_2pyTP)_2(OTf)_2$

N(6)-Pd-N(5)	83.4(3)	C(9A)-N(2A)-C(6A)	106.3(9)
N(6)-Pd-P(2)	94.4(2)	C(14A)-N(3A)-C(11A)	106.3(9)
N(5)-Pd-P(2)	177.7(2)	C(19A)-N(4A)-C(16A)	106.5(9)
N(6)-Pd-P(1)	175.3(3)	C(4B)-N(1B)-C(1B)	108.5(9)
N(5)-Pd-P(1)	92.1(2)	C(9B)-N(2B)-C(6B)	105.8(9)
P(2)-Pd-P(1)	90.22(11)	C(16B)-N(3B)-C(19B)	109.0(9)
C(104)-P(1)-C(101)	106.9(5)	C(11B)-N(4B)-C(14B)	107.2(9)
C(104)-P(1)-C(110)	106.1(5)	C(102)-C(101)-P(1)	113.0(8)
C(101)-P(1)-C(110)	103.5(5)	C(101)-C(102)-C(103)	113.6(9)
C(104)-P(1)-Pd	110.4(4)	C(102)-C(103)-P(2)	112.7(8)
C(101)-P(1)-Pd	116.4(4)	C(109)-C(104)-C(105)	118.5(11)
C(110)-P(1)-Pd	112.8(4)	C(109)-C(104)-P(1)	119.7(9)
C(116)-P(2)-C(103)	106.0(6)	C(105)-C(104)-P(1)	121.8(9)
C(116)-P(2)-C(122)	104.7(6)	C(106)-C(105)-C(104)	119.1(11)
C(103)-P(2)-C(122)	104.6(6)	C(107)-C(106)-C(105)	123.2(12)
C(116)-P(2)-Pd	116.2(4)	C(106)-C(107)-C(108)	117.7(13)
C(103)-P(2)-Pd	115.1(4)	C(109)-C(108)-C(107)	120.1(13)
C(122)-P(2)-Pd	109.2(4)	C(108)-C(109)-C(104)	121.4(11)
C(24A)-N(5)-C(23A)	117.7(10)	C(111)-C(110)-C(115)	120.3(12)
C(24A)-N(5)-Pd	120.0(8)	C(111)-C(110)-P(1)	120.3(10)
C(23A)-N(5)-Pd	122.1(8)	C(115)-C(110)-P(1)	119.4(10)
C(23B)-N(6)-C(24B)	118.3(10)	C(110)-C(111)-C(112)	119.5(12)
C(23B)-N(6)-Pd	120.4(8)	C(113)-C(112)-C(111)	120.0(13)
C(24B)-N(6)-Pd	118.1(8)	C(114)-C(113)-C(112)	119.0(14)
C(4A)-N(1A)-C(1A)	107.0(9)	C(113)-C(114)-C(115)	123.(2)

Table 7. (continued)

C(114)-C(115)-C(110)	118.2(13)	C(4A)-C(5A)-C(6A)	126.7(10)
C(121)-C(116)-C(117)	117.9(13)	C(4A)-C(5A)-C(21A)	117.0(10)
C(121)-C(116)-P(2)	119.5(10)	C(6A)-C(5A)-C(21A)	116.3(10)
C(117)-C(116)-P(2)	122.6(11)	N(2A)-C(6A)-C(5A)	124.8(10)
C(118)-C(117)-C(116)	119.9(14)	N(2A)-C(6A)-C(7A)	109.3(10)
C(119)-C(118)-C(117)	122.(2)	C(5A)-C(6A)-C(7A)	125.7(10)
C(118)-C(119)-C(120)	121.(2)	C(8A)-C(7A)-C(6A)	107.7(10)
C(119)-C(120)-C(121)	114.(2)	C(7A)-C(8A)-C(9A)	107.1(11)
C(116)-C(121)-C(120)	124.3(13)	N(2A)-C(9A)-C(10A)	125.0(10)
C(123)-C(122)-C(127)	120.4(13)	N(2A)-C(9A)-C(8A)	109.6(10)
C(123)-C(122)-P(2)	121.4(11)	C(10A)-C(9A)-C(8A)	125.4(11)
C(127)-C(122)-P(2)	118.0(11)	C(11A)-C(10A)-C(9A)	126.0(11)
C(122)-C(123)-C(124)	120.4(13)	C(11A)-C(10A)-C(26A)	116.5(11)
C(125)-C(124)-C(123)	121.0(14)	C(9A)-C(10A)-C(26A)	117.6(10)
C(124)-C(125)-C(126)	118.4(14)	C(10A)-C(11A)-N(3A)	125.0(11)
C(127)-C(126)-C(125)	122.(2)	C(10A)-C(11A)-C(12A)	126.2(12)
C(126)-C(127)-C(122)	118.0(14)	N(3A)-C(11A)-C(12A)	108.8(10)
N(1A)-C(1A)-C(20A)	125.0(10)	C(13A)-C(12A)-C(11A)	108.4(11)
N(1A)-C(1A)-C(2A)	108.6(9)	C(12A)-C(13A)-C(14A)	106.3(11)
C(20A)-C(1A)-C(2A)	126.3(10)	C(15A)-C(14A)-N(3A)	124.8(11)
C(3A)-C(2A)-C(1A)	108.5(10)	C(15A)-C(14A)-C(13A)	124.8(11)
C(2A)-C(3A)-C(4A)	107.7(10)	N(3A)-C(14A)-C(13A)	110.1(10)
N(1A)-C(4A)-C(5A)	124.8(11)	C(14A)-C(15A)-C(16A)	127.4(11)
N(1A)-C(4A)-C(3A)	108.2(10)	C(14A)-C(15A)-C(33A)	116.0(10)
C(5A)-C(4A)-C(3A)	127.0(10)	C(16A)-C(15A)-C(33A)	116.6(10)

Table 7. (continued)

(4A)-C(16A)-C(15A)	124.9(10)	C(30A)-C(29A)-C(32A)	120.1(13)
N(4A)-C(16A)-C(17A)	109.1(10)	C(29A)-C(30A)-C(31A)	122.9(14)
C(15A)-C(16A)-C(17A)	126.0(11)	C(26A)-C(31A)-C(30A)	121.0(14)
C(18A)-C(17A)-C(16A)	106.2(10)	C(34A)-C(33A)-C(38A)	118.6(11)
C(17A)-C(18A)-C(19A)	108.7(11)	C(34A)-C(33A)-C(15A)	121.4(12)
N(4A)-C(19A)-C(20A)	124.5(10)	C(38A)-C(33A)-C(15A)	119.9(12)
N(4A)-C(19A)-C(18A)	109.5(11)	C(33A)-C(34A)-C(35A)	119.4(13)
C(20A)-C(19A)-C(18A)	125.6(11)	C(36A)-C(35A)-C(34A)	122.2(13)
C(19A)-C(20A)-C(1A)	126.6(10)	C(37A)-C(36A)-C(35A)	118.4(12)
C(19A)-C(20A)-C(40A)	116.5(10)	C(37A)-C(36A)-C(39A)	120.9(13)
C(1A)-C(20A)-C(40A)	116.8(10)	C(35A)-C(36A)-C(39A)	120.7(13)
C(25A)-C(21A)-C(22A)	118.3(10)	C(36A)-C(37A)-C(38A)	120.6(13)
C(25A)-C(21A)-C(5A)	121.8(12)	C(37A)-C(38A)-C(33A)	120.6(13)
C(22A)-C(21A)-C(5A)	119.9(11)	C(41A)-C(40A)-C(45A)	118.2(11)
C(21A)-C(22A)-C(23A)	118.8(11)	C(41A)-C(40A)-C(20A)	121.2(11)
N(5)-C(23A)-C(22A)	122.8(11)	C(45A)-C(40A)-C(20A)	120.6(11)
N(5)-C(24A)-C(25A)	124.4(12)	C(42A)-C(41A)-C(40A)	121.3(12)
C(21A)-C(25A)-C(24A)	117.9(11)	C(41A)-C(42A)-C(43A)	119.4(12)
C(31A)-C(26A)-C(27A)	114.9(12)	C(44A)-C(43A)-C(42A)	120.4(12)
C(31A)-C(26A)-C(10A)	123.8(12)	C(44A)-C(43A)-C(46A)	122.9(13)
C(27A)-C(26A)-C(10A)	121.2(12)	C(42A)-C(43A)-C(46A)	116.7(13)
C(26A)-C(27A)-C(28A)	121.0(12)	C(45A)-C(44A)-C(43A)	118.8(12)
C(29A)-C(28A)-C(27A)	123.7(13)	C(44A)-C(45A)-C(40A)	121.9(12)
C(28A)-C(29A)-C(30A)	116.3(13)	C(20B)-C(1B)-N(1B)	124.7(10)
C(28A)-C(29A)-C(32A)	123.6(14)	C(20B)-C(1B)-C(2B)	127.8(11)

Table 7. (continued)

N(1B)-C(1B)-C(2B)	107.4(10)	C(15B)-C(14B)-N(4B)	125.7(11)
C(3B)-C(2B)-C(1B)	108.3(10)	C(15B)-C(14B)-C(13B)	126.7(11)
C(2B)-C(3B)-C(4B)	108.0(10)	N(4B)-C(14B)-C(13B)	107.6(10)
N(1B)-C(4B)-C(5B)	125.6(10)	C(16B)-C(15B)-C(14B)	127.6(11)
N(1B)-C(4B)-C(3B)	107.7(9)	C(16B)-C(15B)-C(33B)	114.8(10)
C(5B)-C(4B)-C(3B)	126.3(10)	C(14B)-C(15B)-C(33B)	117.6(10)
C(4B)-C(5B)-C(6B)	127.1(10)	C(15B)-C(16B)-N(3B)	126.2(10)
C(4B)-C(5B)-C(21B)	116.7(10)	C(15B)-C(16B)-C(17B)	127.6(10)
C(6B)-C(5B)-C(21B)	116.1(10)	N(3B)-C(16B)-C(17B)	106.2(10)
N(2B)-C(6B)-C(5B)	125.6(10)	C(18B)-C(17B)-C(16B)	109.1(10)
N(2B)-C(6B)-C(7B)	108.8(10)	C(17B)-C(18B)-C(19B)	107.9(10)
C(5B)-C(6B)-C(7B)	125.5(10)	N(3B)-C(19B)-C(20B)	125.4(10)
C(8B)-C(7B)-C(6B)	107.3(10)	N(3B)-C(19B)-C(18B)	107.5(9)
C(7B)-C(8B)-C(9B)	106.9(10)	C(20B)-C(19B)-C(18B)	127.1(10)
N(2B)-C(9B)-C(10B)	125.5(11)	C(1B)-C(20B)-C(19B)	126.3(10)
N(2B)-C(9B)-C(8B)	111.2(10)	C(1B)-C(20B)-C(40B)	116.8(10)
C(10B)-C(9B)-C(8B)	123.2(11)	C(19B)-C(20B)-C(40B)	116.9(10)
C(9B)-C(10B)-C(11B)	124.5(10)	C(22B)-C(21B)-C(25B)	119.6(11)
C(9B)-C(10B)-C(26B)	118.8(10)	C(22B)-C(21B)-C(5B)	121.7(11)
C(11B)-C(10B)-C(26B)	116.7(10)	C(25B)-C(21B)-C(5B)	118.2(11)
N(4B)-C(11B)-C(10B)	124.8(10)	C(21B)-C(22B)-C(23B)	118.3(12)
N(4B)-C(11B)-C(12B)	108.3(10)	N(6)-C(23B)-C(22B)	123.4(12)
C(10B)-C(11B)-C(12B)	126.8(10)	N(6)-C(24B)-C(25B)	123.2(12)
C(13B)-C(12B)-C(11B)	108.8(10)	C(24B)-C(25B)-C(21B)	116.6(12)
C(12B)-C(13B)-C(14B)	108.0(10)	C(27B)-C(26B)-C(31B)	116.8(11)

Table 7. (continued)

C(27B)-C(26B)-C(10B)	121.1(11)	C(42B)-C(43B)-C(46B)	123.6(12)
C(31B)-C(26B)-C(10B)	121.8(11)	C(44B)-C(43B)-C(46B)	120.4(11)
C(26B)-C(27B)-C(28B)	119.1(13)	C(43B)-C(44B)-C(45B)	122.0(11)
C(29B)-C(28B)-C(27B)	122.9(13)	C(44B)-C(45B)-C(40B)	119.7(12)
C(28B)-C(29B)-C(30B)	119.5(13)	O(2)-S(1)-O(3)	115.3(7)
C(28B)-C(29B)-C(32B)	121.0(14)	O(2)-S(1)-O(1)	114.6(6)
C(30B)-C(29B)-C(32B)	119.5(14)	O(3)-S(1)-O(1)	115.8(6)
C(29B)-C(30B)-C(31B)	119.5(13)	O(2)-S(1)-C(1S)	106.5(7)
C(30B)-C(31B)-C(26B)	122.2(12)	O(3)-S(1)-C(1S)	106.3(7)
C(38B)-C(33B)-C(34B)	119.1(11)	O(1)-S(1)-C(1S)	95.3(7)
C(38B)-C(33B)-C(15B)	122.0(12)	F(3)-C(1S)-F(2)	142.(2)
C(34B)-C(33B)-C(15B)	118.8(11)	F(3)-C(1S)-F(1)	109.(2)
C(33B)-C(34B)-C(35B)	120.2(12)	F(2)-C(1S)-F(1)	108.(2)
C(36B)-C(35B)-C(34B)	121.6(13)	F(3)-C(1S)-S(1)	96.(2)
C(35B)-C(36B)-C(37B)	117.3(11)	F(2)-C(1S)-S(1)	93.5(14)
C(35B)-C(36B)-C(39B)	121.1(13)	F(1)-C(1S)-S(1)	89.4(12)
C(37B)-C(36B)-C(39B)	121.5(13)	O(6)-S(2)-O(5)	116.5(9)
C(38B)-C(37B)-C(36B)	120.4(12)	O(6)-S(2)-O(4)	108.9(9)
C(33B)-C(38B)-C(37B)	121.3(13)	O(5)-S(2)-O(4)	118.0(9)
C(41B)-C(40B)-C(45B)	117.4(11)	O(6)-S(2)-C(2S)	100.8(10)
C(41B)-C(40B)-C(20B)	122.3(10)	O(5)-S(2)-C(2S)	102.9(12)
C(45B)-C(40B)-C(20B)	120.3(11)	O(4)-S(2)-C(2S)	107.6(10)
C(42B)-C(41B)-C(40B)	121.4(12)	F(6)-C(2S)-F(4)	107.(2)
C(41B)-C(42B)-C(43B)	123.3(12)	F(6)-C(2S)-F(5)	121.(3)
C(42B)-C(43B)-C(44B)	115.9(11)	F(4)-C(2S)-F(5)	113.(2)

Table 7. (continued)

F(6)-C(2S)-S(2)	112.(2)
F(4)-C(2S)-S(2)	105.(2)
F(5)-C(2S)-S(2)	98.(2)
O(23)-C(3S)-C(4S)	121.(2)

References:

1. Part of this work was present at the 207th American Chemical Society National Meeting, San Diego, CA, March 13-17, 1994, INOR 331.
2. Presidential Young Investigator, 1990-1995: Camille and Henry Dreyfus Teacher-Scholar 1993-1998.
3. (a) Gust, D.; Moore, T. A. *Adv. Photochem.* **1991**, *16*, 1. (b) Gust, D.; Moore, T. A. in *The photosynthetic Reaction Center*, Deisenhofer, J.; Norris, J. R., Eds.; Academic Press: San Diego, CA, 1993, Chap. 14, pp. 419-464. (c) Wasielewski, M. R. in *The photosynthetic Reaction Center*, Deisenhofer, J.; Norris, J. R., Eds.; Academic Press: San Diego, CA, 1993, Chap. 15, pp. 465-511. (d) Wasielewski, M. *Chem. Rev.* **1992**, *92*, 435-461. (e) Paddon-Roow, M. N. *Acc. Chem. Res.* **1994**, *27*, 18-25. (f) Harry, K.; Huber, M. *Angew. Chem.* **1995**, *107*, 927-947.
4. Fox, M. A.; Jones, W. E.; Watkins, D. M. *Chem. Eng. News* **1993**, *71* (11), 38-48.
5. (a) Wagner, R. W; Lindsey, J. S. *J. Am. Chem. Soc.* **1994**, *116*, 9759-9760. (b)

Seth, J; Palaniappan, V.; Johnson, T. E.; Prathapan, S.; Lindsey, J. S.; Bocian, D. F. *J. Am. Chem. Soc.* **1994**, *116*, 10578-10592. (c) Prathapan, S.; Johnson, T. E.; Lindsey, J. S. *J. Am. Chem. Soc.* **1993**, *115*, 7519-7520. (d) Lindsey, J. S.; Prathapan, S.; Johnson, T. E.; Wagner, R. W. *Tetrahedron* **1994**, *50*, 8941-8968.

6. Wasielewski, M. R.; Gaines, G. L. III; Wiederrecht, G. P.; Svec, W. A. ; Niemczyk, M. P. *J. Am. Chem. Soc.* **1993**, *115*, 10442-10443

7. (a) Helms, A.; Heiler, D.; McLendon, G. *J. Am. Chem. Soc.* **1992**, *114*, 6227-6238. (b) Helms, A.; Heiler, D.; McLendon, G. *J. Am. Chem. Soc.* **1991**, *113*, 4325-4327. (c) McLendon, G. *Acc. Chem. Res.* **1988**, *21*, 160-167.

8. (a) Sessler, J. L.; Johnson, M. R.; Creager, S. E.; Fettinger, J. C.; Ibers, J. A. *J Am. Chem. Soc.* **1990**, *112*, 9310-9329. (b) Sessler, J. L.; Capuano, V. L.; Harriman, A. *J Am. Chem. Soc.* **1993**, *115*, 4618-4628.

9. (a) Osuka, A.; Maruyama, K. *J. Am. Chem. Soc.* **1988**, *110*, 4454-4456. (b) Toshi, N.; Osuka, A.; Maruyama, K. *J. Am. Chem. Soc.* **1990**, *112*, 3054-3059. (c) Osuka, A.; Maruyama,K.; Mataga, N; Asahi, T.; Yamazaki, I.; Tamai, J.; *J. Am. Chem. Soc.* **1990**, *112*,4958-4959. (d) Osuka, A.; Yamada, H.; Maruyama, K.; Mataga, N.; Asahi, T.; Ohkouchi, M.; Okada, T.; Yamazaki, I.; Nishimura, Y. *J. Am. Chem. Soc.* **1993**, *115*, 9439-9452. (e) Osuka, A; Nagata, T.; Maruyama, K. *Chem. Lett.* **1991**, 481-484. (f) Osuka, A; Nagata, T.; Maruyama, K. *Chem. Lett.*

1991, 1687-1690. (g) Osuka, A; Liu, B.-L.; Maruyama, K. *Chem. Lett.* **1993**, 949-952.

10. (a). Sessler, J. L.; Wang, B.; Harriman, A. *J. Am. Chem. Soc.* **1993**, *115*, 10418. (b) Sessler, J. L.; Wang, B.; Harriman, A. *J. Am. Chem. Soc.* **1995**, *117*, 704.

11. (a) Odobel, F.; Sauvage, J-P.; Harriman, A. *Tetrahedron Lett.* **1993**, *34*, 8113-8116. (b) Harriman, A.; Odobel, F.; Sauvage, J-P. *J. Am. Chem. Soc.* **1994**, *116*, 5481-5482. (c) Collin, J-P.; Harriman, A.; Heitz, V.; Odobel, F.; Sauvage, J-P. *J. Am. Chem. Soc.* **1994**, *116*, 5679.

12. Similar compounds were reported by Drain and Lehn (Drain, C. M.; Lehn, J-M; *J Chem. Soc., Chem. Commun.*, **1994**, 2313). The complexes reported in this publication were characterized only by spectroscopic data.

13. Fleisher, E.B.; Shachter, A. M.; *Inorg. Chem.* **1991**, *30*, 3763.

14. Fuhrhop, J.; Smith, K. M. *Laboratory Methods in Porphyrin and Metalloporphyrin Research*; Elsevier: New York, 1975; p 42.

15. Price, J. H.; Williamson, A. N.; Schramm, R. F.; Wayland, B. B.; *Inorg. Chem.*, **1972**, *6*, 1280.

16. (a) Oliver, D. L.; Anderson, G. K.; *Polyhedron* **1992**, *11*, 2415. (b) Fallis, S.; Anderson, G. K.; Rath, N. P. *Organometallics*, **1991**, *10*, 3180.

17. Renzi, A. E.; Panunzi, A.; Vitagloano, A.; Paiaro, G. *J. Chem. Soc., Chem. Comm.* **1976**, 47.

18. SHELXTL-PLUS, Siemens Analytical X-ray, Inc., Madison, WI.

19. SHELXL-93, G. M. Sheldrick, *J. Appl. Cryst.* in preparation.

20. All X-ray scattering factors and anomalous dispersion terms were obtained from the "International Tables for Crystallography", Vol C, pp. 4.2.6.8 and 6.1.1.4.

21. Siedle, A. R.; Pignolet, L. H. *Inorg. Chem.* **1982**, *21*, 135-141.

22. Annibale, G.; Bonivento, M.; Canovese, L.; Cattalini, L.; Michelon, G.; Tobe, M. L. *Inorg. Chem.* **1985**, *24*, 797-800.

23. Horike, M.; Kai, Y.; Yasuoka, N.; Hasai, N. *J. Organometal. Chem.* **1975**, *86*, 269-279.

24. Stang, P. J.; Cao, D. H.; Poulter, G. T.; Arif, A. M. *Organometallics* **1995**, *14*, 1110-1114.

GENERAL CONCLUSIONS

This dissertation focuses on the preparation of derivatized porphyrins and multi-porphyrin systems. We have prepared a series thiol-derivatized porphyrins and metalloporphyrins which have varying numbers of thiol appendages attached to the porphyrin ring through amide linkages at different locations. In addition, new synthetic strategies for the synthesis of porphyrin-containing multi-component systems have been developed. These new materials are of great relevance to the area of molecular assembly and supramolecular chemistry.

A series of thiol-derivatized porphyrins and the corresponding Co and Zn containing metalloporphyrins was synthesized from 5-(*p*-aminophenyl)triphenylporphyrin, 5α,15α-bis(*o*-aminophenyl) porphyrin, and α,α,α,α-tetrakis(*o*-aminophenyl)porphyrin. The thiol-derivatized porphyrins form oriented monomolecular layers on gold surfaces. Gold electrodes that have been chemically modified with cobalt thiol porphyrin exhibit electrocatalytic potencies for the reduction of O_2 which vary as a function of the number and location of the thiol appendages. The monolayer formed by bis thiol-porphyrins, in which the porphyrin rings are largely parallel to the gold surface, has a higher electrocatalytic activity compared with that from the monolayer formed by mono thiol porphyrin where the porphyrin rings are roughly perpendicular to the gold surface. A fundamental breakthrough in this research involved the first demonstration of the influence of surface architecture on chemical properties.

A series of mono-, bis- and tetra-porphyrin assemblies has also been prepared by utilizing the well defined and versatile chemistry of square planar Pt(II) and Pd(II) coordination complexes. Starting with monopyridyl-triphenylporphyrin and Pd(II) or Pt(II) ions, we have been able to place different porphyrin subunits at chosen positions and fixed distances around the center metal ions. An X-ray crystal structure of a Pd-linked bisporphyrin assembly has been solved. This is the first molecular structure determined by single-crystal X-ray diffraction of a metal ion-templated multi-porphyrin assembly. This straightforward synthetic strategy provides an easy method for the preparation of porphyrin-containing multi-component systems.

ACKNOWLEDGEMENTS

I would like to thank Keith Woo. I am grateful for your encouragement, guidance, patience, and most of all, for your energy and enthusiasm for research. I wouldn't have reached this stage without you. You have taught me many things, inside and outside of chemistry, which are invaluble to me.

Secondly, I would like to thank Dr. Robert Angelici, Dr. John Verkade, Dr. Alan Schwabacher and Dr. Scott Chumbley for being on my committee. Thank you for your time and advice.

I am also grateful to former and present Woo group members. Along with teaching me English, life in America, and the techniques needed for my research, Lisa Berreau, Mannar Maurya, Jean-Pierre Djukic, Jim Goll, Alan Hays, Dan Smith were a tremendous help with preparation for my seminars and oral exam. Lisa Berreau, who joined this group at the same time as I, was always there to help me out when I was in trouble. Steven Gray offered a lot of help in editing my thesis. Chris Hamaker brought the updated news of the sports world. Teasing with our freshman Joe Thorman released my tension in the thesis writing and endless corrections. It is a joy to know you and work with you. I carry away special memories of each of you.

I would like to thank the other research groups at Iowa State for their loans or gifts of chemicals and equipment for my research.

I would also like to thank Dr. Porter's group for the help in the study of

monolayer formation and electrochemistry and Dr. Petrich's group for the photophysical study of multiporphyrin assemblies. I would like to acknowledge Leonard Thomas for his work involving the crystal structure reported here. I also acknowledge the help of Dave Scott, Karen Ann Smith, and Kamel Herrata in obtaining NMR and mass spectral data.

I am extremely grateful to my parents for their loving support throughout the years. They are my inspiration and I strive to make them proud of me at all times.

Last, I would like thank my wife Danhong for her love, support and understanding.